

The Lifecycle of New Zealand Atmospheric Rivers and Relationship with the Madden-Julian Oscillation

Hamish D Prince¹, Peter B Gibson², and Nicolas J. Cullen³

¹University of Wisconsin Madison, Department of Atmospheric and Oceanic Sciences

²NIWA

³School of Geography

May 25, 2023

Abstract

New Zealand atmospheric river (AR) lifecycles are analyzed to examine the synoptic conditions that produce extreme precipitation and regular flooding. An AR lifecycle tracking algorithm, novel to the region, is utilized to identify the genesis location of New Zealand ARs: the location where moisture fluxes enhance and become distinct synoptic features capable of producing impactful weather conditions. Genesis locations of ARs that later impact New Zealand cover a broad region extending from the Southern Indian Ocean (90°E) into the South Pacific (170°W) with the highest genesis frequency being in the Tasman Sea. The most impactful ARs, associated with heavy precipitation, tend to originate from distinct regions based on landfall location. Impactful North Island ARs tend to originate from subtropical regions to the northwest of New Zealand, while impactful South Island ARs are associated with genesis over southeast Australia. The synoptic conditions of impactful AR genesis are identified with North Island ARs typically associated with a cyclone in the central Tasman Sea along with a distant, persistent low pressure off the coast of West Antarctica. South Island AR genesis typically occurs in conjunction with moist conditions over Australia associated with a zonal synoptic-scale wavetrain. The Madden-Julian oscillation (MJO) is examined as a potential source of variability that modulates New Zealand AR lifecycles. It appears that the MJO modulates AR characteristics, especially during Phase 5, typically bringing more frequent, slow moving ARs with greater moisture fluxes to the North Island of New Zealand.

The Lifecycle of New Zealand Atmospheric Rivers and Relationship with the Madden-Julian Oscillation

H. D. Prince¹, P. B. Gibson², and N. J. Cullen³

¹University of Wisconsin Madison, Department of Atmospheric and Oceanic Sciences, USA

²National Institute of Water and Atmospheric Research, NZ

³University of Otago, School of Geography, NZ

Corresponding author: Hamish Prince (prince.hamishd@gmail.com)

Key Points:

- New Zealand atmospheric rivers (ARs) tend to have genesis within the Tasman Sea and terminate in the South Pacific Ocean.
- Impactful ARs originate further from landfall, in the north Tasman Sea for the North Island and southern Australia for the South Island.
- New Zealand ARs are modulated by the MJO with phase 5 notably bringing anomalous meridional moisture flux and AR frequency over the country.

Abstract

New Zealand atmospheric river (AR) lifecycles are analyzed to examine the synoptic conditions that produce extreme precipitation and regular flooding. An AR lifecycle tracking algorithm, novel to the region, is utilized to identify the genesis location of New Zealand ARs: the location where moisture fluxes enhance and become distinct synoptic features capable of producing impactful weather conditions. Genesis locations of ARs that later impact New Zealand cover a broad region extending from the Southern Indian Ocean (90°E) into the South Pacific (170°W) with the highest genesis frequency being in the Tasman Sea. The most impactful ARs, associated with heavy precipitation, tend to originate from distinct regions based on landfall location. Impactful North Island ARs tend to originate from subtropical regions to the northwest of New Zealand, while impactful South Island ARs are associated with genesis over southeast Australia. The synoptic conditions of impactful AR genesis are identified with North Island ARs typically associated with a cyclone in the central Tasman Sea along with a distant, persistent low pressure off the coast of West Antarctica. South Island AR genesis typically occurs in conjunction with moist conditions over Australia associated with a zonal synoptic-scale wavetrain. The Madden–Julian oscillation (MJO) is examined as a potential source of variability that modulates New Zealand AR lifecycles. It appears that the MJO modulates AR characteristics, especially during Phase 5, typically bringing more frequent, slow moving ARs with greater moisture fluxes to the North Island of New Zealand.

Plain Language Summary

The occurrence of atmospheric rivers (ARs) in New Zealand regularly results in extreme precipitation and flooding. This study presents the lifecycle of atmospheric rivers, identifying the atmospheric conditions that allow for ARs to form which then cause precipitation in New Zealand. The majority of New Zealand ARs tend to come from the Tasman Sea and then propagate across the South Pacific Ocean. The ARs that cause extreme precipitation originate from distinct regions in the Tasman Sea and over southern Australia. Northern landfalling ARs are associated with a large trough and a cyclone in the north Tasman Sea while southern ARs in New Zealand are associated with a cyclone position to the south of Australia. The Madden-Julian Oscillation, the position of tropical deep convection, is examined as a modulator of AR lifecycle characteristics. Phase 5 of the MJO is identified as an important phase for increasing the moisture flux and AR

activity over northern New Zealand, indicating an opportunity to improve seasonal-to-subseasonal forecasting.

1 Introduction

Flooding regularly causes hazardous conditions and substantial damage to infrastructure and property in New Zealand, resulting in significant environmental and socioeconomic impacts (Revell et al., 2019; Prince et al., 2021a). Historical individual flood events are recorded to cost more than USD\$25 million (based on adjusted insurance claim data) with recent events exceeding USD\$100 million (Reid et al., 2021; ICNZ, 2023). Identifying the atmospheric conditions across all spatiotemporal scales associated with hazardous conditions allows for an accurate impact-based assessment of geophysical properties. Furthermore, describing the specific atmospheric dynamics associated with such events provides a physically-based, dynamical understanding (compared to commonly cited probabilistic changes, e.g. Stone et al., 2022; Rhoades et al., 2021) of how changing atmospheric circulations may impact livelihoods.

An increasingly common method for studying the atmospheric controls on heavy precipitation and flooding is to identify landfalling atmospheric rivers (ARs), plumes of enhanced midlatitude water vapor transport, and their associated dynamics (Ralph et al., 2019). Numerous studies in recent years have identified that precipitation in New Zealand is dominated by the occurrence of ARs, with the vast majority of heavy precipitation events occurring during these extreme moisture fluxes (Kingston et al., 2016; Prince et al., 2021a; Reid et al., 2021; Shu et al., 2021). Prince et al., (2021a) presented a climatology of New Zealand ARs that account for up to 75% of total precipitation and >90% of heavy rainfall on selected West Coast weather stations. A more comprehensive calculation of New Zealand AR precipitation impacts for weather stations across the country (from the NIWA CliFlo database; <https://cliflo.niwa.co.nz/>) is presented in Figure 1 (corroborating Shu et al., 2021). There is a distinct spatial structure to the amount of precipitation ARs deliver in NZ, which is related to topography. On the western side of both islands, ARs account for between 50% and 85% of total annual precipitation (70% to 90% of extreme precipitation), and account for between 30% and 50% on eastern sides of the country (less than 50% of extreme precipitation).

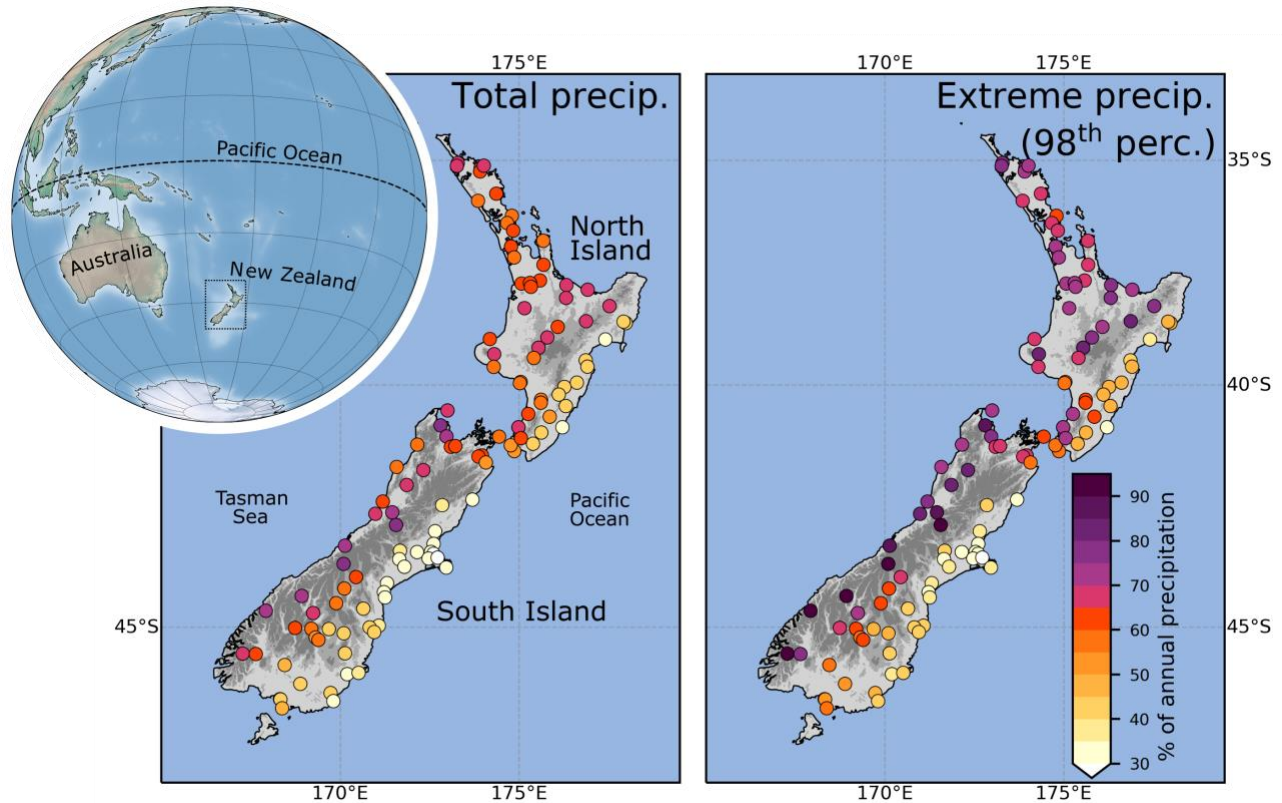


Figure 1. Mean percentage of (left) annual precipitation and (right) annual extreme precipitation (in the 98th percentile) from ARs in New Zealand from the NIWA CliFlo weather station network (<https://cliflo.niwa.co.nz/>). The presented 118 stations were selected with hourly precipitation records spanning more than 10 years with less than 10% missing data. Position of New Zealand in the Southwest Pacific basin shown in upper left and topography of New Zealand is shown with gray shading over the country with the Southern Alps (> 1000 m.a.s.l.) identified as the dark gray region extending the length of the South Island.

The broad synoptic scale conditions associated with landfalling ARs in various regions of New Zealand was presented by Prince et al. (2021a), highlighting the important orientations of the dipole pressure anomalies directing moisture laden air masses towards various coastlines of New Zealand. Prince et al. (2021a) and Reid et al. (2021) both discuss the seasonality and impact of ARs, with almost double the amount of ARs occurring in summer compared to in winter. Furthermore, AR precipitation is distinctly related to the moisture flux and duration, as defined by the AR rank; Ralph et al. (2019), especially for the western coast of New Zealand (Prince et al., 2021; Reid et al., 2021). Pohl et al., (2021) highlight the importance of the vapor transport orientation towards the landmass of New Zealand for producing extreme precipitation, which

89 directly relates to the pressure anomalies and preferential geostrophic flow. Results from Kingston
90 et al. (2021) and Prince et al. (2021a) further demonstrate the importance of landfalling moisture
91 flux direction through flooding case studies and calculated composites, respectively. Intense
92 moisture flux across the Tasman Sea, directed towards the mountainous regions of New Zealand,
93 has also been shown as a key driving mechanism in producing both heavy snowfall and snow/ice
94 melt (Little et al., 2019; Cullen et al., 2019; Kropac et al., 2021; Porhemmat et al. 2021). These
95 studies have all focused on the landfalling characteristics and statistics of New Zealand ARs ,with
96 the full dynamical description of New Zealand ARs lifecycle, genesis and termination, remaining
97 elusive.

98 The modulation of extreme weather and particularly extreme precipitation in New Zealand
99 through larger scale climate modes and oscillations is an emerging avenue of study which adds
100 understanding to seasonal-to-subseasonal forecasting and teleconnections (Mariotti et al., 2020).
101 The Southern Annular Mode (SAM), El Niño Southern Oscillation (ENSO), Interdecadal Pacific
102 Oscillation (IPO), and the Madden-Julian Oscillation (MJO) have all been shown to influence
103 weather regimes that impact New Zealand (Salinger et al., 2001; Kidston et al., 2009; Fauchereau
104 et al., 2016). The SAM, ENSO and IPO are low frequency, large-scale climate modes that manifest
105 as variations in wind speed, surface pressure, and sea surface temperatures at monthly to decadal
106 time scales (Salinger et al., 2001; Fogt and Marshall, 2020). Due to the large spatiotemporal scales
107 of SAM, ENSO, and IPO, the synoptic-scale impacts on New Zealand are not straightforward, and
108 rather appear as statistical anomalies on the climate scale.

109 The MJO however, is a convectively coupled, eastward propagating tropical wave that
110 follows a 30 to 60-day cycle that has direct dynamical influences (Zhang et al., 2020). The direct
111 thermodynamic signature allows for effective understanding of teleconnections propagating from
112 regions of enhanced tropical convection, through upper-tropospheric divergence and the
113 generation of poleward extending stationary Rossby waves (Hoskins and Karoly, 1981; Henderson
114 et al., 2017). Midlatitude precipitation anomalies in particular are described well throughout the
115 MJO lifecycle through propagating Rossby waves (Wang et al., 2023). The Northern Hemisphere
116 teleconnections of the MJO have received a lot of attention, most recently, focusing on AR
117 occurrence in North America (Zhou et al., 2021; Toride and Hakim, 2022; Wang et al., 2023).
118 Fauchereau et al. (2016) demonstrated that, for New Zealand, the MJO has a direct influence of
119 the type of weather regimes that influence the country, suggesting an ability to improve

predictability of impactful weather events as modulated by the MJO. Importantly, moist, west to northwesterly flows toward the country can be up to 50% more or less frequent based on the phase of the MJO. Pohl et al. (2022) goes on to demonstrate that New Zealand weather types are closely linked to AR occurrence, therefore, it is likely that the lifecycle of New Zealand landfalling ARs are also influenced by the MJO and the shifting location of tropical deep convection. The role of MJO on AR lifecycles forms the secondary focus of this study due to its importance for moisture flux (and presumably ARs) in New Zealand and the potential scientific advances that MJO-AR relationships can elicit as demonstrated for the North Pacific (Zhou et al., 2021; Toride and Hakim, 2022).

Tracking ARs throughout their lifecycle, including identifying conditions conducive to their formation and controls on lifecycle characteristics, has become an active research topic (Guan and Waliser, 2019; Kim and Chiang 2021). Recent advances in AR lifecycle tracking algorithms provide details such as the genesis location, travel speed, age and termination location of ARs (Guan and Waliser, 2019). AR lifecycle tracking on the West Coast of the USA has allowed for a unique understanding of the initial, distal atmospheric conditions conducive to the development of heavy precipitation and consequently substantial societal impacts to the region. ARs that travel further over the ocean prior to landfall tend to have greater integrated vapor transport (IVT; Zhou and Kim, 2019). Prince et al. (2021b) also demonstrates that the spatial distribution of AR genesis tends to shift further from the coastline for more damaging ARs, increasing the distance travelled over ocean prior to landfall and increasing the vapor transport (corroborating with Zhou and Kim, 2019). The identified AR genesis location (and associated time step) is the point in time and space when a region of moisture flux increases in magnitude (from quiescent conditions), becoming sufficiently large and intense to be considered an AR and consequently, a synoptic-scale feature capable of producing heavy precipitation. AR genesis can therefore be considered as the strengthening of lower-level winds (often through a pre-cold frontal lower level jet) within a moist environment, often associated with a developing midlatitude cyclone (Ralph et al., 2018). The presence of strong vapor transport can also generate a positive feedback for cyclonic intensification, with additional latent heating generating lower level diabatic potential vorticity (Lackmann, 2002; Zhang et al., 2019).

These emerging studies on AR lifecycle were all focused on the west coast of North America with AR genesis across the North Pacific (Sellars et al., 2017; Zhou et al., 2018; Zhou

and Kim, 2019; Kim and Chiang, 2021). The focus of this study is to examine the lifecycle, specifically the genesis, of ARs that make landfall in New Zealand in order to provide insight into the synoptic patterns and large-scale dynamics associated with the transport of moisture leading to heavy precipitation events. The genesis and termination locations of New Zealand ARs are examined for ARs throughout the entire year, followed by an assessment of how these vary based on landfall location. The modulation of AR genesis location based on extreme precipitation is presented at four individual weather stations, with an examination of the atmospheric conditions associated with AR genesis for these locations. Lagged composites of AR genesis are calculated, examining the atmospheric conditions prior and following AR genesis, to examine the antecedent and subsequent conditions for impactful AR genesis. Finally, an examination of the role of MJO on AR life cycles in New Zealand is presented to provide the first examination of the role of MJO on New Zealand ARs and subsequent extreme precipitation.

2 Data and Methods

A historical climatology of landfalling ARs in New Zealand is developed from the ERA-Interim reanalysis of 6-hourly instantaneous fields of global IVT (eastward and northward water vapor fluxes) from 1979 to 2019 (40 years) at 1.5° resolution (Dee et al., 2011). Landfalling ARs in New Zealand are identified using the Guan and Waliser (2019) Version 3, Tracking Atmospheric Rivers Globally as Elongated Targets (tARget) algorithm (henceforth GW₁₉). ARs are detected as objects of coherent, elongated regions of increased vapor transport (IVT) as described in Guan and Waliser (2015, 2019). GW₁₉ is a widely used AR detection algorithm and has undergone extensive validation and iterations of improvements, with the most recent version being a benchmark for object-based global AR tracking (Guan and Waliser, 2015, 2017, 2019; Guan et al., 2018). Examples of AR lifecycles are shown in Figure 2 for New Zealand, with identified genesis and termination regions. While only a single AR lifecycle tracking algorithm is used in this study (GW₁₉), validation from Zhou et al. (2021) has shown that new lifecycle tracking algorithms (namely from Guan and Waliser, 2019, Zhou and Kim, 2019 and Shearer et al., 2020) tend to perform consistently in identifying genesis location, especially for ARs of stronger magnitude.

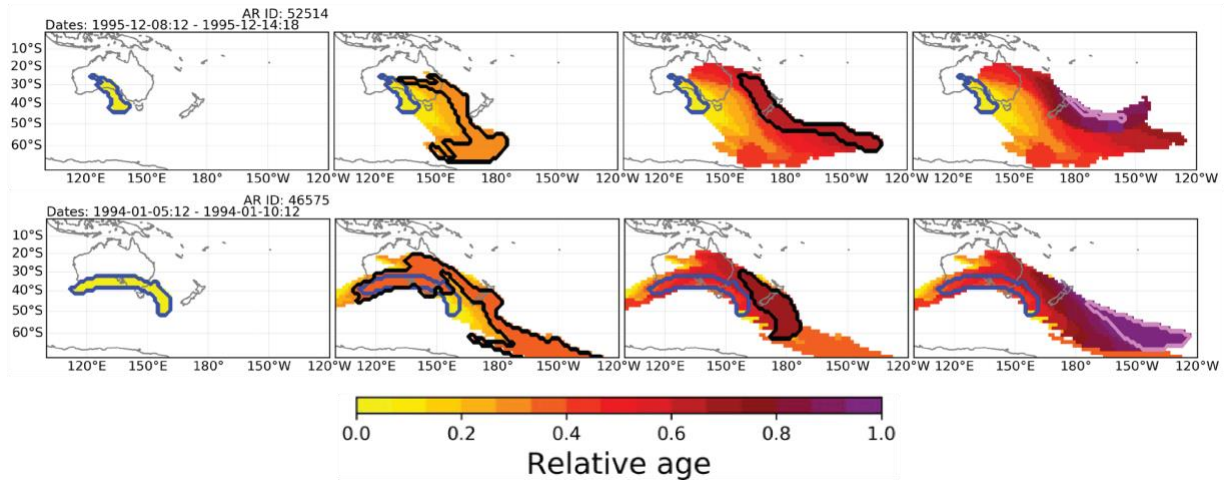


Figure 2. Examples of two AR lifecycles that made landfall in New Zealand and produced substantial precipitation (in the top 5 ARs recorded at the Hokitika rain gauge; exceeding 600 mm within 3 days). The genesis location is identified with the blue outline and the yellow color and the termination location is identified in purple. The relative age begins at zero at genesis and scales linearly to termination at unity.

GW₁₉ assigns individual ARs a unique identification allowing each landfalling AR (an AR that crosses the coastline of New Zealand) to be tracked throughout its lifecycle. The genesis and termination locations are identified as the grid cells where an AR object is first detected and where the final timestep of its presence is identified. A spatial relationship algorithm is applied in GW₁₉ to quantify the relationship between detected AR objects between time and space to assess the persistence of the same AR object throughout a lifecycle. An additional measure analyzed herein is the lifecycle frequency, which is considered as the amount of time an AR is present for each grid cell throughout its entire lifecycle, considering all time steps the AR is detected. The AR lifecycle frequency may then be calculated over a set period (i.e. a year) to calculate the frequency of time ARs are present in each cell.

Hourly precipitation records were examined from four locations on the western side of New Zealand spanning the latitudinal range of the country (from north to south: Auckland, Taranaki, Hokitika, and Fiordland). These precipitation records are used to examine the lifecycle properties and atmospheric conditions for ARs that cause heavy precipitation; the ARs with the potential to cause extensive damage. Storm-total precipitation is calculated as the amount of precipitation that falls within 12-hours of an AR being present over the weather station. The 75th

percentile of AR storm-total precipitation is chosen as the cut off to select the most extreme storms, above which the amount of precipitation increases exponentially (Figure 3). Changes in AR genesis with landfalling precipitation impact is examined using a one-sided Fishers-exact test (at the 95% level; e.g. Orskaug et al., 2011), to examine differences in frequency of events with differing sample sizes. Atmospheric composites and anomalies are calculated for all and impactful ARs using Era-Interim 500 hPa geopotential height, vertically integrated water vapor (IWV), and vertically integrated vapor transport (IVT).

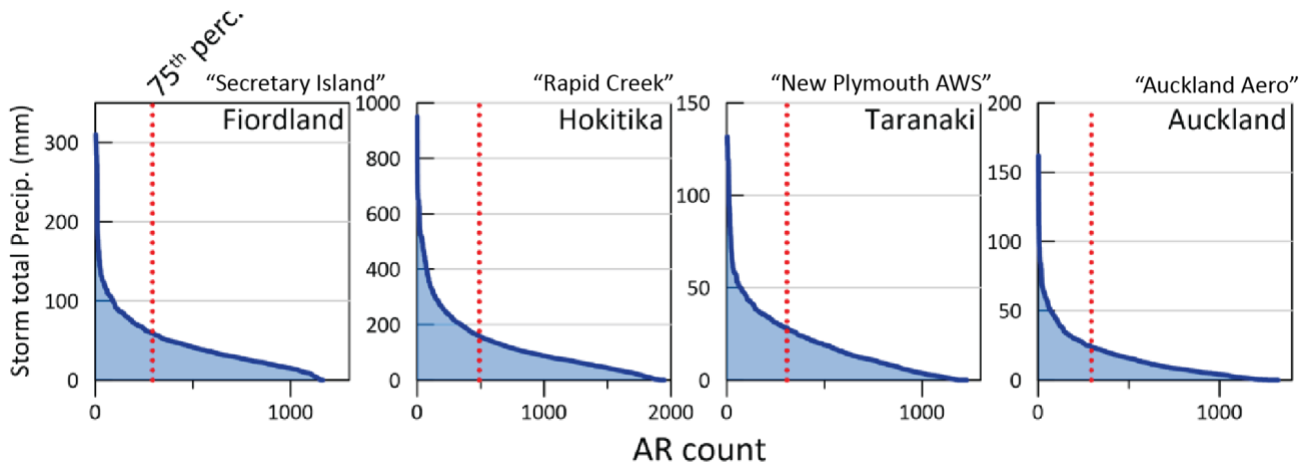


Figure 3. Storm total precipitation associated with landfalling ARs from four selected weather stations in New Zealand (named above figure) used throughout this research. The ARs are ordered along the x-axis from greatest to least storm total precipitation. The 75th percentile in storm total precipitation is identified with the red dotted line. ARs left of this line are selected as those that are most impactful.

The multivariate MJO index (Wheeler and Hendon, 2003) is used to examine the role MJO has on modulating New Zealand ARs. The index consists of two amplitudes (RMM1 and RMM2) from empirical orthogonal functions of tropical zonal winds and outgoing longwave radiation categorized into 8 distinct phases. For each phase, MJO days are identified when the combined magnitude ($\sqrt{\text{RMM1}^2 + \text{RMM2}^2}$) exceeds 1, a common distinction for identifying MJO days (Henderson et al., 2017; Zhou et al., 2021). New Zealand landfalling ARs that have genesis during an MJO phase are identified, however, since ARs can exist over multiple days it is possible for an AR to have genesis in one MJO phase and termination in another. The initial conditions are the focus of this study and so genesis during each phase is the focus to connect downstream impacts

(in New Zealand) over the entire AR lifecycle to the conditions that were present at the time of genesis (following similar justification to Zhou et al., 2021). Across all landfall locations, approximately 62% of landfalling ARs have a genesis during an identified phase of the MJO, with New Zealand AR genesis occurring on 12-19% of all days with an identified MJO.

3 Results

3.1 New Zealand AR lifecycles

We begin by examining AR lifecycles for all ARs that make landfall in New Zealand irrespective of their landfall location, magnitude, or moisture flux direction. The genesis region for New Zealand ARs stretches from 90°E to 160°W, from the Indian to the Pacific Ocean, with the highest frequency of AR genesis located in the Tasman Sea, westward of the North Island (Figure 4a). Tasman Sea genesis frequencies exceed 6 per year, with the highest grid cell frequencies exceeding 10 per year. The greatest genesis frequencies are located immediately adjacent to New Zealand, typically to the north-west. While AR genesis frequency does decrease over the landmass of Australia, it remains elevated indicating that AR genesis is not limited to maritime locations and advected moisture over the landmass of Australia is able to meet the characteristics of a genesis AR. The eastward extent of AR genesis downwind of New Zealand is notable and may also be associated with ARs that have genesis at the point of landfall with a large shape that extends well beyond the landmass of New Zealand (Prince et al., 2021b). This eastern genesis region will also reflect the genesis of ARs that make landfall on the east coast of New Zealand (Figure 5; Prince et al., 2021a).

Termination locations for New Zealand ARs extend across the entire South Pacific from 150°E to 60°W (Figure 4b), with an average of 1.5 ARs per year terminating through the Drake Passage, between South America and the Antarctic Peninsula. Similar to genesis, the highest termination rates are immediately adjacent to the landmass of New Zealand representing ARs that have termination at the time or shortly after landfall. A region of increased termination extends from the southern end of New Zealand to the southeast, possibly indicating the direction most ARs travel following landfall. Notably, over 3 ARs per year on average that landfall in New Zealand reach the Antarctic continent, extending from Victoria Land and the front of the Ross Ice Shelf, across the coastline of West Antarctic and to the western edge of the Antarctic Peninsula (Figure 4b).

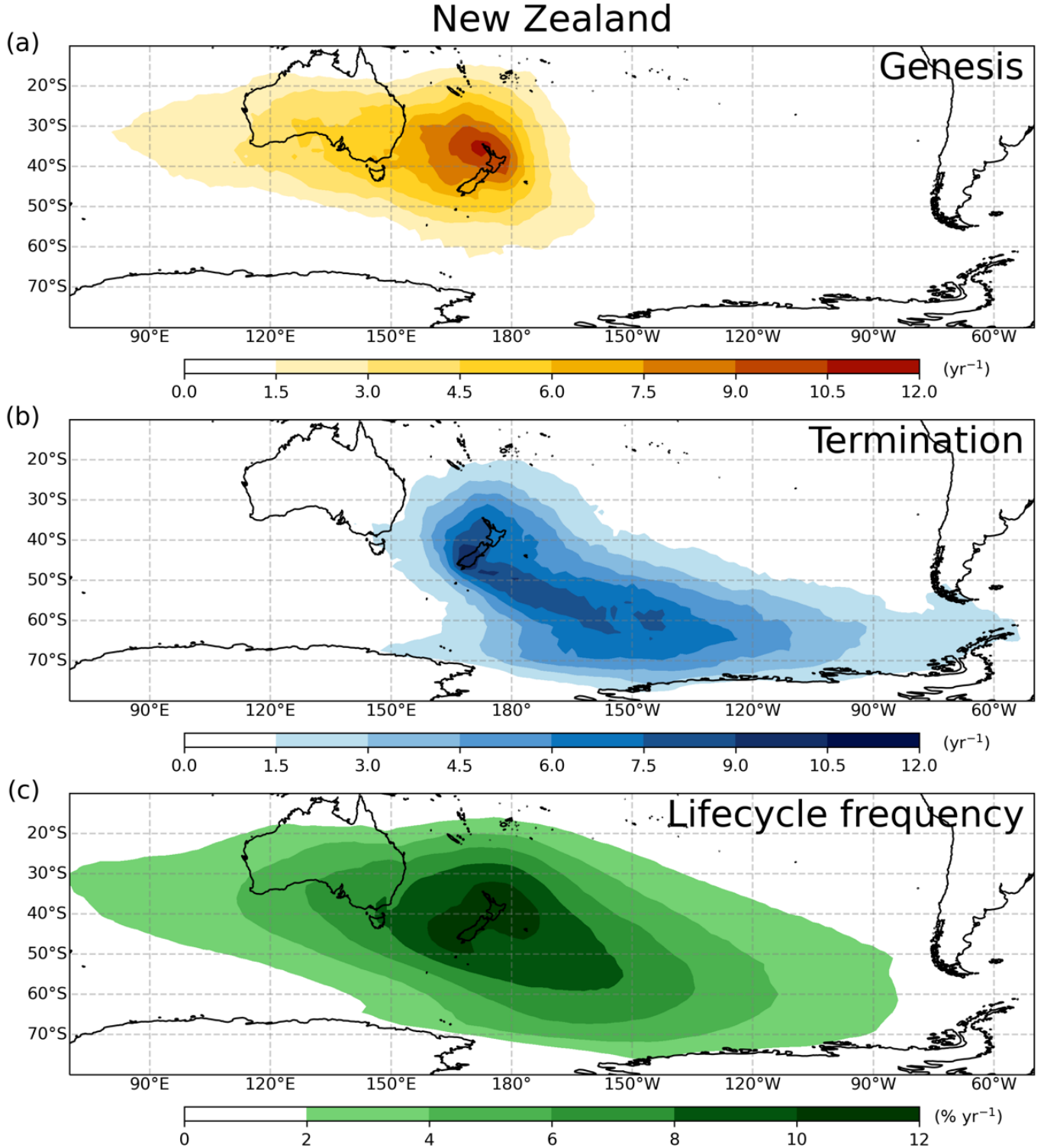


Figure 4. Mean frequency of AR (a) genesis and (b) termination for ARs that make landfall in New Zealand at any point throughout their lifecycle (in counts per year) between 1979 and 2019. (c) Lifecycle frequency of all AR objects for New Zealand landfalling ARs are shown as a percent of annual time steps.

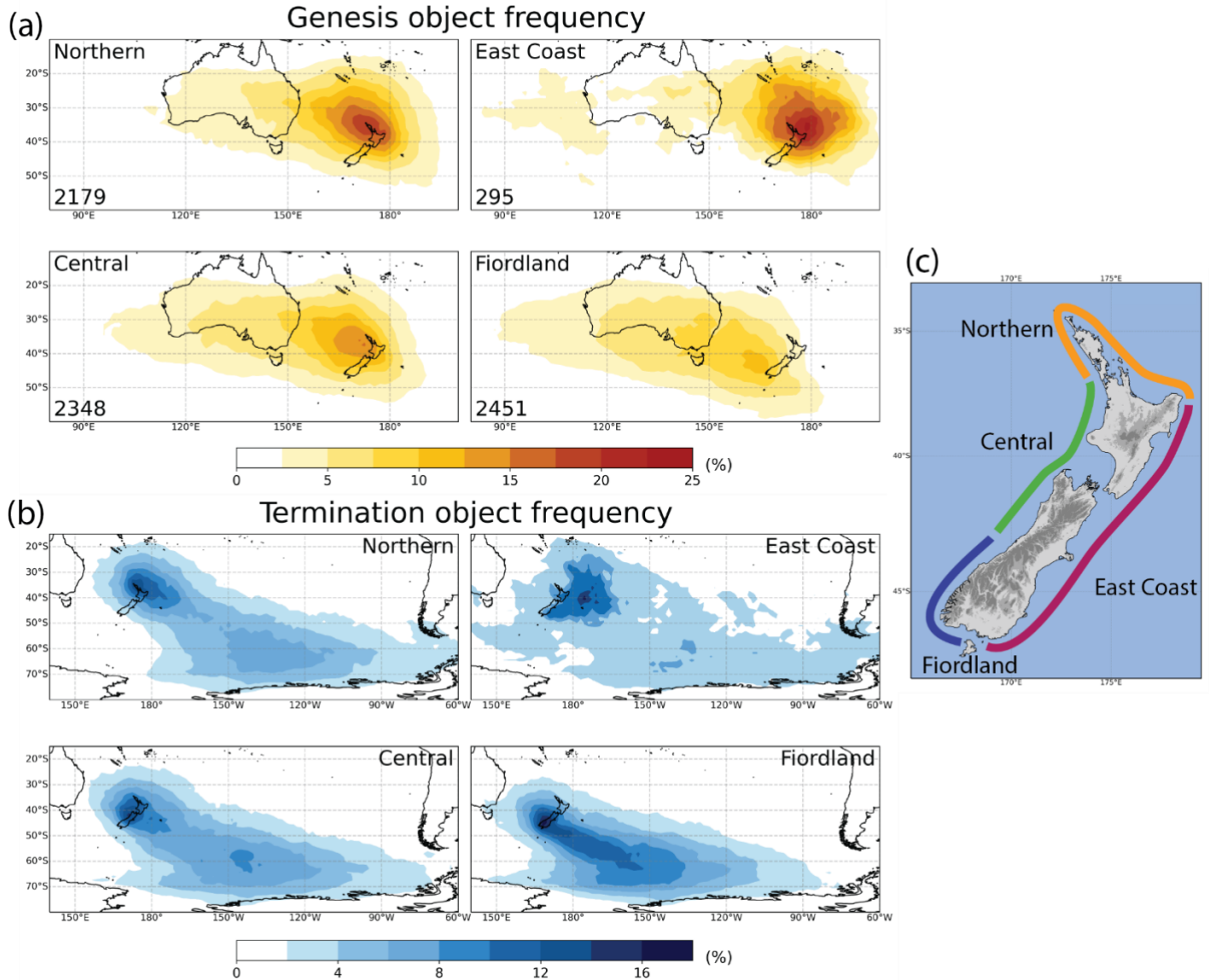


Figure 5. AR genesis (a) and termination (b) frequency for ARs that make landfall in New Zealand separated by regions as identified in (c) shown as percentages. For landfall to be selected in this figure, the moisture flux of the AR must be directed from the ocean and towards the land. Total number of AR lifecycles shown in the lower left corner in (a).

These termination locations are also well within the northern most extent of seasonal sea ice cover around Antarctica (Parkinson and Cavalieri, 2012). The range between the westward extent of genesis (90°E) and the eastward extent of termination (60°W) is over 210° of longitude, extending more than half way around the globe, demonstrating the importance of planetary scale circulation features on synoptic-scale cyclonic processes that initiate precipitation in New Zealand.

Mapping the AR lifecycle frequency further adds to this understanding by demonstrating where ARs that make landfall in New Zealand tend to occur, rather than their instantaneous genesis or termination statistics (Figure 4c). The lifecycle frequency reveals important information about the duration of AR conditions rather than the instantaneous genesis or termination object. Over the landmass of New Zealand, AR frequencies of 10-12% of timesteps within the year are observed which matches well with previous, location specific New Zealand AR frequencies (Prince et al., 2021a). Furthermore, ARs that make landfall in New Zealand occur over southeast Australia (New South Wales and Victoria) for 6-8% and Western Australia for 2-4% of annual timesteps. The lifecycle map also reveals that New Zealand landfalling ARs are also present southward of 70°S, well within the range of Antarctic sea ice for up to 2% of annual timesteps, corresponding to AR conditions (associated with New Zealand ARs) on 7 days within a year.

Dividing the genesis and termination frequencies based on landfall location further reveals the nature of AR lifecycles for various regions around the country (Figure 5). ARs that make landfall on the western side of New Zealand (Central and Fiordland in Figure 5) have the largest spread of genesis locations with up to 5% of landfalling ARs with genesis in the Indian Ocean, westward of Australia (120°E). As observed in Figure 4, the genesis frequency increases with proximity to the landfall location, increasing to up to 15% in locations adjacent to the coastline. Elevated genesis frequencies of over 2.5% extend northward up to 20°S and across central Australia. ARs that make landfall on the Northern coast of New Zealand have a more concentrated genesis region, with frequencies over 2.5% remaining eastward of 120°E, over the landmass of Australia. Towards the coastline, Northern ARs have genesis frequencies over 20%. East Coast landfalling ARs have the most unique genesis region, being constrained mostly eastward of Australia in the Tasman Sea and South Pacific Ocean. The core region of AR genesis for the East Coast is at about 180°E, to the northeast of New Zealand.

The spatial distribution of AR termination separated by region also reveals further insight into the lifecycle of New Zealand landfalling ARs. Central and Northern landfalling ARs have similar termination regions, with up to 4% of landfalling ARs having termination on the coast of Western Antarctica. These regions also display two regions of enhanced termination, over the landmass of New Zealand (over 12% of ARs) and in the South Pacific centered at 140°W and 60°S (up to 8%). About 2% of Northern and Central ARs cross the entire South Pacific Ocean and have termination in the Drake Passage. Fiordland ARs do not travel as far, with almost all termination

occurring westward of the Antarctic Peninsula and less than 2% of ARs having termination eastward of 90°W. Fiordland ARs exhibit a narrow band of increased AR termination indicating a preferential pathway for ARs that landfall in this region, extending to the southeast of the South Island with frequencies up to 12%. East Coast ARs tend to all have termination immediately east of the North Island of New Zealand at 40°S and eastward of 180°E. The colocation of East Coast AR genesis and termination regions suggests that ARs that make landfall in this region do not travel far and have relatively short lifetimes compared to those that make landfall in other regions of New Zealand.

3.2 Genesis frequency as a function of impact

A key question in this research is the role that genesis has on the impact of New Zealand landfalling ARs. The difference in genesis frequency between all ARs and those that produce impactful weather events (precipitation in the stations 75th percentile) is presented in Figure 6 across four locations spanning the length of the western coast of New Zealand (from south to north, Fiordland, Hokitika, Taranaki, and Auckland). As found in Figures 4 and 5, AR genesis for all locations on the western coast extends over Australia and towards 90°E, with those making landfall further south having genesis regions extend further westward. The distribution of genesis locations appears to shift notably when considering impactful ARs (75th percentile precipitation) across all landfall locations (statistically significant, at the 95% level from a one-sided Fisher-exact test). The median genesis centroid and relationship between storm total precipitation and IVT is shown in Supporting Information S1.

For Auckland, ARs tend to have more frequent genesis (frequencies up to 5% greater) in the north Tasman Sea stretching between Brisbane and New Caledonia between 30°S and 40°S of rates that are for individual grid cells. The reduced frequency to the south of the distribution demonstrates that impactful ARs for Auckland tend to come from north of 35°S. Further south, Taranaki exhibits a similar region of enhanced AR genesis in the North Tasman Sea, between the top of the North Island and New Caledonia with an extended zonal range stretching northwest across Australia. In the middle of the South Island, impactful ARs in Hokitika tend to have genesis along the western side of the Tasman Sea, on the east coast of Australia with a broad range of increased genesis across much of southern Australia. In Fiordland, at the southern end of New Zealand, impactful ARs only have a small region of increased genesis in a narrow band along the

southern coast of Australia. In summary, impactful North Island ARs tend to come from subtropical regions to the northwest of New Zealand, while impactful South Island ARs are associated with genesis over southeastern Australia, with the western Tasman Sea being a key region of impactful AR genesis for all regions.

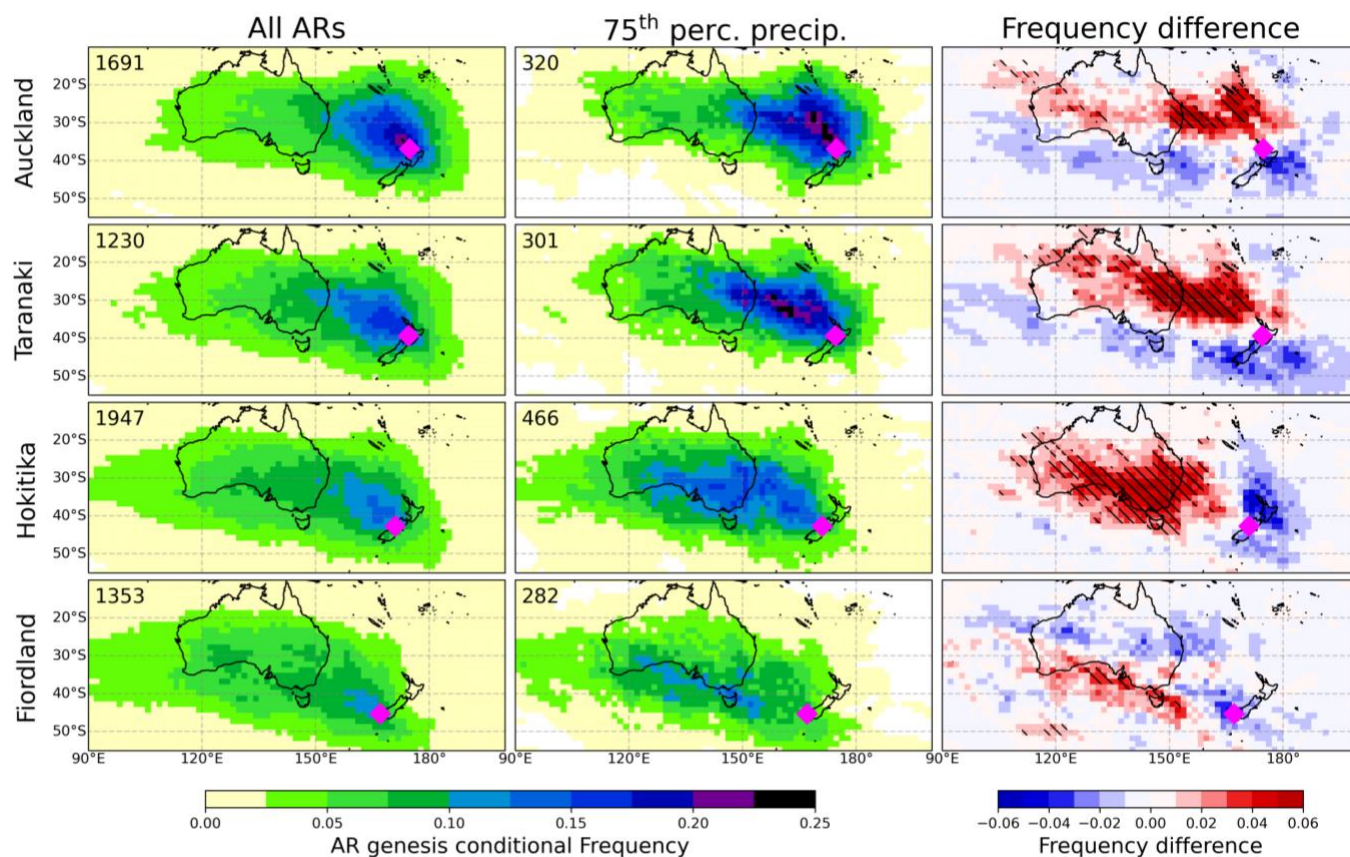


Figure 6. The conditional frequency of atmospheric river (AR) genesis for ARs making landfall at the four weather stations identified in Figure 1 for all landfalling ARs (left) and those that produce precipitation in the 75th percentile (center). Conditional frequency is the probability an AR object originates from a grid cell given that it makes landfall in each location and causes precipitation in the specified range (i.e., exceeding the 75th percentile). The numerical absolute increase in frequency (center column minus the left column) is shown (right) with statistical significance ($p < 0.05$) shown with dashed lines (from a one-sided Fisher-exact test).

3.3 Synoptic conditions during AR genesis

To further investigate characteristics of these primary AR genesis regions, atmospheric composites of vertically integrated water vapor (IWV), vertically integrated water vapor transport (IVT), and 500 hPa surface heights are assessed for the four individual landfall locations for ARs

that occur throughout the entire year (Figure 7). Genesis of all ARs for Auckland is associated with a low pressure centered to the west of the South Island of New Zealand with higher pressures to the northeast of the North Island. This pressure dipole initiates an anomalously moist, northwesterly geostrophic flow directed toward the North Island of New Zealand. Considering the other landfall locations, the location of this pressure dipole and associated moist geostrophic flow shifts southward as expected. AR genesis for all locations in Figure 7 has a weak high-pressure anomaly off the coast of Antarctic at about 50°S between 90°E and 110°E, suggesting the presence of a wave packet, with embedded synoptic scale waves, directed to the northeast. Notably, for Fiordland ARs, the moisture anomaly stretches across the entirety of Australia, suggesting that AR genesis that landfall in Fiordland is associated with broad moist conditions across Australia.

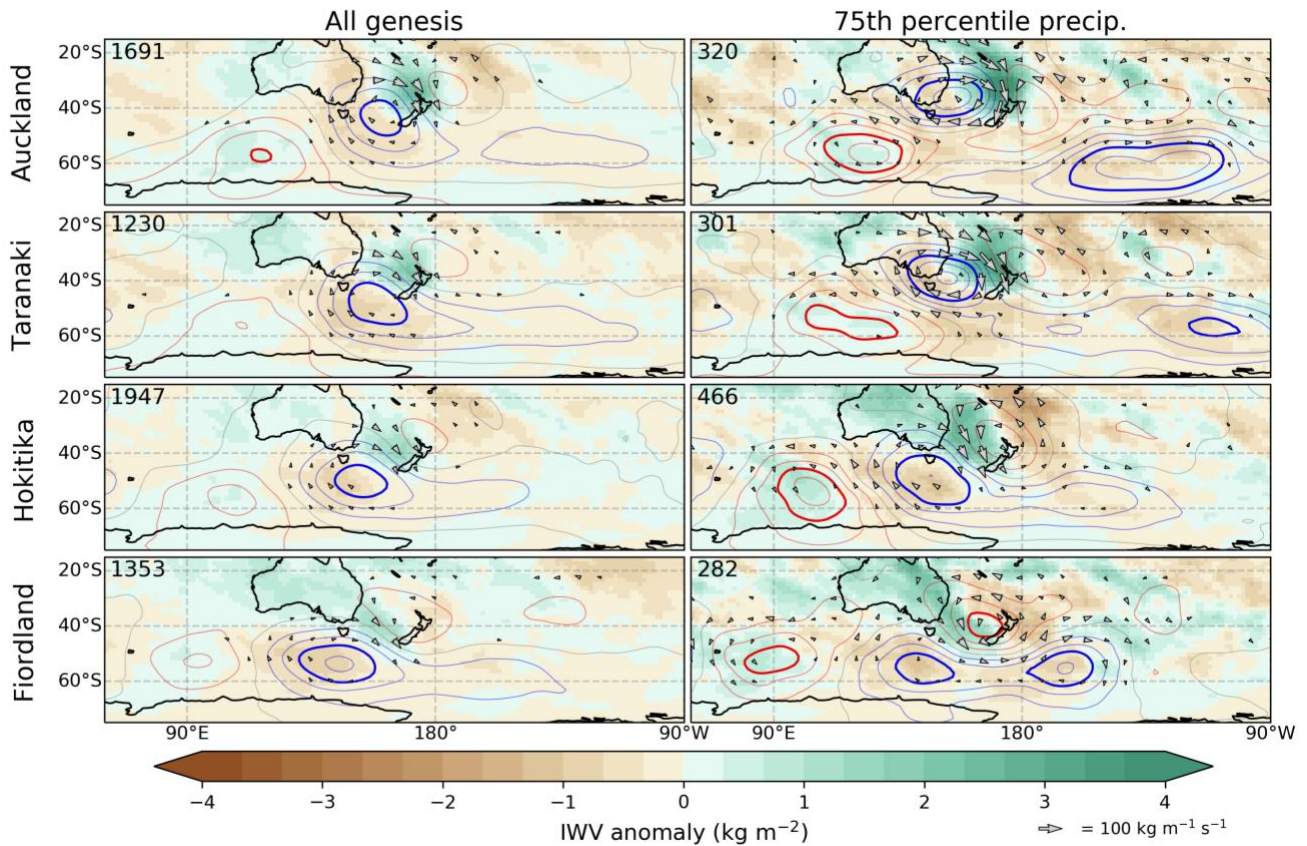


Figure 7. Atmospheric conditions at the time of atmospheric rivers (AR) genesis shown with composites of anomalous vertically integrated water vapor (IWV; green and brown), 500 hpa height anomalous (red and blue 10 m contours, 30 m in bold) and vapor flux vector anomaly (arrows) for all landfalling ARs (left) and those that produce precipitation in the 75th percentile (right).

Considering the most impactful AR conditions reveals enhanced moisture flux, IWV and geopotential height anomalies at genesis (Figure 7). For Auckland, the cyclonic anomaly deepens and shifts to the northwest, rotating the pressure dipole and allowing for a much more meridional flow, producing a much more moist northerly flow towards New Zealand. Interestingly, these impactful ARs for the North Island are also associated with a large low pressure region in the South Pacific Ocean centered at 60°S off the coast of Antarctica, centered between 180°W and 90°W. This additional geopotential anomaly combines with the previously noted tripole to trace a planetary-scale wave from 90°E to 90°W (half a hemisphere) with an embedded wave packet, with an embedded shortwave trough initiating AR genesis for the North Island of New Zealand. These features of enhanced geopotential anomalies, northward rotated moisture flux, greater moisture anomalies and the presence of a planetary-scale trough are apparent for both Auckland and Taranaki impactful (75th percentile precipitation) AR genesis.

South Island impactful AR genesis anomalies reveals a more mixed spatial pattern. In Hokitika, the cyclonic anomaly shifts westward and broadens with enhanced northerly moisture advection. For Fiordland, the high pressure located over New Zealand strengthens while two cyclonic anomalies are distributed to the south of New Zealand at 55°S. For both South Island locations, impactful ARs are associated with substantial moist anomalies over the landmass of Australia paired with substantial dry advection to the east of New Zealand. The upwind high pressure anomalies also become much more pronounced for the impactful ARs, a feature that is observed for impactful genesis for all landfall locations.

3.4 Lagged composite analysis

To further examine the preconditions of ARs in New Zealand a lagged composite analysis is undertaken by calculating mean atmospheric conditions at the time of genesis along with 2 and 5 days prior and following AR genesis for all and impactful ARs. Lagged composites are only shown for Hokitika and Auckland as representative locations, with the results from Taranaki and Fiordland are presented in the supplementary materials (Supporting Information S2 and S3). For all ARs in Hokitika, there is no consistent pressure anomaly, moisture flux or organized regions of anomalous moisture at 5 days prior to genesis (Figure 8). At 2 days prior and genesis, there is development and intensification of the low pressure anomaly in the composite with anomalous

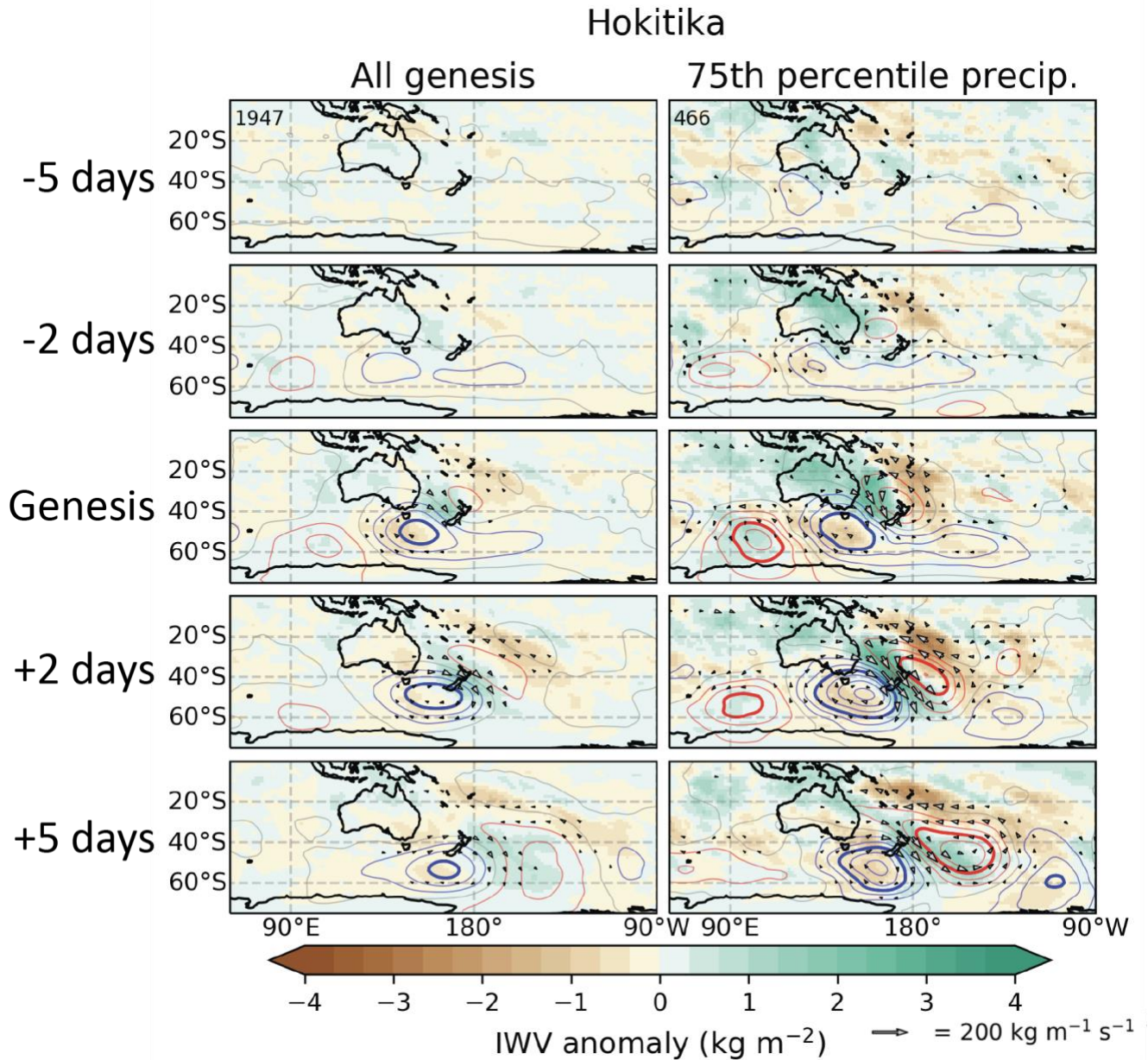


Figure 8. Synoptic-scale composites (of the same properties as Figure 7) on the day of genesis and 2 and 5 days preceding and following the genesis of ARs that make landfall in Hokitika for all ARs (left) and those that produce precipitation exceeding the 75th percentile (right).

moisture flux occurring at the time of genesis, when conditions first meet AR characteristics. After 2 days from genesis the noted anomalies persist, and intensify, demonstrating the normal progression of an AR intensifying and making landfall. After 5 days following genesis the moisture anomaly has typically moved past New Zealand as the cyclonic feature translates eastward indicating that on average, AR conditions have made landfall and passed over the country within

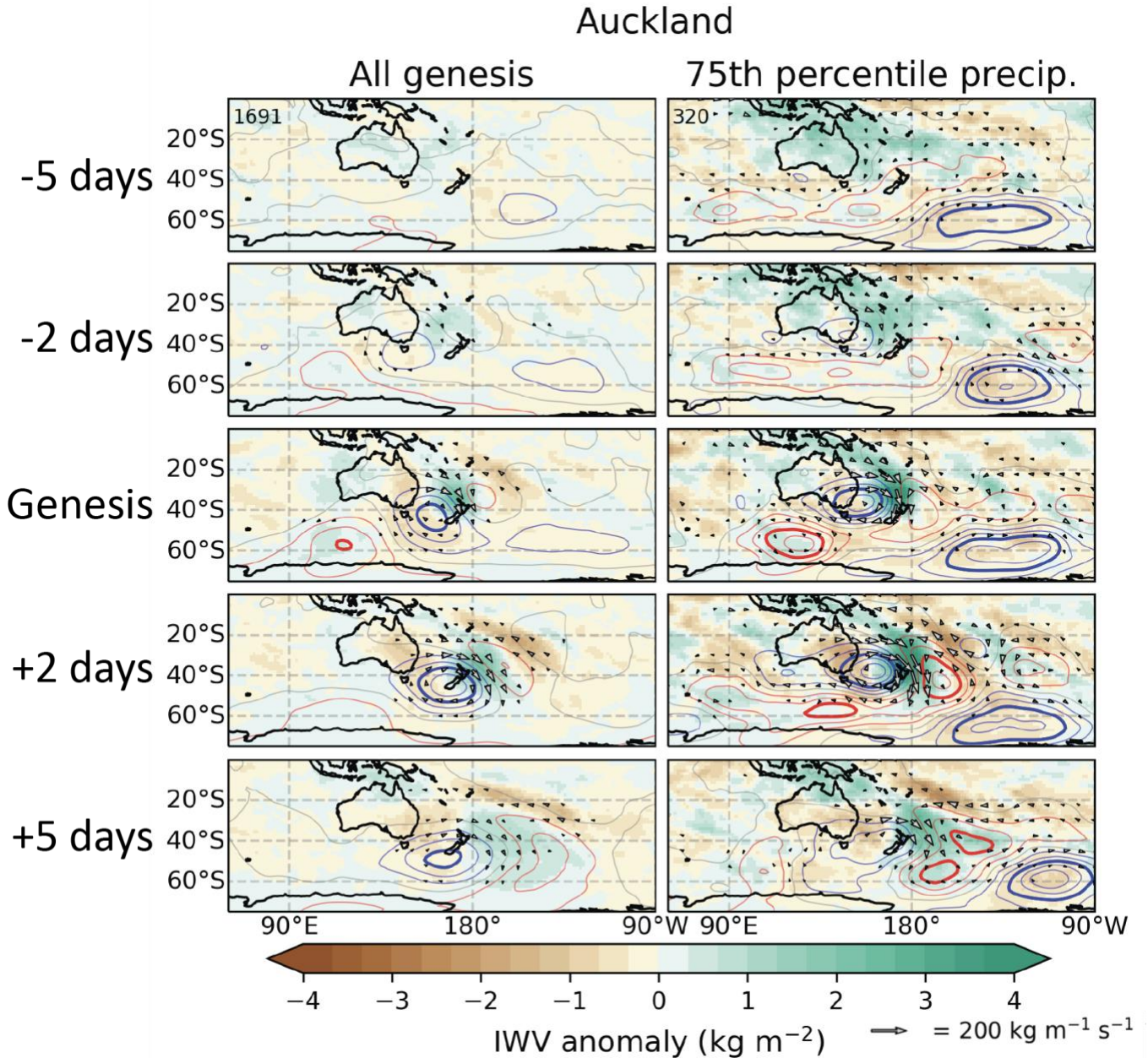
5 days. Impactful Hokitika ARs have a large moisture anomaly 2 days prior to genesis associated with a low that is passing to the south of Australia. Following genesis, impactful ARs are associated with a strengthening of all anomalies of pressure, IWV, and IVT observed up to 5 days following genesis.

Similar to Hokitika, Auckland AR genesis for all ARs does not have a signal in pressure, IWV or IVT at 5 days prior (Figure 9). At 2 days prior to genesis, moistening can be seen to the northwest of New Zealand with a low pressure in the south Tasman Sea in the composite. Following genesis, the cyclonic anomaly shifts eastward to be positioned over New Zealand which shifts the core of the enhanced moisture flux offshore to the east of Auckland, with all anomalies easing by 5 days following genesis. The lifecycle of impactful ARs for Auckland has some notable differences, namely, a large, stationary low pressure anomaly to the southeast of New Zealand, off the coast of Antarctica at about 135°W and 60°S . This low pressure remains relatively unchanged at a constant pressure anomaly and position over the 10 days centered around impactful ARs genesis. Another notable feature is the broad moist anomaly over much of Australia up to 5 days prior to impactful AR genesis. In the following 5 days leading up to genesis, a small cyclonic anomaly passes over the south of Australia, organizing this broad region of moisture into a narrow corridor along the leading edge of the cyclone, associated with the poleward flowing air of the circulation. By the time genesis occurs, the previously noted full planetary scale trough is apparent which persists for up to 5 days following genesis. As noted for Hokitika, the pressure anomalies tend to strengthen 2 days following genesis for impactful ARs, driving further development of the moisture flux in the events that produce substantial precipitation.

3.5 MJO impact on AR lifecycle characteristics

The role of the MJO on AR lifecycle characteristics is examined as an initial quantification of its impact on the weather systems that produce precipitation in New Zealand. The mean atmospheric conditions during the 8 MJO phases around New Zealand are shown in Supporting Information S4 and S5 accompanied by composites of New Zealand landfalling ARs that have genesis during each phase. Four individual AR lifecycle properties are examined at the four locations identified in Figure 6 during the 8 phases of the MJO: AR frequency, maximum IVT, AR travel speed, and median precipitation (Figure 10). AR travel speed is the mean speed that the AR object travels which will be broadly associated with the eastward translation of midlatitude

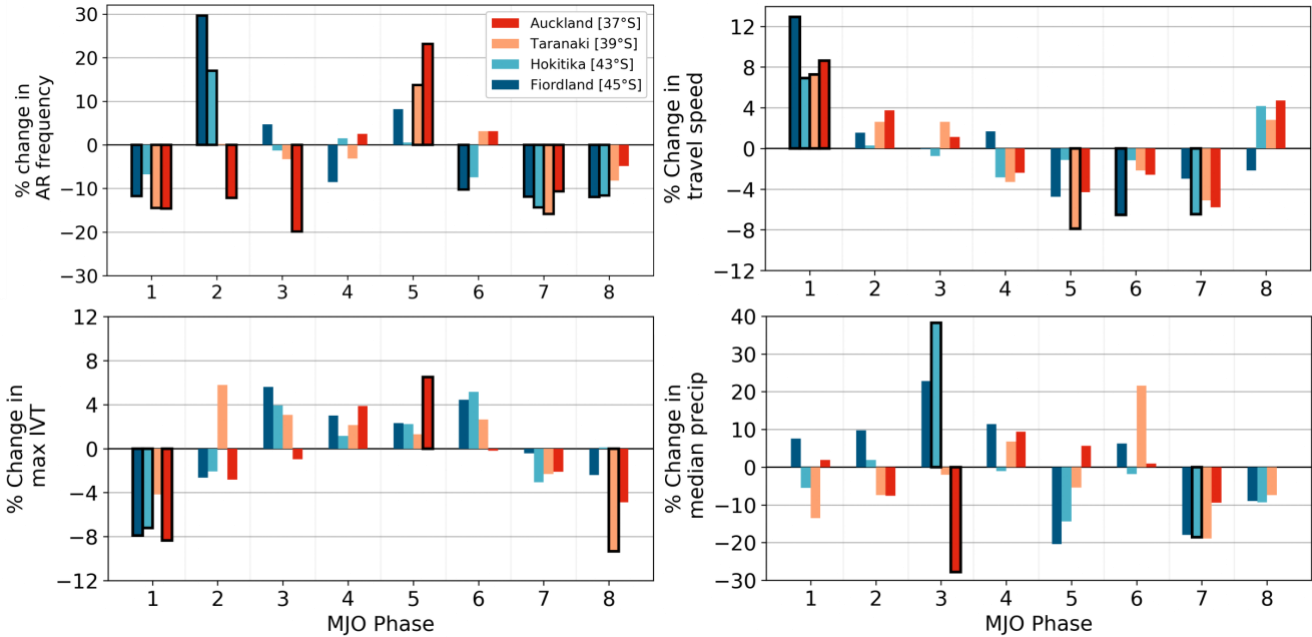
421 cyclones. A slower AR travel speed will be associated with a more stationary synoptic system
 422 possibly associated with blocking.



423 **Figure 9.** Synoptic-scale composites (of the same properties as Figure 7) on the day of genesis and
 424 2 and 5 days preceding and following the genesis of ARs that make landfall in Auckland for all
 425 ARs (left) and those that produce precipitation exceeding the 75th percentile (right).

426 Maximum IVT and AR travel speed both demonstrate a distinct modulation with the
 427 progression of the MJO. In phase 1 landfalling IVT is statistically significantly lower (an 8%
 428 decrease) in Auckland, Hokitika, and Fiordland. Moving through phases 2 to 4, the sign of the

429 difference changes to positive, however, these differences are not significant. At phase 5, Auckland
 430 experiences significantly greater maximum IVT (a 5% increase in magnitude). Then moving
 431 through to phase 8, the sign of the difference flips again with Taranaki experiencing significantly
 432 lower maximum IVT. Generally, it appears the IVT tends to be decreased during phases 1, 2, 7
 433 and 8, while IVT tends to be greater during phases 3 through to 6. AR travel speed (the speed that
 434 an AR object is translated geographically) also has a distinct cycle. ARs travel faster (statistically
 435 significant) for all landfall locations (up to 12% faster) in phase 1. Through phases 2 to 4 there is
 436 no substantial difference, while in phases 5, 6 and 7 ARs appear to travel slower with statistical
 437 significance in Fiordland, Hokitika, and Taranaki. Summarizing these two cycles, ARs tend to
 438 have lower landfalling IVT and travel faster in phases 1, 2 and 8, while having greater IVT and
 439 slower travel speeds in the middle phases, 4, 5, and 6.



440 **Figure 10.** Percent change in AR frequency, maximum IVT, AR travel speed and median
 441 precipitation for ARs that make landfall at the various locations in New Zealand during MJO
 442 phases. Statistically significant differences at the 95% level shown with bold outlines.

443 AR frequency has a complex relationship with MJO phase, however, cyclicity appears
 444 when examining individual landfall locations. In Auckland and Taranaki, AR frequency peaks in
 445 phase 5 with substantially lower frequencies during phase 1, 2, 3, 7, and 8. In Hokitika and
 446 Fiordland, AR frequency peaks in phase 2 with mostly reduced frequencies in all other phases.
 447 Median precipitation also exhibits an intriguing relationship with MJO phase, with the largest

anomalies occurring in phase 3 where Hokitika (and Fiordland to an extent) has increased median precipitation, while Auckland experiences significantly reduced median precipitation. All other phases do not have a significant impact on median precipitation, with the exception of phase 7, where there is an apparent reduction in all locations (significant in Hokitika). Interestingly, maximum IVT modulations and median precipitation statistics do not appear to covary with MJO phase.

To aid in the discussion of the role of MJO on New Zealand ARs, the spatial differences of AR lifecycle frequency is presented in Figure 11 (along with moisture, IVT, and pressure anomalies) for notable MJO phases 1, 2, 5, and 7. A positive anomaly in lifecycle frequency demonstrates that ARs (that makes landfall in New Zealand) tend to spend a longer duration at a given location than when considering all landfalling ARs. Phase 1 is characterized by reduced moisture to the north of New Zealand with a broad high pressure over the Tasman Sea and a low to the south of New Zealand. AR lifecycle frequencies are reduced over a large region of Australia and the South Pacific Ocean including much of New Zealand. Notably, the meridional pressure dipole produces a zonal moisture flux anomaly to the south of Australia, originating from the Indian Ocean that experiences increased AR occurrence and increased advection of moisture during phase 1. Phase 2 has a similar pattern that is translated eastward as the central region of tropical convection also shifts eastward. Increased atmospheric moisture in the eastern Indian Ocean allows for increased AR occurrence in the south of Australia, which stretches to the South Island of New Zealand. By phase 7 the region of increased moisture has shifted to be directly north of New Zealand, with increased AR occurrence over much of Australia and to the north of New Zealand. Phase 5 is associated with a poleward pointing geostrophic wind with a low pressure to the west of New Zealand and a high pressure to the east. Phase 5 is also associated with a large low pressure in the Amundsen-Bellingshausen Sea. Phase 7 has much drier conditions in the Indian Ocean with reduced AR occurrence over Australia and New Zealand. The region of convection is shifted into the Pacific Ocean with increased AR occurrence stretching across the Pacific Ocean.

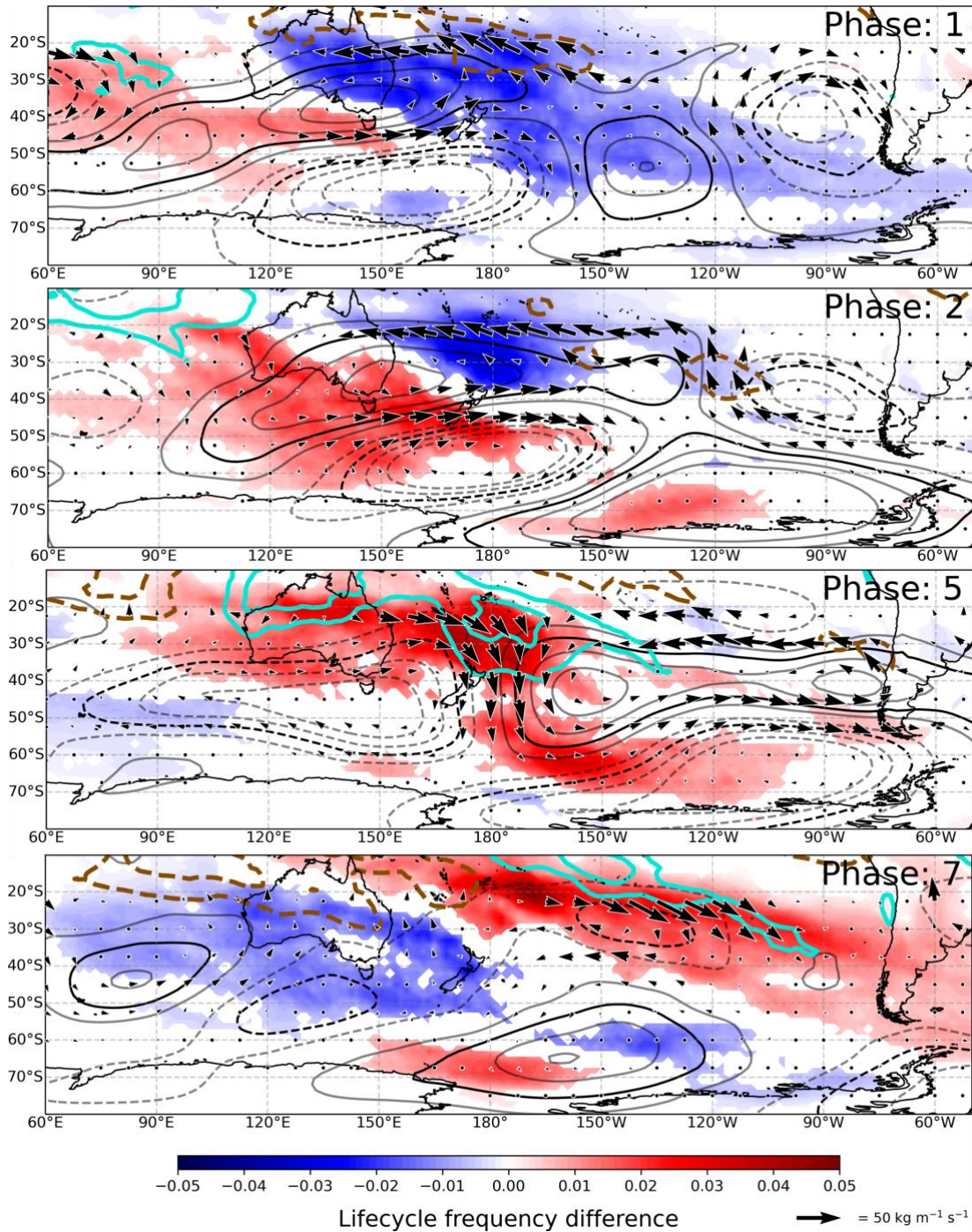


Figure 11. AR lifecycle frequency anomalies (red/blue shading) during selected MJO phases for ARs that make landfall in New Zealand (only significant anomalies at the 5% level are shown). 500z height anomalies shown with black contours (5 m interval; solid for positive, dashed for negative). IVT anomaly shown with black vectors (southward of 20°S). IWV anomalies in aqua/brown contours (+/- 1 and 2 mm of precipitable water). All atmospheric fields averaged from 10 day means following AR genesis within each MJO phase.

4 Discussion

4.1 New Zealand AR lifecycles

The composite and lagged-composite analysis (Figures 7, 8, and 9) allow for interpretation of the initial dynamical conditions that generate AR conditions for New Zealand, with a particular focus on impactful events. A schematic of the major geopotential and precipitable moisture anomalies during AR genesis is presented in Figure 12 for both the North and South Islands. Impactful South Island AR genesis tends to be associated with increased water vapor over much of Australia associated with a cyclone positioned to the south of Tasmania (50°S). The preconditioning of South Island ARs through moist anomalies over Australia has not been explicitly noted in previous studies. Prince et al. (2021a) and Kingston et al. (2021) identify the conditions during landfall with increased moisture advection immediately westward of New Zealand. We show here that this anomalous vapor flux landfalling on the South Island of New Zealand tends to be associated with greater than average precipitable water not just over the Tasman Sea but extending back over the Australian continent.

Impactful North Island AR genesis is characterized by a wavetrain within a broad trough with elevated moisture over the Coral Sea (northeast of Australia) and broad dry anomalies over Australia (Figure 12). The persistent low-pressure anomaly in the Amundsen Sea, lasting for over 10 days, speaks further to the stationary nature of this large scale trough (Figure 9). The location, magnitude, and size of this low-pressure anomaly resembles the characteristics of the Amundsen Sea Low (Raphael et al., 2016) suggesting, a linkage between Antarctic atmospheric dynamics and extreme weather in New Zealand. The same large-scale dynamics that initiate the Amundsen Sea Low may setup conditions favorable for impactful precipitation in the North Island of New Zealand.

The large-scale Rossby wave train for North Island ARs also bears resemblance to the synoptic conditions that produce Australian northwest cloudbands, a large-scale cloud feature related to widespread precipitation and warm advection over Australia (Reid et al., 2019; Black et al., 2021). Black et al. (2021) discuss the role of this large-scale trough in fluxing momentum equatorward, into the subtropical jet stream over New Zealand. This synoptic pattern is also associated with AR activity over Australia and the climatology of Australian northwest cloudbands also matches the climatology of ARs in New Zealand and Australia with maximum occurrence in

the summer (Prince et al., 2021a; Reid et al., 2019, 2022) The source of this planetary-scale wave that produces these numerous weather events for New Zealand and Australia requires further examination and remains an interesting research question. The presented composites also only resembles the mean conditions during AR genesis; an exploration of the various types of AR genesis for New Zealand would reveal further details to better constrain the synoptic drivers since they could vary somewhat between events, as have been studied for the Western U.S (e.g. Zhou and Kim, 2019; Prince et al., 2021b).

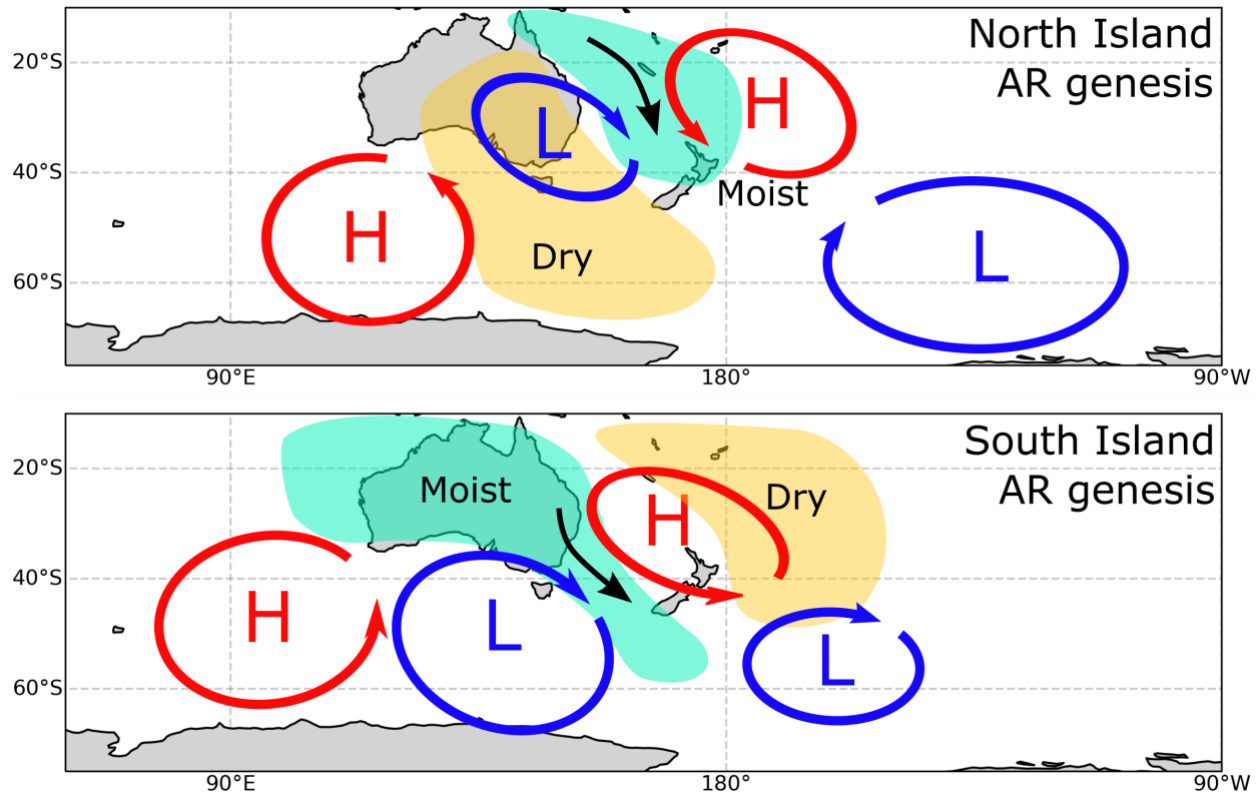


Figure 12. Schematic of the synoptic-scale setup for the genesis of impactful ARs that make landfall in the North (upper) and South (lower) Islands of New Zealand. Moisture anomalies shown with green and brown and pressure anomalies identified with blue and red regions.

The spatial extent of New Zealand AR genesis reveals insight in the passage of cyclones and accumulation of moisture that passes over New Zealand, highlighting the broad region of genesis extending back into the Indian Ocean through to termination in the South Pacific and extending through the Drake Passage. The maximum westward extent of New Zealand AR genesis extends approximately 90° west (with frequencies greater than 5%), almost half the longitudinal extent of AR genesis for corresponding west coast landfall locations in North America (Oregon

and Washington, between 35-40°N; Prince et al., 2021b). We speculate that the presence of the Australian landmass may be considered as the first order difference, inhibiting evaporation and initiating precipitation of transiting cyclones, limiting the supply of moisture available for progressing midlatitude storms. However, an adjacent moisture source is not necessarily a requirement of an AR, with examples from North Africa and the Middle East demonstrating the rapid advection of moisture over broad landmass and deserts (namely over the Arabian Peninsula; Esfandiari and Lashkari 2020; Dezfuli 2020) before initiating precipitation in mountainous regions. It is important to note however, that AR precipitable water does not necessarily come from the genesis region (Sodemann and Stohl, 2013), but rather ARs gain and lose moisture throughout their entire lifecycle. Therefore, the conditions immediately upstream of AR precipitation may be equally as important as the genesis region, suggesting that conditions in the Tasman Sea, such as sea surface temperature may be fundamentally important in controlling the amount of moisture that is advected over New Zealand. Further assessment of the source of moisture in New Zealand ARs could reveal fascinating insight into the particular regions of interest for the generation of moisture for New Zealand precipitation.

The dynamic difference between the North Pacific and westward of New Zealand (Tasman Sea and Southern Indian Ocean) cannot be ignored here and may be equally, if not more, important than the prior moisture source argument. The Northern Hemisphere jet stream maximum situated to the east of Japan (downwind of the Tibetan Plateau) is associated with substantial baroclinic growth in the north Pacific and consequently results in a broad region of enhanced transient eddy activity across the entire north Pacific basin (James, 1994), which is associated with broad AR genesis and elevated AR tracks (Zhang and Villarini, 2018; Guan and Waliser, 2019; Zhou and Kim, 2019; Prince et al., 2021b). The region of maximum cyclogenesis immediately westward of New Zealand is much closer to New Zealand than cyclogenesis for North America, with maximum cyclogenesis occurring over eastern Australia (Trenberth, 1991; Sinclair, 1994, 1995; Hoskins and Hodges, 2005). The cyclones that come further from the east, over the southern Indian Ocean (the hemispheric maximum in cyclone activity and eddy kinetic energy) tend to migrate poleward before reaching New Zealand, terminating well south of Australia (Sinclair, 1995; Hoskins and Hodges, 2005). While this westward region in the Indian Ocean does have enhanced AR genesis activity (Guan and Waliser, 2019), these ARs tend to have a substantial meridional component following the poleward migration of the cyclones, terminating to the south of Australia and

avoiding landfall with New Zealand. This understanding is in congruence with the results presented here; New Zealand ARs tend to come from a smaller upstream region stretching across Australia back to 90°E. The eastward propagation of New Zealand ARs following landfall, which extends well beyond 90° in longitude, further demonstrates that New Zealand is positioned closer to a region of AR genesis (and presumably cyclone genesis as demonstrated by Hoskins and Hodges, 2005), where ARs make landfall relatively early in their lifecycle. The unique characteristics of New Zealand AR lifecycles are crucial for understanding the occurrence of extreme precipitation in New Zealand and must be considered when interpreting future climate impacts for New Zealand.

4.2 Role of the MJO on New Zealand ARs

The presented connection between MJO and ARs in New Zealand generally agree with the role the MJO has on New Zealand weather types (Fauchereau et al., 2016). Phase 5 produces notable increases in North Island AR frequency, moisture flux and AR travel speed while aligns with the northerly flow and north Tasman Sea cyclone typically associated with this phase (Fauchereau et al., 2016). Interestingly, while phase 5 produces anomalous moisture flux and AR frequencies, it is not associated with increased precipitation, shown here and by Fauchereau et al. 2016. The anomalously low precipitation (and AR frequency) on the western coast during phase 7 (Figure 10) also agrees with the reduced west coast precipitation presented by Fauchereau et al. (2016), associated with anomalous easterly flow over the country. The increased AR frequency in phase 2 in the South Island is shown by Fauchereau et al. (2016) as increased precipitation on the South Island West Coast. The synoptic conditions are calculated as 10-day averages following the MJO phase following the methodology presented by Zhou et al. (2021) to capture the potential teleconnections initiated by the deep tropical convection associated with the MJO. Fauchereau et al. (2016) demonstrate that the geopotential height anomaly near New Zealand is stable within 10-days of a given MJO phase, consistent with the relevant timescales of stationary Rossby waves, providing confidence in the presented results.

The motivation to examine the potential role of the MJO on New Zealand AR genesis was to examine whether the geopotential anomalies associated with each phase resembled the conditions during AR genesis (as presented in Figures 7, 8, 9, and 12). The MJO does modulate the AR frequency for New Zealand landfalling ARs ($\pm 30\%$ in their occurrence). The associated

geopotential anomalies, especially associated with phase 5 sets up a low pressure in the Tasman Sea that has some resemblance to North Island AR composites. While the AR geopotential height composites will certainly involve interactions from a variety of wave sources, the position of the pressure dipole over New Zealand during phase 5 is certainly a feature expected to produce increased North Island AR activity. The exploratory analysis presented here acts as a benchmark to continue exploring the dynamical explanation for precipitation variability in New Zealand. Modern studies of MJO teleconnections have focused on North America, which has provided significant understanding of the role of tropical convection plays on seasonal-to-subseasonal forecasting (Wang et al. 2023). The results presented herein and by Fauchereau et al. (2016) highlight the potential of building understanding of tropical teleconnections for New Zealand.

5 Conclusions

In this study, we present the first assessment of New Zealand AR lifecycles, identifying the regions where New Zealand landfalling ARs are first detected and the synoptic conditions associated with initiating ARs conditions. The genesis conditions of the most impactful ARs are examined for various locations across New Zealand, with an assessment of the synoptic conditions prior to and following genesis. Impactful AR genesis for the North Island of New Zealand is associated with an embedded shortwave within a distinct planetary-scale trough extending over New Zealand. This identified synoptic pattern is not dissimilar to synoptic conditions that produce northwest cloudbands over Australia and the possible connection between Australian moisture anomalies and precipitation with New Zealand ARs is demonstrated. South Island AR genesis resembles a more typical synoptic scale wavetrain extending across New Zealand associated with moist conditions over Australia. North Island and South Island ARs appear to come from distinctly different geographic regions with the typical regions of genesis modulating for the most impactful events.

The role of MJO on modulating New Zealand AR lifecycles is also examined through 10-day composite analysis and changing AR characteristics. There is a distinct modulation in AR moisture flux and travel speed with phase 8 and 1 being associated with reduced AR frequency, low moisture flux, and faster travel speeds. The middle phases (4, 5, and 6) appear to be associated with increased moisture flux, increased AR frequency and slower travel speeds. These results appear consistent with the current understanding of MJO teleconnections in New Zealand. These

results highlight the potential for developing seasonal-to-subseasonal forecasts for the New Zealand region by identifying the role tropical dynamics play in generating midlatitude conditions that enhance precipitation.

Acknowledgments

This research undertaken by H. D. Prince is funded by Fulbright New Zealand.

Data Availability Statement

The AR data are available at <https://ucla.box.com/ARcatalog>. Development of the AR detection algorithm and databases was supported by NASA. AR detection is based on the algorithm originally introduced in Guan and Waliser (2015), refined in Guan et al. (2018), and further enhanced in Guan and Waliser (2019) with tracking capability. Precipitation data is retrieved from the NIWA CliFlo weather station network (<https://cliflo.niwa.co.nz/>). Atmospheric data is retrieved from the ECMWF ERA-Interim repository (<https://apps.ecmwf.int/datasets/data/interim-full-daily/levtype=sfc/>) and MJO timeseries is calculated by Wheeler and Hendon (2003) and retrieved from the Australian Bureau of Meteorology (<http://www.bom.gov.au/climate/mjo/>). Analysis was conducted in Python with figures produced primarily using the xarray and Cartopy packages.

References

- Black, A. S., Risbey, J. S., Chapman, C. C., Monselesan, D. P., Moore, T. S., Pook, M. J., Richardson, D., Sloyan, B. M., Squire, D. T. and Tozer, C. R. (2021). Australian Northwest cloudbands and their relationship to atmospheric rivers and precipitation. *Monthly Weather Review*, **149**(4), 1125–1139. <https://doi.org/10.1175/MWR-D-20-0308.1>
- Cullen, N. J., P. B. Gibson, T. Mölg, J. P. Conway, P. Sirguey, and D. G. Kingston (2019). The influence of weather systems in controlling mass balance in the Southern Alps of New Zealand. *J. Geophys. Res. Atmos.*, **124**, 4514–4529, <https://doi.org/10.1029/2018JD030052>.
- Dee, D. P., and Coauthors, 2011: The ERA-Interim reanalysis: Configuration and performance of the data assimilation system. *Quart. J. Roy. Meteor. Soc.*, **137**, 553–597, <https://doi.org/10.1002/qj.828>.
- Dezfuli, A. (2020). Rare atmospheric river caused record floods across the Middle East. *Bulletin of the American Meteorological Society*, **101**(4), E394–E400. <https://doi.org/10.1175/BAMS-D-19-0247.1>
- Esfandiari, N., and H. Lashkari, 2020: Identifying atmospheric river events and their paths into Iran. *Theor. Appl. Climatol.*, **140**, 1125–1137, <https://doi.org/10.1007/s00704-020-03148-w>

- Fauchereau, N., Pohl, B. and Lorrey, A. (2016). Extratropical impacts of the Madden-Julian Oscillation over New Zealand from a weather regime perspective. *Journal of Climate*, **29**(6), 2161–2175. <https://doi.org/10.1175/JCLI-D-15-0152.1>
- Fogt, R. L. and Marshall, G. J. (2020). The Southern Annular Mode: Variability, trends, and climate impacts across the Southern Hemisphere. *WIREs Climate Change*, **11**(4), e652. <https://doi.org/10.1002/wcc.652>
- Guan, B. and Waliser, D. E. (2019). Tracking atmospheric rivers globally: Spatial distributions and temporal evolution of life cycle characteristics. *J. Geophys. Res. Atmos.*, **124**, 12 523–12 552, <https://doi.org/10.1029/2019JD031205>.
- Guan, B., & Waliser, D. E. (2017). Atmospheric rivers in 20 year weather and climate simulations: A multimodel, global evaluation. *Journal of Geophysical Research: Atmospheres*, **122**, 5556–5581. <https://doi.org/10.1002/2016JD026174>
- Guan, B., and D. E. Waliser, (2015). Detection of atmospheric rivers: Evaluation and application of an algorithm for global studies. *J. Geophys. Res. Atmos.*, **120**, 12 514–12 535, <https://doi.org/10.1002/2015JD024257>
- Guan, B., Waliser, D. E., & Ralph, F. M. (2018). An intercomparison between reanalysis and dropsonde observations of the total water vapor transport in individual atmospheric rivers. *Journal of Hydrometeorology*, **19**(2), 321–337. <https://doi.org/10.1175/JHM-D-17-0114.1>
- Henderson, S. A., Maloney, E. D., Son, S.-W. (2017). Madden-Julian Oscillation Pacific Teleconnections: The impact of the basic state and MJO representation in General Circulation Models. *Journal of Climate*, **30**(12), 4567–4587. <https://doi.org/10.1175/JCLI-D-16-0789.1>
- Hoskins, B. J. and Hodges, K. I. (2005). A new perspective on Southern Hemisphere storm tracks. *Journal of Climate*, **18**(20), 4108–4129. <https://doi.org/10.1175/JCLI3570.1>
- Hoskins, B. J. and Karoly, D. J. (1981). The steady linear response of a spherical atmosphere to thermal and orographic forcing. *Journal of the Atmospheric Sciences*, **38**(6), 1179–1196. [https://doi.org/10.1175/1520-0469\(1981\)038<1179:TSLROA>2.0.CO;2](https://doi.org/10.1175/1520-0469(1981)038<1179:TSLROA>2.0.CO;2)
- ICNZ, 2023: Costs of natural disasters. Insurance Council of New Zealand, accessed 10 May 2023, <https://www.icnz.org.nz/natural-disasters/cost-of-natural-disasters/>
- James, I. N. (1994). Introduction to Circulating Atmospheres. *Cambridge University Press*, New York, USA
- Kidston, J., Renwick, J. A. and McGregor, J. (2009). Hemispheric-scale seasonality of the Southern Annular Mode and impacts on the climate of New Zealand. *Journal of Climate*, **22**(18), 4759–4770. <https://doi.org/10.1175/2009JCLI2640.1>
- Kim, S. and Chiang, J. C. H. (2021). Atmospheric river lifecycle characteristics shaped by synoptic conditions at genesis. *International Journal of Climatology*, **42**(1), 521–538. <https://doi.org/10.1002/joc.7258>
- Kingston, D. G., D. A. Lavers, and D. M. Hannah (2016). Floods in the Southern Alps of New Zealand: The importance of atmospheric rivers. *Hydrol. Processes*, **30**, 5063–5070, <https://doi.org/10.1002/hyp.10982>.
- Kingston, D. G., Lavers, D. A. and Hannah, D. M. (2021). Characteristics and large-scale drivers of atmospheric rivers associated with extreme floods in New Zealand. *International Journal of Climatology*, **42**(5), 3208–3224. <https://doi.org/10.1002/joc.7415>
- Kropač, E., Mölg, T., Cullen, N. J., Collier, E., Pickler, C. and Turton, J. V. (2021). A detailed, multi-scale assessment of an atmospheric river event and its impact on extreme glacier melt

- in the Southern Alps of New Zealand. *Journal of Geophysical Research: Atmospheres*, **126**, e2020JD034217. <https://doi.org/10.1029/2020JD034217>
- Lackman, G. M. (2002). Cold-frontal potential vorticity maxima, the low-level jet, and moisture transport in extratropical cyclones. *Monthly Weather Review*, **130**(1), 59-74. [https://doi.org/10.1175/1520-0493\(2002\)130<0059:CFPVMT>2.0.CO;2](https://doi.org/10.1175/1520-0493(2002)130<0059:CFPVMT>2.0.CO;2)
- Little, K., D. G. Kingston, N. J. Cullen, and P. B. Gibson (2019). The role of atmospheric rivers for extreme ablation and snowfall events in the Southern Alps of New Zealand. *Geophys. Res. Lett.*, **46**, 2761–2771, <https://doi.org/10.1029/2018GL081669>
- Mariotti, A., C. Baggett, E. A. Barnes, E. Becker, A. Butler, D. C. Collins, P.A. Dirmeyer, L. Ferranti, N. C. Johnson, J. Jones, B. P. Kirtman, A. L. Lang, A. Molod, M. Newman, A. W. Robertson, S. Schubert, D. E. Waliser, and J. Albers (2020). Windows of opportunity for skillful forecasts subseasonal to seasonal and beyond. *Bulletin of the American Meteorological Society*, **101**(5), E608-E625. <https://doi.org/10.1175/BAMS-D-18-0326.1>
- Orskaug, E., Scheel, I., Frigessi, A., Guttorp, P., Haugen J. E., Tveito, O. E. and Haug, O. (2011). Evaluation of a dynamic downscaling of precipitation over the Norwegian mainland. *Tellus*, **63A**, 746-756. <https://doi.org/10.1111/j.1600-0870.2011.00525.x>
- Pohl, B., Prince, H. D., Wille, J., Kingston, D. G., Cullen, N. J. and Fauchereau, N. (2023). Atmospheric rivers and weather types in Aotearoa New Zealand: a two-way story. *Journal of Geophysical Research: Atmospheres*, **Accepted**.
- Pohl, B., Sturman, A., Renwick, J., Quénol, H., Fauchereau, N., Lorrey and Pergaud, J. (2021). Precipitation and temperature anomalies over Aotearoa New Zealand analysed by weather types and descriptors of atmospheric centres of action. *International Journal of Climatology*, **43**(1), 331-353. <https://doi.org/10.1002/joc.7762>
- Porhemmat, R., Purdie, H., Zawar-Reza, P., Zammit, C. and Kerr, T. (2021). Moisture transport during large snowfall events in the New Zealand Southern Alps: The role of atmospheric rivers. *Journal of Hydrometeorology*, **22**(2), 425-444. <https://doi.org/10.1175/JHM-D-20-0044.1>
- Prince, H. D., Cullen, N. J., Gibson, P. B., Conway, J. and Kingston, D. G. (2021a). A climatology of atmospheric rivers in New Zealand. *Journal of Climate*, **34**(11), 4383-4402. <https://doi.org/10.1175/JCLI-D-20-0664.1>
- Prince, H. D., Gibson, P. B., DeFlorio, M. J., Corringham, T. W., Cobb, A., Guan, B., et al. (2021b). Genesis locations of the costliest atmospheric rivers impacting the western United States. *Geophysical Research Letters*, **48**, e2021GL093947. <https://doi.org/10.1029/2021GL093947>
- Ralph, F. M., J. J. Rutz, J. M. Cordeira, M. Dettinger, M. Anderson, D. Reynolds, L. J. Schick, and C. Smallcomb (2019). A scale to characterize the strength and impacts of atmospheric rivers. *Bull. Amer. Meteor. Soc.*, **100**, 269–289, <https://doi.org/10.1175/BAMS-D-18-0023.1>.
- Ralph, F. M., M. D. Dettinger, M. M. Cairns, T. J. Galarneau, and J. Eylander, 2018: Defining “atmospheric river”: How the Glossary of Meteorology helped resolve a debate. *Bull. Amer. Meteor. Soc.*, **99**, 837–839, <https://doi.org/10.1175/BAMS-D-17-0157.1>
- Raphael, M. N., Marshall, G. J., Turner, J., Fogt, R. L., Schneider, D., Dixon, D. A., Hoskings, J. S., Jones, J. M. and Hobbs, W. R. (2016). The Amundsen Sea Low: Variability, change, and impact on Antarctic Climate. *Bulletin of the American Meteorological Society*, **97**(1), 111-121. <https://doi.org/10.1175/BAMS-D-14-00018.1>

- Reid, K. J., King, A. D., Lane, T. P. and Hudson, D. (2022). Tropical, subtropical, and extratropical atmospheric rivers in the Australian region. *Journal of Climate*, **35**(9), 2697-2708. <https://doi.org/10.1175/JCLI-D-21-0606.1>
- Reid, K. J., Rosier, S. M., Harrington, L. J., King, A. D. and Lane, T. P. (2021). Extreme rainfall in New Zealand and its association with atmospheric rivers. *Environmental Research Letters*, **16**(4), 044012, <https://doi.org/10.1088/1748-9326/abeae0>
- Reid, K. J., Simmonds, I., Vincent, C. L. and King, A. D. (2019). The Australian Northwest Cloudband: Climatology, Mechanisms, and association with precipitation. *Journal of Climate*, **32**(20), 6665-6684. <https://doi.org/10.1175/JCLI-D-19-0031.1>
- Revell, M., Carey-Smith, T. and Moore, S. (2019). A severe frontal rain event over the lower North Island of New Zealand with intense embedded convective banding. *Weather and Climate*, **39**(1), 14-27. <https://doi.org/10.2307/26892909>
- Rhoades, A. M., Risser, M. D., Stone, D. A., Wehner, M. D. and Jones, A. D. (2021). Implications of warming on western United States landfalling atmospheric rivers and their flood damages. *Weather and Climate Extremes*, **32**, 100326. <https://doi.org/10.1016/j.wace.2021.100326>
- Salinger, M. J., Renwick, J. A. and Mullan, A. B. (2001). Interdecadal Pacific Oscillation and South Pacific Climate. *International Journal of Climatology*, **21**, 1705-1721. <https://doi.org/10.1002/joc.691>
- Sellars, S. L., Kawzenuk, B., Nguyen, P., Ralph, F. M., and Sorooshian, S. (2017). Genesis, pathways, and terminations of intense global water vapor transport in association with large-scale climate patterns. *Geophysical Research Letters*, **44**, 12465–12475. <https://doi.org/10.1002/2017gl075495>
- Shearer, E. J., Nguyen, P., Sellars, S. L., Analui, B., Kawzenuk, B., Hsu, K. and Sorooshian, S. (2020). Examination of global midlatitude atmospheric river lifecycles using an object-oriented methodology. *Journal of Geophysical Research: Atmospheres*, **125**, e2020JD033425. <https://doi.org/10.1029/2020jd033425>
- Shu, J., Shamseldin, A. Y. and Weller, E. (2021). The impact of atmospheric rivers on rainfall in New Zealand. *Scientific Reports*, **11**, 5869. <https://doi.org/10.1038/s41598-021-85297-0>
- Sinclair, M. R. (1994). An objective cyclone climatology for the Southern Hemisphere. *Mon. Wea. Rev.*, **122**, 2239–2256, [https://doi.org/10.1175/1520-0493\(1994\)122<2239:AOCFT.2.0.CO;2](https://doi.org/10.1175/1520-0493(1994)122<2239:AOCFT.2.0.CO;2)
- Sinclair, M. R. (1995). A climatology of cyclogenesis for the Southern Hemisphere. *Monthly Weather Review*, **123**(6), 1601-1619. [https://doi.org/10.1175/1520-0493\(1995\)123<1601:ACOCFT>2.0.CO;2](https://doi.org/10.1175/1520-0493(1995)123<1601:ACOCFT>2.0.CO;2)
- Sodemann, H., and A. Stohl, (2013). Moisture origin and meridional transport in atmospheric rivers and their association with multiple cyclones. *Mon. Wea. Rev.*, **141**, 2850–2868, <https://doi.org/10.1175/MWR-D-12-00256.1>
- Stone, D., Rosier, S. M., Bird, L., Harrington, L. J., Rana, S., Stuart, S. and Dean, S. M. (2022). The effect of experiment conditioning on estimates of human influence on extreme weather. *Weather and Climate Extremes*, **36**, 100427. <https://doi.org/10.1016/j.wace.2022.100427>
- Thompson, D. W. J. and Renwick, J. (2006). The Southern Annular Mode and New Zealand climate. *Water and Atmosphere*, **14**(2), 23-25
- Toride, K. and Hakim, G. J. (2022). What distinguished MJO events associated with atmospheric rivers? *Journal of Climate*, **35**(18), 6135-6149. <https://doi.org/10.1175/JCLI-D-21-0493.1>

- 788 Trenberth, K. E. (1991). Storm tracks in the Southern Hemisphere. *J. Atmos. Sci.*, **48**, 2159–2178,
789 [https://doi.org/10.1175/1520-0469\(1991\)048<2159:STITSH.2.0.CO;2](https://doi.org/10.1175/1520-0469(1991)048<2159:STITSH.2.0.CO;2).
- 790 Wang, J., DeFlorio, M. J., Guan, B. and Castellano, C. M. (2023). Seasonality of MJO impacts on
791 precipitation extremes over the Western United States. *Journal of Hydrometeorology*,
792 **24**(1), 151–166. <https://doi.org/10.1175/JHM-D-22-0089.1>
- 793 Wheeler, M. C., and H. H. Hendon, 2004: An all-season realtime multivariate MJO index:
794 Development of an index for monitoring and prediction. *Mon. Wea. Rev.*, **132**, 1917–1932,
795 [doi:10.1175/1520-0493\(2004\)132,1917:AARMMI.2.0.CO;2](https://doi.org/10.1175/1520-0493(2004)132<1917:AARMMI.2.0.CO;2).
- 796 Zhang, C., Adames, Á. F., Khouider, B., Wang, B. and Yang, D. (2020). Four theories of the
797 Madden-Julian Oscillation. *Reviews of Geophysics*, **58**, e2019RG000685.
798 <https://doi.org/10.1029/2019RG000685>
- 799 Zhang, W., and Villarini, G. (2018). Uncovering the role of the East Asian jet stream and
800 heterogeneities in atmospheric rivers affecting the western United States. *Proceedings of*
801 *the National Academy of Sciences of the United States of America*, **115**(50), 891–896.
802 <https://doi.org/10.1073/pnas.1717883115>
- 803 Zhang, Z., Ralph, F. M. and Zheng, M. (2019). The relationship between extratropical cyclones
804 strength and atmospheric river intensity and position. *Geophysical Research Letters*, **46**,
805 1814–1823. <https://doi.org/10.1029/2018GL079071>
- 806 Zhou, Y., and Kim, H. (2019). Impact of distinct origin locations on the life cycles of landfalling
807 atmospheric rivers over the U.S. West Coast. *Journal of Geophysical Research:*
808 *Atmospheres*, **124**, 11897–11909. <https://doi.org/10.1029/2019JD031218>
- 809 Zhou, Y., Kim, H. and Guan, B. (2018) Life cycle of atmospheric rivers: identification and
810 climatological characteristics. *Journal of Geophysical Research: Atmospheres*, **123**, 12–
811 715
- 812 Zhou, Y., Kim, H. and Waliser, D. E. (2021). Atmospheric river lifecycles responses to the
813 Madden-Julian Oscillation. *Geophysical Research Letters*, **48**, e2020GL090983.
814 <https://doi.org/10.1029/2020GL090983>

The Lifecycle of New Zealand Atmospheric Rivers and Relationship with the Madden-Julian Oscillation

H. D. Prince¹, P. B. Gibson², and N. J. Cullen³

¹University of Wisconsin Madison, Department of Atmospheric and Oceanic Sciences, USA

²National Institute of Water and Atmospheric Research, NZ

³University of Otago, School of Geography, NZ

Corresponding author: Hamish Prince (prince.hamishd@gmail.com)

Key Points:

- New Zealand atmospheric rivers (ARs) tend to have genesis within the Tasman Sea and terminate in the South Pacific Ocean.
- Impactful ARs originate further from landfall, in the north Tasman Sea for the North Island and southern Australia for the South Island.
- New Zealand ARs are modulated by the MJO with phase 5 notably bringing anomalous meridional moisture flux and AR frequency over the country.

Abstract

New Zealand atmospheric river (AR) lifecycles are analyzed to examine the synoptic conditions that produce extreme precipitation and regular flooding. An AR lifecycle tracking algorithm, novel to the region, is utilized to identify the genesis location of New Zealand ARs: the location where moisture fluxes enhance and become distinct synoptic features capable of producing impactful weather conditions. Genesis locations of ARs that later impact New Zealand cover a broad region extending from the Southern Indian Ocean (90°E) into the South Pacific (170°W) with the highest genesis frequency being in the Tasman Sea. The most impactful ARs, associated with heavy precipitation, tend to originate from distinct regions based on landfall location. Impactful North Island ARs tend to originate from subtropical regions to the northwest of New Zealand, while impactful South Island ARs are associated with genesis over southeast Australia. The synoptic conditions of impactful AR genesis are identified with North Island ARs typically associated with a cyclone in the central Tasman Sea along with a distant, persistent low pressure off the coast of West Antarctica. South Island AR genesis typically occurs in conjunction with moist conditions over Australia associated with a zonal synoptic-scale wavetrain. The Madden–Julian oscillation (MJO) is examined as a potential source of variability that modulates New Zealand AR lifecycles. It appears that the MJO modulates AR characteristics, especially during Phase 5, typically bringing more frequent, slow moving ARs with greater moisture fluxes to the North Island of New Zealand.

Plain Language Summary

The occurrence of atmospheric rivers (ARs) in New Zealand regularly results in extreme precipitation and flooding. This study presents the lifecycle of atmospheric rivers, identifying the atmospheric conditions that allow for ARs to form which then cause precipitation in New Zealand. The majority of New Zealand ARs tend to come from the Tasman Sea and then propagate across the South Pacific Ocean. The ARs that cause extreme precipitation originate from distinct regions in the Tasman Sea and over southern Australia. Northern landfalling ARs are associated with a large trough and a cyclone in the north Tasman Sea while southern ARs in New Zealand are associated with a cyclone position to the south of Australia. The Madden-Julian Oscillation, the position of tropical deep convection, is examined as a modulator of AR lifecycle characteristics. Phase 5 of the MJO is identified as an important phase for increasing the moisture flux and AR

activity over northern New Zealand, indicating an opportunity to improve seasonal-to-subseasonal forecasting.

1 Introduction

Flooding regularly causes hazardous conditions and substantial damage to infrastructure and property in New Zealand, resulting in significant environmental and socioeconomic impacts (Revell et al., 2019; Prince et al., 2021a). Historical individual flood events are recorded to cost more than USD\$25 million (based on adjusted insurance claim data) with recent events exceeding USD\$100 million (Reid et al., 2021; ICNZ, 2023). Identifying the atmospheric conditions across all spatiotemporal scales associated with hazardous conditions allows for an accurate impact-based assessment of geophysical properties. Furthermore, describing the specific atmospheric dynamics associated with such events provides a physically-based, dynamical understanding (compared to commonly cited probabilistic changes, e.g. Stone et al., 2022; Rhoades et al., 2021) of how changing atmospheric circulations may impact livelihoods.

An increasingly common method for studying the atmospheric controls on heavy precipitation and flooding is to identify landfalling atmospheric rivers (ARs), plumes of enhanced midlatitude water vapor transport, and their associated dynamics (Ralph et al., 2019). Numerous studies in recent years have identified that precipitation in New Zealand is dominated by the occurrence of ARs, with the vast majority of heavy precipitation events occurring during these extreme moisture fluxes (Kingston et al., 2016; Prince et al., 2021a; Reid et al., 2021; Shu et al., 2021). Prince et al., (2021a) presented a climatology of New Zealand ARs that account for up to 75% of total precipitation and >90% of heavy rainfall on selected West Coast weather stations. A more comprehensive calculation of New Zealand AR precipitation impacts for weather stations across the country (from the NIWA CliFlo database; <https://cliflo.niwa.co.nz/>) is presented in Figure 1 (corroborating Shu et al., 2021). There is a distinct spatial structure to the amount of precipitation ARs deliver in NZ, which is related to topography. On the western side of both islands, ARs account for between 50% and 85% of total annual precipitation (70% to 90% of extreme precipitation), and account for between 30% and 50% on eastern sides of the country (less than 50% of extreme precipitation).

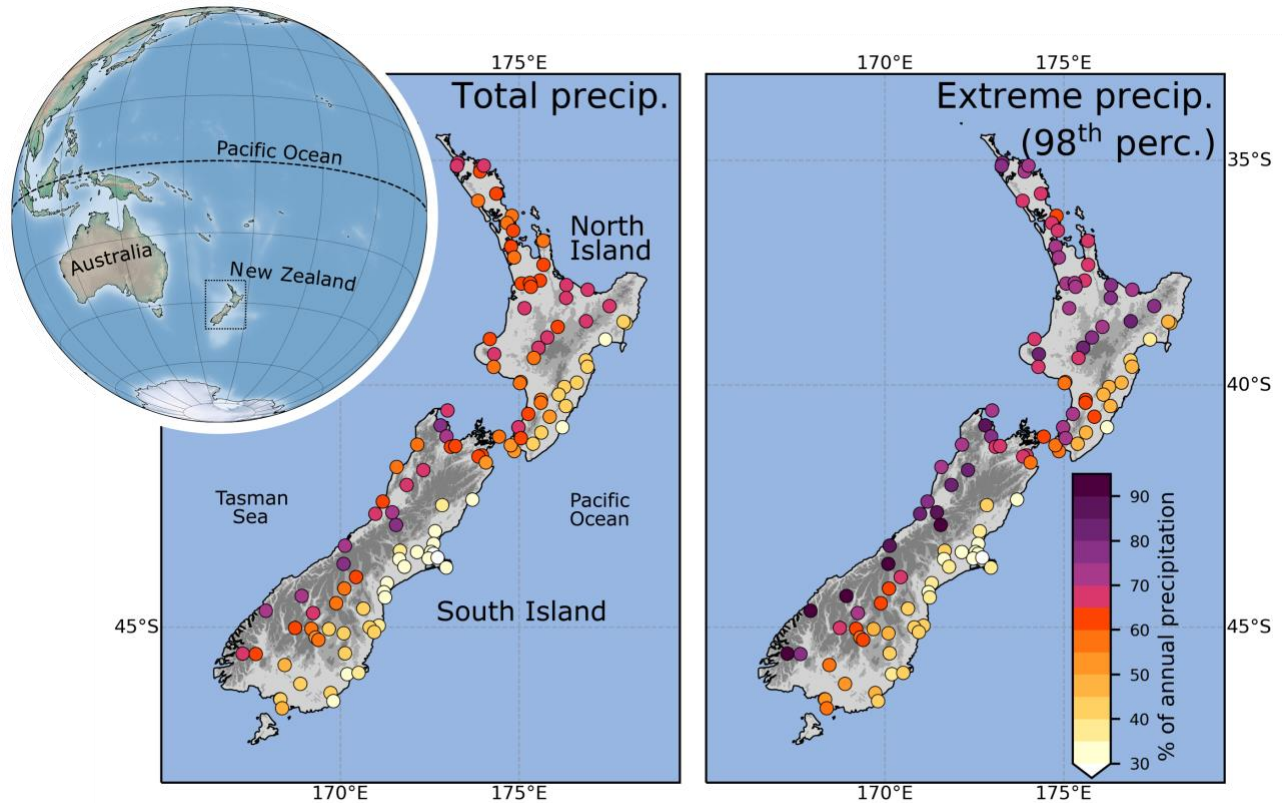


Figure 1. Mean percentage of (left) annual precipitation and (right) annual extreme precipitation (in the 98th percentile) from ARs in New Zealand from the NIWA CliFlo weather station network (<https://cliflo.niwa.co.nz/>). The presented 118 stations were selected with hourly precipitation records spanning more than 10 years with less than 10% missing data. Position of New Zealand in the Southwest Pacific basin shown in upper left and topography of New Zealand is shown with gray shading over the country with the Southern Alps (> 1000 m.a.s.l.) identified as the dark gray region extending the length of the South Island.

The broad synoptic scale conditions associated with landfalling ARs in various regions of New Zealand was presented by Prince et al. (2021a), highlighting the important orientations of the dipole pressure anomalies directing moisture laden air masses towards various coastlines of New Zealand. Prince et al. (2021a) and Reid et al. (2021) both discuss the seasonality and impact of ARs, with almost double the amount of ARs occurring in summer compared to in winter. Furthermore, AR precipitation is distinctly related to the moisture flux and duration, as defined by the AR rank; Ralph et al. (2019), especially for the western coast of New Zealand (Prince et al., 2021; Reid et al., 2021). Pohl et al., (2021) highlight the importance of the vapor transport orientation towards the landmass of New Zealand for producing extreme precipitation, which

89 directly relates to the pressure anomalies and preferential geostrophic flow. Results from Kingston
90 et al. (2021) and Prince et al. (2021a) further demonstrate the importance of landfalling moisture
91 flux direction through flooding case studies and calculated composites, respectively. Intense
92 moisture flux across the Tasman Sea, directed towards the mountainous regions of New Zealand,
93 has also been shown as a key driving mechanism in producing both heavy snowfall and snow/ice
94 melt (Little et al., 2019; Cullen et al., 2019; Kropac et al., 2021; Porhemmat et al. 2021). These
95 studies have all focused on the landfalling characteristics and statistics of New Zealand ARs ,with
96 the full dynamical description of New Zealand ARs lifecycle, genesis and termination, remaining
97 elusive.

98 The modulation of extreme weather and particularly extreme precipitation in New Zealand
99 through larger scale climate modes and oscillations is an emerging avenue of study which adds
100 understanding to seasonal-to-subseasonal forecasting and teleconnections (Mariotti et al., 2020).
101 The Southern Annular Mode (SAM), El Niño Southern Oscillation (ENSO), Interdecadal Pacific
102 Oscillation (IPO), and the Madden-Julian Oscillation (MJO) have all been shown to influence
103 weather regimes that impact New Zealand (Salinger et al., 2001; Kidston et al., 2009; Fauchereau
104 et al., 2016). The SAM, ENSO and IPO are low frequency, large-scale climate modes that manifest
105 as variations in wind speed, surface pressure, and sea surface temperatures at monthly to decadal
106 time scales (Salinger et al., 2001; Fogt and Marshall, 2020). Due to the large spatiotemporal scales
107 of SAM, ENSO, and IPO, the synoptic-scale impacts on New Zealand are not straightforward, and
108 rather appear as statistical anomalies on the climate scale.

109 The MJO however, is a convectively coupled, eastward propagating tropical wave that
110 follows a 30 to 60-day cycle that has direct dynamical influences (Zhang et al., 2020). The direct
111 thermodynamic signature allows for effective understanding of teleconnections propagating from
112 regions of enhanced tropical convection, through upper-tropospheric divergence and the
113 generation of poleward extending stationary Rossby waves (Hoskins and Karoly, 1981; Henderson
114 et al., 2017). Midlatitude precipitation anomalies in particular are described well throughout the
115 MJO lifecycle through propagating Rossby waves (Wang et al., 2023). The Northern Hemisphere
116 teleconnections of the MJO have received a lot of attention, most recently, focusing on AR
117 occurrence in North America (Zhou et al., 2021; Toride and Hakim, 2022; Wang et al., 2023).
118 Fauchereau et al. (2016) demonstrated that, for New Zealand, the MJO has a direct influence of
119 the type of weather regimes that influence the country, suggesting an ability to improve

predictability of impactful weather events as modulated by the MJO. Importantly, moist, west to northwesterly flows toward the country can be up to 50% more or less frequent based on the phase of the MJO. Pohl et al. (2022) goes on to demonstrate that New Zealand weather types are closely linked to AR occurrence, therefore, it is likely that the lifecycle of New Zealand landfalling ARs are also influenced by the MJO and the shifting location of tropical deep convection. The role of MJO on AR lifecycles forms the secondary focus of this study due to its importance for moisture flux (and presumably ARs) in New Zealand and the potential scientific advances that MJO-AR relationships can elicit as demonstrated for the North Pacific (Zhou et al., 2021; Toride and Hakim, 2022).

Tracking ARs throughout their lifecycle, including identifying conditions conducive to their formation and controls on lifecycle characteristics, has become an active research topic (Guan and Waliser, 2019; Kim and Chiang 2021). Recent advances in AR lifecycle tracking algorithms provide details such as the genesis location, travel speed, age and termination location of ARs (Guan and Waliser, 2019). AR lifecycle tracking on the West Coast of the USA has allowed for a unique understanding of the initial, distal atmospheric conditions conducive to the development of heavy precipitation and consequently substantial societal impacts to the region. ARs that travel further over the ocean prior to landfall tend to have greater integrated vapor transport (IVT; Zhou and Kim, 2019). Prince et al. (2021b) also demonstrates that the spatial distribution of AR genesis tends to shift further from the coastline for more damaging ARs, increasing the distance travelled over ocean prior to landfall and increasing the vapor transport (corroborating with Zhou and Kim, 2019). The identified AR genesis location (and associated time step) is the point in time and space when a region of moisture flux increases in magnitude (from quiescent conditions), becoming sufficiently large and intense to be considered an AR and consequently, a synoptic-scale feature capable of producing heavy precipitation. AR genesis can therefore be considered as the strengthening of lower-level winds (often through a pre-cold frontal lower level jet) within a moist environment, often associated with a developing midlatitude cyclone (Ralph et al., 2018). The presence of strong vapor transport can also generate a positive feedback for cyclonic intensification, with additional latent heating generating lower level diabatic potential vorticity (Lackmann, 2002; Zhang et al., 2019).

These emerging studies on AR lifecycle were all focused on the west coast of North America with AR genesis across the North Pacific (Sellars et al., 2017; Zhou et al., 2018; Zhou

and Kim, 2019; Kim and Chiang, 2021). The focus of this study is to examine the lifecycle, specifically the genesis, of ARs that make landfall in New Zealand in order to provide insight into the synoptic patterns and large-scale dynamics associated with the transport of moisture leading to heavy precipitation events. The genesis and termination locations of New Zealand ARs are examined for ARs throughout the entire year, followed by an assessment of how these vary based on landfall location. The modulation of AR genesis location based on extreme precipitation is presented at four individual weather stations, with an examination of the atmospheric conditions associated with AR genesis for these locations. Lagged composites of AR genesis are calculated, examining the atmospheric conditions prior and following AR genesis, to examine the antecedent and subsequent conditions for impactful AR genesis. Finally, an examination of the role of MJO on AR life cycles in New Zealand is presented to provide the first examination of the role of MJO on New Zealand ARs and subsequent extreme precipitation.

2 Data and Methods

A historical climatology of landfalling ARs in New Zealand is developed from the ERA-Interim reanalysis of 6-hourly instantaneous fields of global IVT (eastward and northward water vapor fluxes) from 1979 to 2019 (40 years) at 1.5° resolution (Dee et al., 2011). Landfalling ARs in New Zealand are identified using the Guan and Waliser (2019) Version 3, Tracking Atmospheric Rivers Globally as Elongated Targets (tARget) algorithm (henceforth GW₁₉). ARs are detected as objects of coherent, elongated regions of increased vapor transport (IVT) as described in Guan and Waliser (2015, 2019). GW₁₉ is a widely used AR detection algorithm and has undergone extensive validation and iterations of improvements, with the most recent version being a benchmark for object-based global AR tracking (Guan and Waliser, 2015, 2017, 2019; Guan et al., 2018). Examples of AR lifecycles are shown in Figure 2 for New Zealand, with identified genesis and termination regions. While only a single AR lifecycle tracking algorithm is used in this study (GW₁₉), validation from Zhou et al. (2021) has shown that new lifecycle tracking algorithms (namely from Guan and Waliser, 2019, Zhou and Kim, 2019 and Shearer et al., 2020) tend to perform consistently in identifying genesis location, especially for ARs of stronger magnitude.

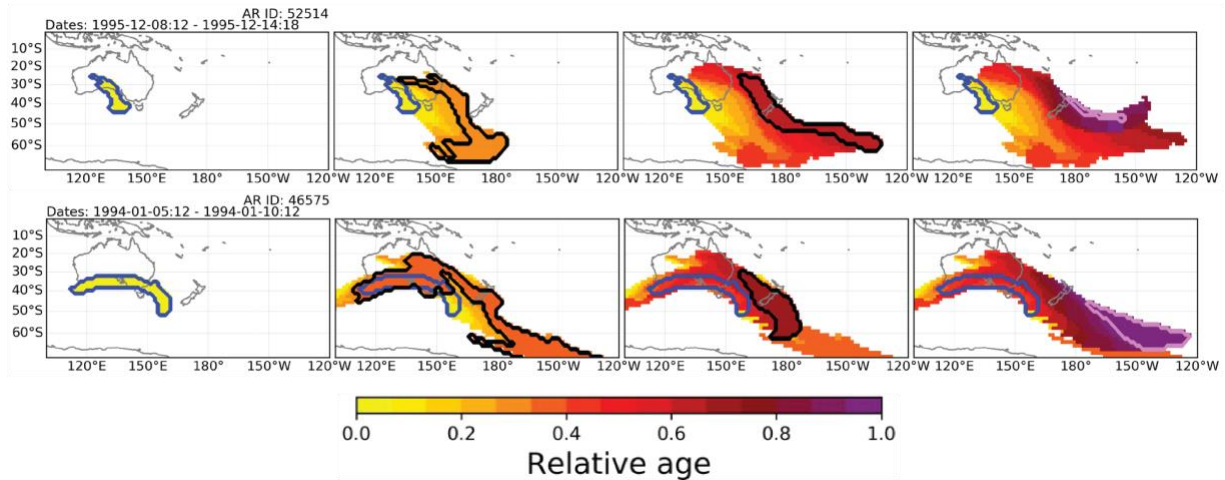


Figure 2. Examples of two AR lifecycles that made landfall in New Zealand and produced substantial precipitation (in the top 5 ARs recorded at the Hokitika rain gauge; exceeding 600 mm within 3 days). The genesis location is identified with the blue outline and the yellow color and the termination location is identified in purple. The relative age begins at zero at genesis and scales linearly to termination at unity.

GW₁₉ assigns individual ARs a unique identification allowing each landfalling AR (an AR that crosses the coastline of New Zealand) to be tracked throughout its lifecycle. The genesis and termination locations are identified as the grid cells where an AR object is first detected and where the final timestep of its presence is identified. A spatial relationship algorithm is applied in GW₁₉ to quantify the relationship between detected AR objects between time and space to assess the persistence of the same AR object throughout a lifecycle. An additional measure analyzed herein is the lifecycle frequency, which is considered as the amount of time an AR is present for each grid cell throughout its entire lifecycle, considering all time steps the AR is detected. The AR lifecycle frequency may then be calculated over a set period (i.e. a year) to calculate the frequency of time ARs are present in each cell.

Hourly precipitation records were examined from four locations on the western side of New Zealand spanning the latitudinal range of the country (from north to south: Auckland, Taranaki, Hokitika, and Fiordland). These precipitation records are used to examine the lifecycle properties and atmospheric conditions for ARs that cause heavy precipitation; the ARs with the potential to cause extensive damage. Storm-total precipitation is calculated as the amount of precipitation that falls within 12-hours of an AR being present over the weather station. The 75th

percentile of AR storm-total precipitation is chosen as the cut off to select the most extreme storms, above which the amount of precipitation increases exponentially (Figure 3). Changes in AR genesis with landfalling precipitation impact is examined using a one-sided Fishers-exact test (at the 95% level; e.g. Orskaug et al., 2011), to examine differences in frequency of events with differing sample sizes. Atmospheric composites and anomalies are calculated for all and impactful ARs using Era-Interim 500 hPa geopotential height, vertically integrated water vapor (IWV), and vertically integrated vapor transport (IVT).

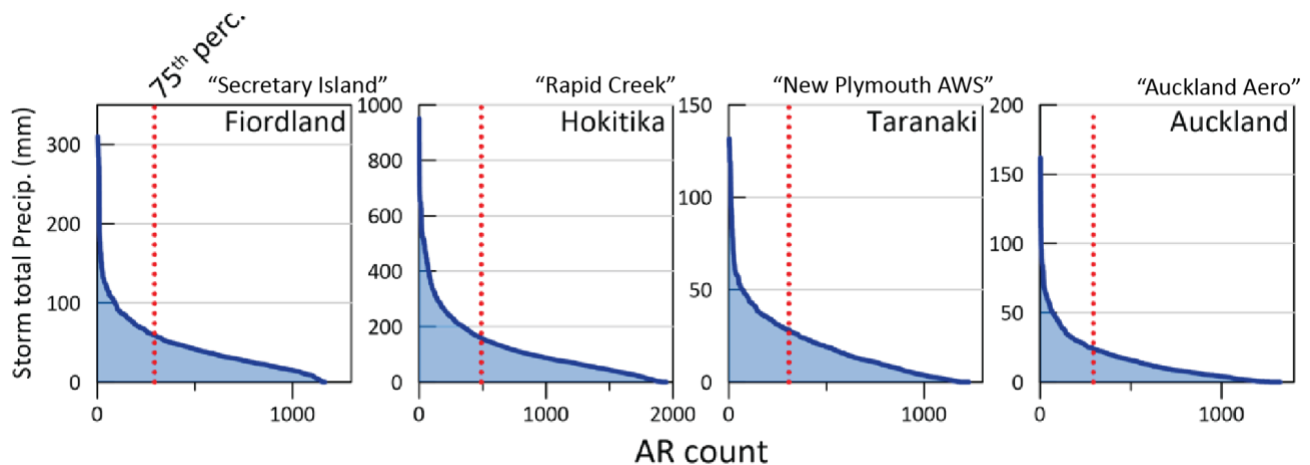


Figure 3. Storm total precipitation associated with landfalling ARs from four selected weather stations in New Zealand (named above figure) used throughout this research. The ARs are ordered along the x-axis from greatest to least storm total precipitation. The 75th percentile in storm total precipitation is identified with the red dotted line. ARs left of this line are selected as those that are most impactful.

The multivariate MJO index (Wheeler and Hendon, 2003) is used to examine the role MJO has on modulating New Zealand ARs. The index consists of two amplitudes (RMM1 and RMM2) from empirical orthogonal functions of tropical zonal winds and outgoing longwave radiation categorized into 8 distinct phases. For each phase, MJO days are identified when the combined magnitude ($\sqrt{\text{RMM1}^2 + \text{RMM2}^2}$) exceeds 1, a common distinction for identifying MJO days (Henderson et al., 2017; Zhou et al., 2021). New Zealand landfalling ARs that have genesis during an MJO phase are identified, however, since ARs can exist over multiple days it is possible for an AR to have genesis in one MJO phase and termination in another. The initial conditions are the focus of this study and so genesis during each phase is the focus to connect downstream impacts

(in New Zealand) over the entire AR lifecycle to the conditions that were present at the time of genesis (following similar justification to Zhou et al., 2021). Across all landfall locations, approximately 62% of landfalling ARs have a genesis during an identified phase of the MJO, with New Zealand AR genesis occurring on 12-19% of all days with an identified MJO.

3 Results

3.1 New Zealand AR lifecycles

We begin by examining AR lifecycles for all ARs that make landfall in New Zealand irrespective of their landfall location, magnitude, or moisture flux direction. The genesis region for New Zealand ARs stretches from 90°E to 160°W, from the Indian to the Pacific Ocean, with the highest frequency of AR genesis located in the Tasman Sea, westward of the North Island (Figure 4a). Tasman Sea genesis frequencies exceed 6 per year, with the highest grid cell frequencies exceeding 10 per year. The greatest genesis frequencies are located immediately adjacent to New Zealand, typically to the north-west. While AR genesis frequency does decrease over the landmass of Australia, it remains elevated indicating that AR genesis is not limited to maritime locations and advected moisture over the landmass of Australia is able to meet the characteristics of a genesis AR. The eastward extent of AR genesis downwind of New Zealand is notable and may also be associated with ARs that have genesis at the point of landfall with a large shape that extends well beyond the landmass of New Zealand (Prince et al., 2021b). This eastern genesis region will also reflect the genesis of ARs that make landfall on the east coast of New Zealand (Figure 5; Prince et al., 2021a).

Termination locations for New Zealand ARs extend across the entire South Pacific from 150°E to 60°W (Figure 4b), with an average of 1.5 ARs per year terminating through the Drake Passage, between South America and the Antarctic Peninsula. Similar to genesis, the highest termination rates are immediately adjacent to the landmass of New Zealand representing ARs that have termination at the time or shortly after landfall. A region of increased termination extends from the southern end of New Zealand to the southeast, possibly indicating the direction most ARs travel following landfall. Notably, over 3 ARs per year on average that landfall in New Zealand reach the Antarctic continent, extending from Victoria Land and the front of the Ross Ice Shelf, across the coastline of West Antarctic and to the western edge of the Antarctic Peninsula (Figure 4b).

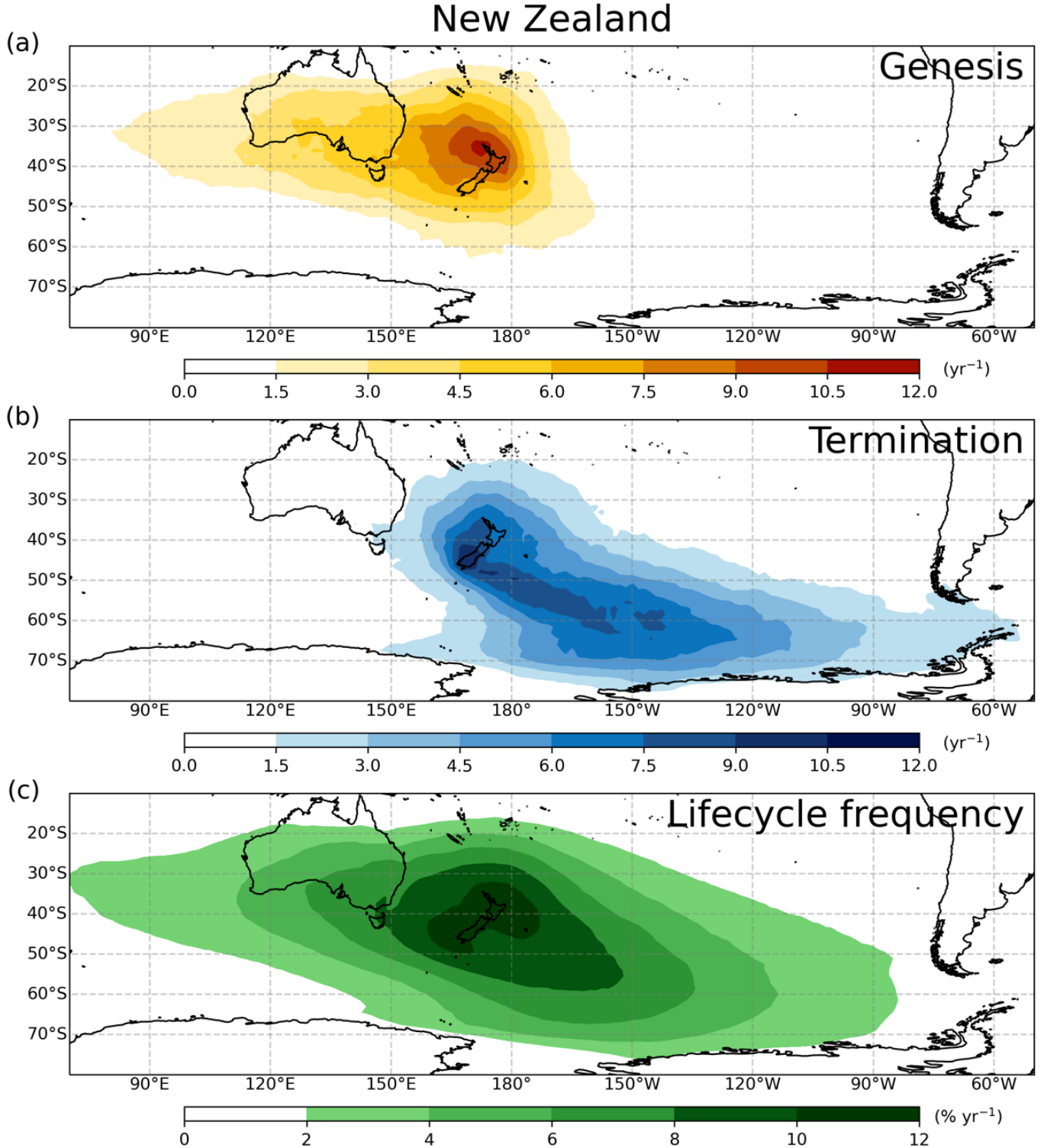


Figure 4. Mean frequency of AR (a) genesis and (b) termination for ARs that make landfall in New Zealand at any point throughout their lifecycle (in counts per year) between 1979 and 2019. (c) Lifecycle frequency of all AR objects for New Zealand landfalling ARs are shown as a percent of annual time steps.

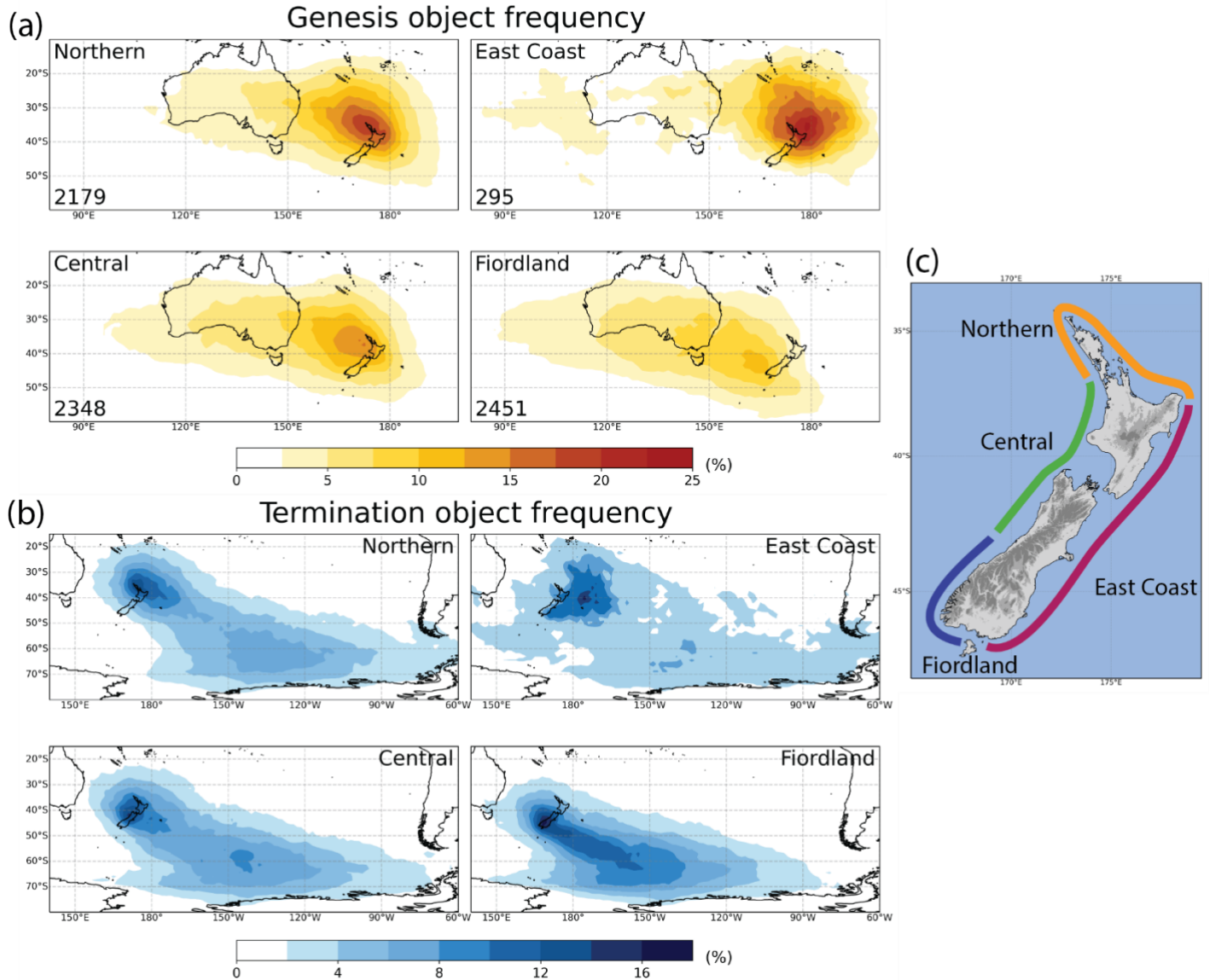


Figure 5. AR genesis (a) and termination (b) frequency for ARs that make landfall in New Zealand separated by regions as identified in (c) shown as percentages. For landfall to be selected in this figure, the moisture flux of the AR must be directed from the ocean and towards the land. Total number of AR lifecycles shown in the lower left corner in (a).

These termination locations are also well within the northern most extent of seasonal sea ice cover around Antarctica (Parkinson and Cavalieri, 2012). The range between the westward extent of genesis (90°E) and the eastward extent of termination (60°W) is over 210° of longitude, extending more than half way around the globe, demonstrating the importance of planetary scale circulation features on synoptic-scale cyclonic processes that initiate precipitation in New Zealand.

Mapping the AR lifecycle frequency further adds to this understanding by demonstrating where ARs that make landfall in New Zealand tend to occur, rather than their instantaneous genesis or termination statistics (Figure 4c). The lifecycle frequency reveals important information about the duration of AR conditions rather than the instantaneous genesis or termination object. Over the landmass of New Zealand, AR frequencies of 10-12% of timesteps within the year are observed which matches well with previous, location specific New Zealand AR frequencies (Prince et al., 2021a). Furthermore, ARs that make landfall in New Zealand occur over southeast Australia (New South Wales and Victoria) for 6-8% and Western Australia for 2-4% of annual timesteps. The lifecycle map also reveals that New Zealand landfalling ARs are also present southward of 70°S, well within the range of Antarctic sea ice for up to 2% of annual timesteps, corresponding to AR conditions (associated with New Zealand ARs) on 7 days within a year.

Dividing the genesis and termination frequencies based on landfall location further reveals the nature of AR lifecycles for various regions around the country (Figure 5). ARs that make landfall on the western side of New Zealand (Central and Fiordland in Figure 5) have the largest spread of genesis locations with up to 5% of landfalling ARs with genesis in the Indian Ocean, westward of Australia (120°E). As observed in Figure 4, the genesis frequency increases with proximity to the landfall location, increasing to up to 15% in locations adjacent to the coastline. Elevated genesis frequencies of over 2.5% extend northward up to 20°S and across central Australia. ARs that make landfall on the Northern coast of New Zealand have a more concentrated genesis region, with frequencies over 2.5% remaining eastward of 120°E, over the landmass of Australia. Towards the coastline, Northern ARs have genesis frequencies over 20%. East Coast landfalling ARs have the most unique genesis region, being constrained mostly eastward of Australia in the Tasman Sea and South Pacific Ocean. The core region of AR genesis for the East Coast is at about 180°E, to the northeast of New Zealand.

The spatial distribution of AR termination separated by region also reveals further insight into the lifecycle of New Zealand landfalling ARs. Central and Northern landfalling ARs have similar termination regions, with up to 4% of landfalling ARs having termination on the coast of Western Antarctica. These regions also display two regions of enhanced termination, over the landmass of New Zealand (over 12% of ARs) and in the South Pacific centered at 140°W and 60°S (up to 8%). About 2% of Northern and Central ARs cross the entire South Pacific Ocean and have termination in the Drake Passage. Fiordland ARs do not travel as far, with almost all termination

occurring westward of the Antarctic Peninsula and less than 2% of ARs having termination eastward of 90°W. Fiordland ARs exhibit a narrow band of increased AR termination indicating a preferential pathway for ARs that landfall in this region, extending to the southeast of the South Island with frequencies up to 12%. East Coast ARs tend to all have termination immediately east of the North Island of New Zealand at 40°S and eastward of 180°E. The colocation of East Coast AR genesis and termination regions suggests that ARs that make landfall in this region do not travel far and have relatively short lifetimes compared to those that make landfall in other regions of New Zealand.

3.2 Genesis frequency as a function of impact

A key question in this research is the role that genesis has on the impact of New Zealand landfalling ARs. The difference in genesis frequency between all ARs and those that produce impactful weather events (precipitation in the stations 75th percentile) is presented in Figure 6 across four locations spanning the length of the western coast of New Zealand (from south to north, Fiordland, Hokitika, Taranaki, and Auckland). As found in Figures 4 and 5, AR genesis for all locations on the western coast extends over Australia and towards 90°E, with those making landfall further south having genesis regions extend further westward. The distribution of genesis locations appears to shift notably when considering impactful ARs (75th percentile precipitation) across all landfall locations (statistically significant, at the 95% level from a one-sided Fisher-exact test). The median genesis centroid and relationship between storm total precipitation and IVT is shown in Supporting Information S1.

For Auckland, ARs tend to have more frequent genesis (frequencies up to 5% greater) in the north Tasman Sea stretching between Brisbane and New Caledonia between 30°S and 40°S of rates that are for individual grid cells. The reduced frequency to the south of the distribution demonstrates that impactful ARs for Auckland tend to come from north of 35°S. Further south, Taranaki exhibits a similar region of enhanced AR genesis in the North Tasman Sea, between the top of the North Island and New Caledonia with an extended zonal range stretching northwest across Australia. In the middle of the South Island, impactful ARs in Hokitika tend to have genesis along the western side of the Tasman Sea, on the east coast of Australia with a broad range of increased genesis across much of southern Australia. In Fiordland, at the southern end of New Zealand, impactful ARs only have a small region of increased genesis in a narrow band along the

southern coast of Australia. In summary, impactful North Island ARs tend to come from subtropical regions to the northwest of New Zealand, while impactful South Island ARs are associated with genesis over southeastern Australia, with the western Tasman Sea being a key region of impactful AR genesis for all regions.

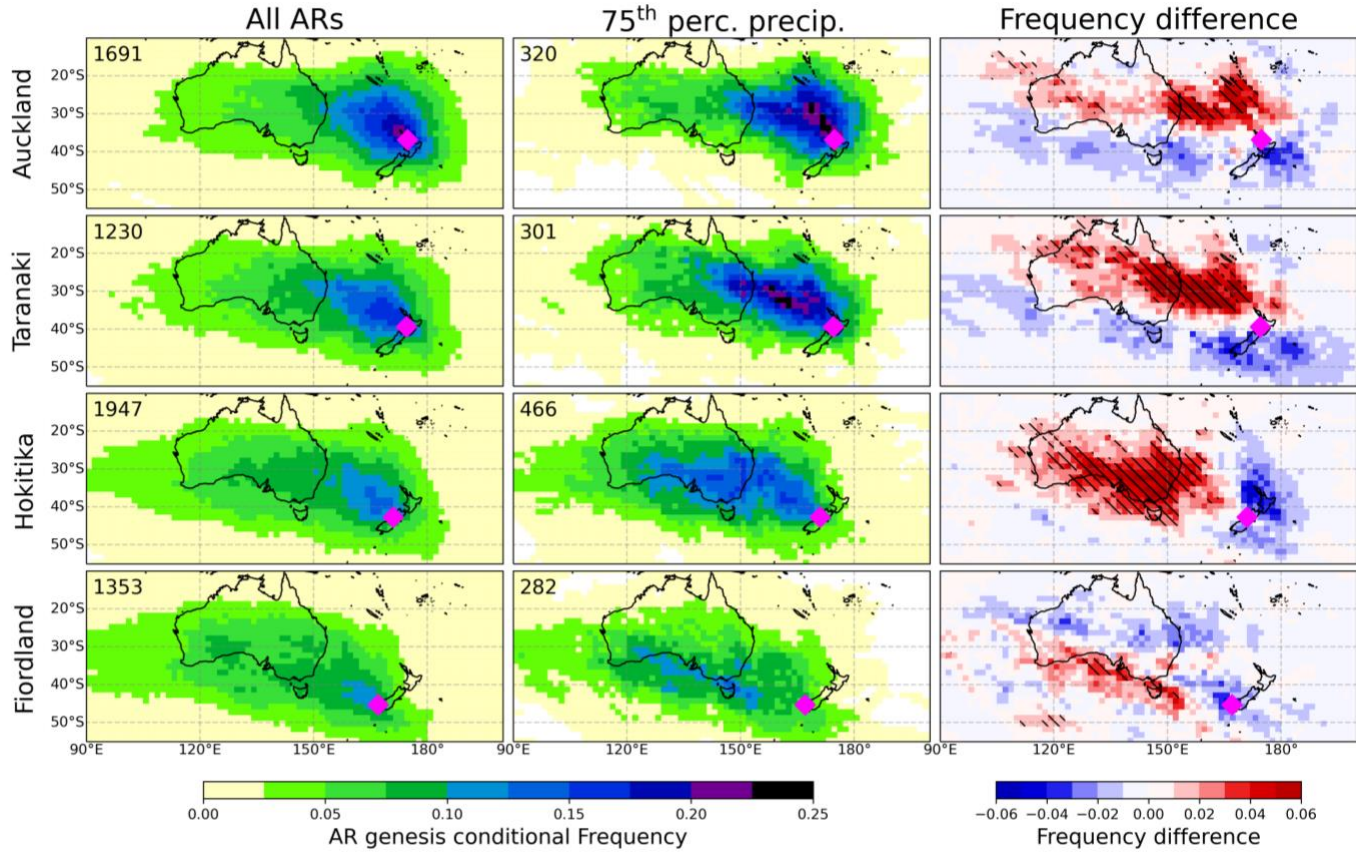


Figure 6. The conditional frequency of atmospheric river (AR) genesis for ARs making landfall at the four weather stations identified in Figure 1 for all landfalling ARs (left) and those that produce precipitation in the 75th percentile (center). Conditional frequency is the probability an AR object originates from a grid cell given that it makes landfall in each location and causes precipitation in the specified range (i.e., exceeding the 75th percentile). The numerical absolute increase in frequency (center column minus the left column) is shown (right) with statistical significance ($p < 0.05$) shown with dashed lines (from a one-sided Fisher-exact test).

3.3 Synoptic conditions during AR genesis

To further investigate characteristics of these primary AR genesis regions, atmospheric composites of vertically integrated water vapor (IWV), vertically integrated water vapor transport (IVT), and 500 hPa surface heights are assessed for the four individual landfall locations for ARs

that occur throughout the entire year (Figure 7). Genesis of all ARs for Auckland is associated with a low pressure centered to the west of the South Island of New Zealand with higher pressures to the northeast of the North Island. This pressure dipole initiates an anomalously moist, northwesterly geostrophic flow directed toward the North Island of New Zealand. Considering the other landfall locations, the location of this pressure dipole and associated moist geostrophic flow shifts southward as expected. AR genesis for all locations in Figure 7 has a weak high-pressure anomaly off the coast of Antarctic at about 50°S between 90°E and 110°E, suggesting the presence of a wave packet, with embedded synoptic scale waves, directed to the northeast. Notably, for Fiordland ARs, the moisture anomaly stretches across the entirety of Australia, suggesting that AR genesis that landfall in Fiordland is associated with broad moist conditions across Australia.

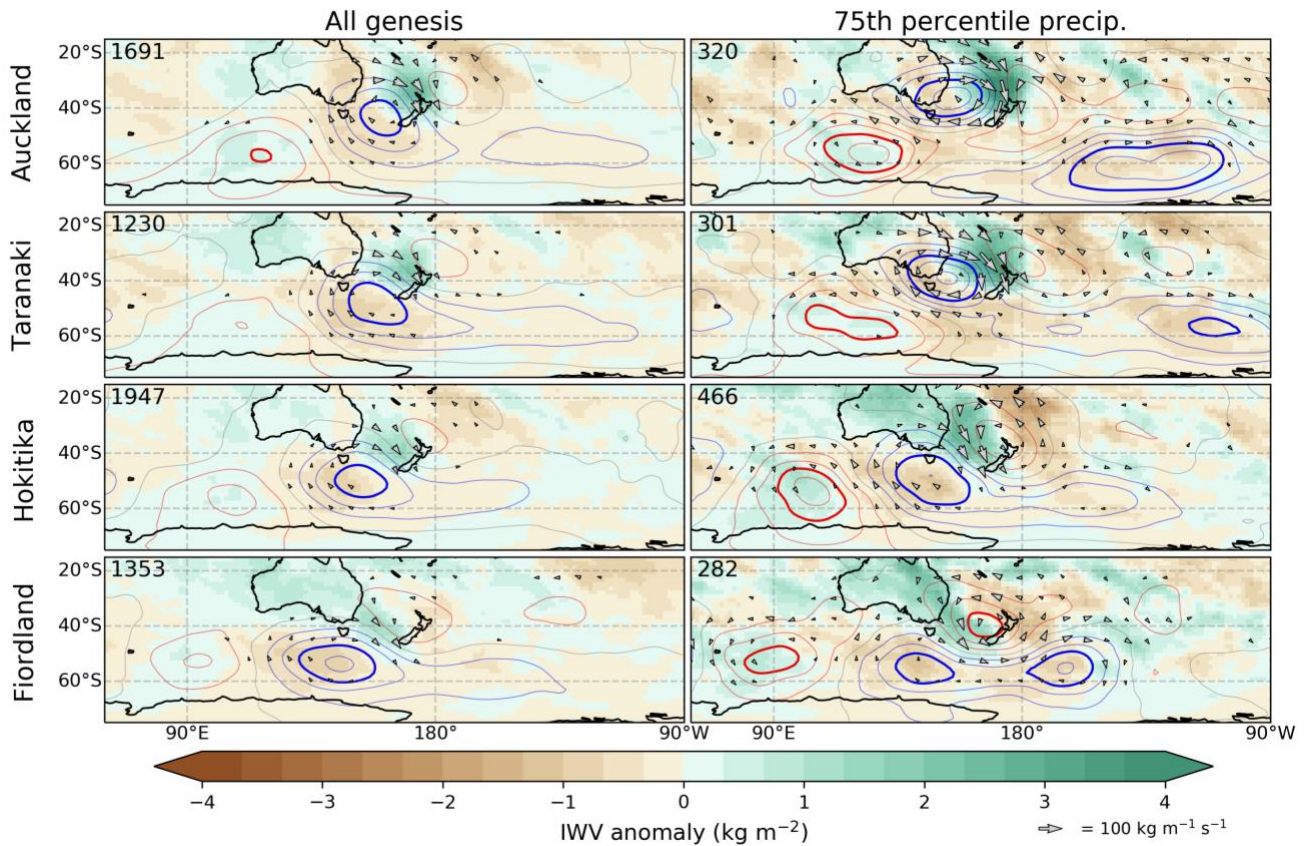


Figure 7. Atmospheric conditions at the time of atmospheric rivers (AR) genesis shown with composites of anomalous vertically integrated water vapor (IWV; green and brown), 500 hpa height anomalies (red and blue 10 m contours, 30 m in bold) and vapor flux vector anomaly (arrows) for all landfalling ARs (left) and those that produce precipitation in the 75th percentile (right).

Considering the most impactful AR conditions reveals enhanced moisture flux, IWV and geopotential height anomalies at genesis (Figure 7). For Auckland, the cyclonic anomaly deepens and shifts to the northwest, rotating the pressure dipole and allowing for a much more meridional flow, producing a much more moist northerly flow towards New Zealand. Interestingly, these impactful ARs for the North Island are also associated with a large low pressure region in the South Pacific Ocean centered at 60°S off the coast of Antarctica, centered between 180°W and 90°W. This additional geopotential anomaly combines with the previously noted tripole to trace a planetary-scale wave from 90°E to 90°W (half a hemisphere) with an embedded wave packet, with an embedded shortwave trough initiating AR genesis for the North Island of New Zealand. These features of enhanced geopotential anomalies, northward rotated moisture flux, greater moisture anomalies and the presence of a planetary-scale trough are apparent for both Auckland and Taranaki impactful (75th percentile precipitation) AR genesis.

South Island impactful AR genesis anomalies reveals a more mixed spatial pattern. In Hokitika, the cyclonic anomaly shifts westward and broadens with enhanced northerly moisture advection. For Fiordland, the high pressure located over New Zealand strengthens while two cyclonic anomalies are distributed to the south of New Zealand at 55°S. For both South Island locations, impactful ARs are associated with substantial moist anomalies over the landmass of Australia paired with substantial dry advection to the east of New Zealand. The upwind high pressure anomalies also become much more pronounced for the impactful ARs, a feature that is observed for impactful genesis for all landfall locations.

3.4 Lagged composite analysis

To further examine the preconditions of ARs in New Zealand a lagged composite analysis is undertaken by calculating mean atmospheric conditions at the time of genesis along with 2 and 5 days prior and following AR genesis for all and impactful ARs. Lagged composites are only shown for Hokitika and Auckland as representative locations, with the results from Taranaki and Fiordland are presented in the supplementary materials (Supporting Information S2 and S3). For all ARs in Hokitika, there is no consistent pressure anomaly, moisture flux or organized regions of anomalous moisture at 5 days prior to genesis (Figure 8). At 2 days prior and genesis, there is development and intensification of the low pressure anomaly in the composite with anomalous

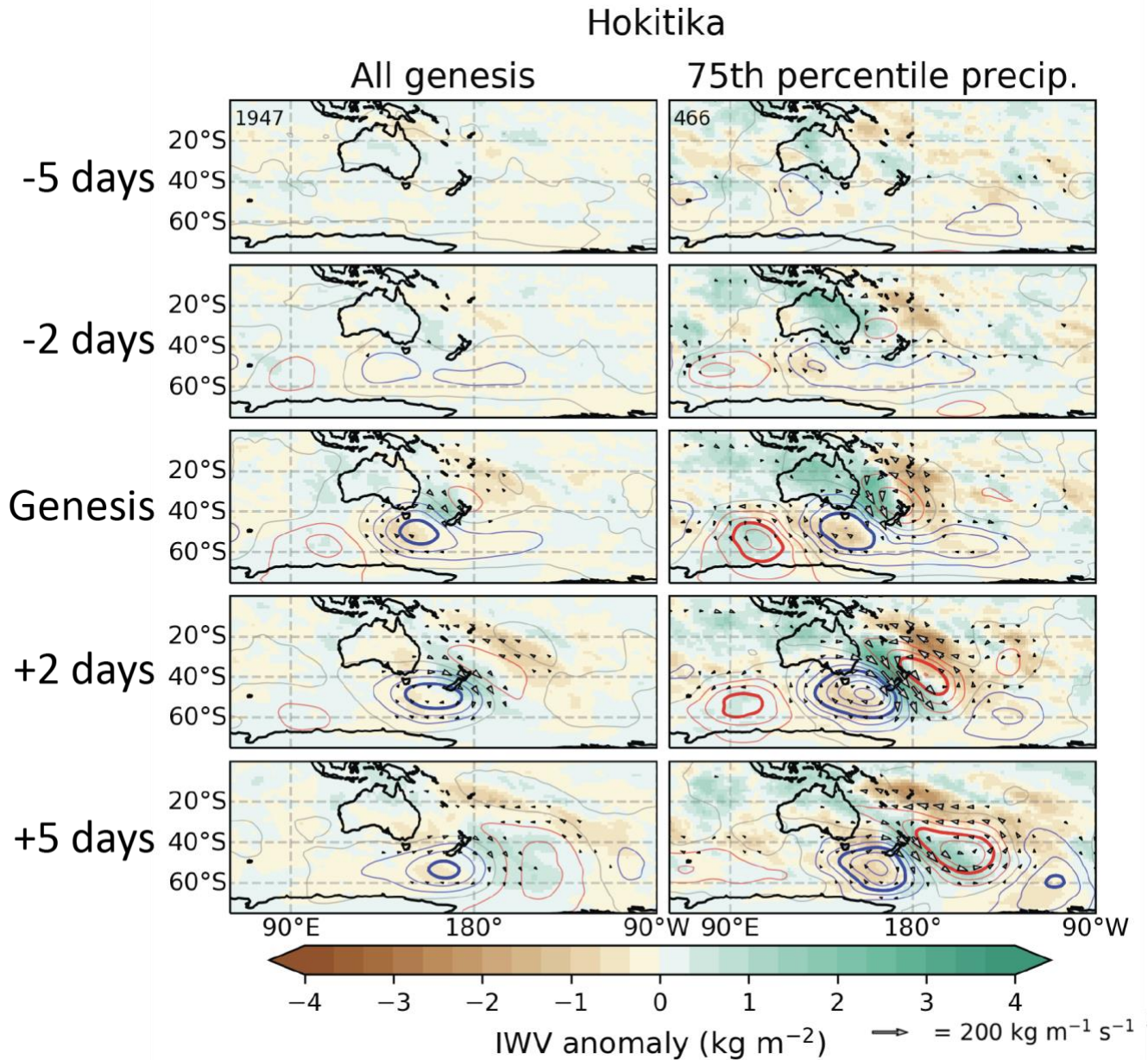


Figure 8. Synoptic-scale composites (of the same properties as Figure 7) on the day of genesis and 2 and 5 days preceding and following the genesis of ARs that make landfall in Hokitika for all ARs (left) and those that produce precipitation exceeding the 75th percentile (right).

moisture flux occurring at the time of genesis, when conditions first meet AR characteristics. After 2 days from genesis the noted anomalies persist, and intensify, demonstrating the normal progression of an AR intensifying and making landfall. After 5 days following genesis the moisture anomaly has typically moved past New Zealand as the cyclonic feature translates eastward indicating that on average, AR conditions have made landfall and passed over the country within

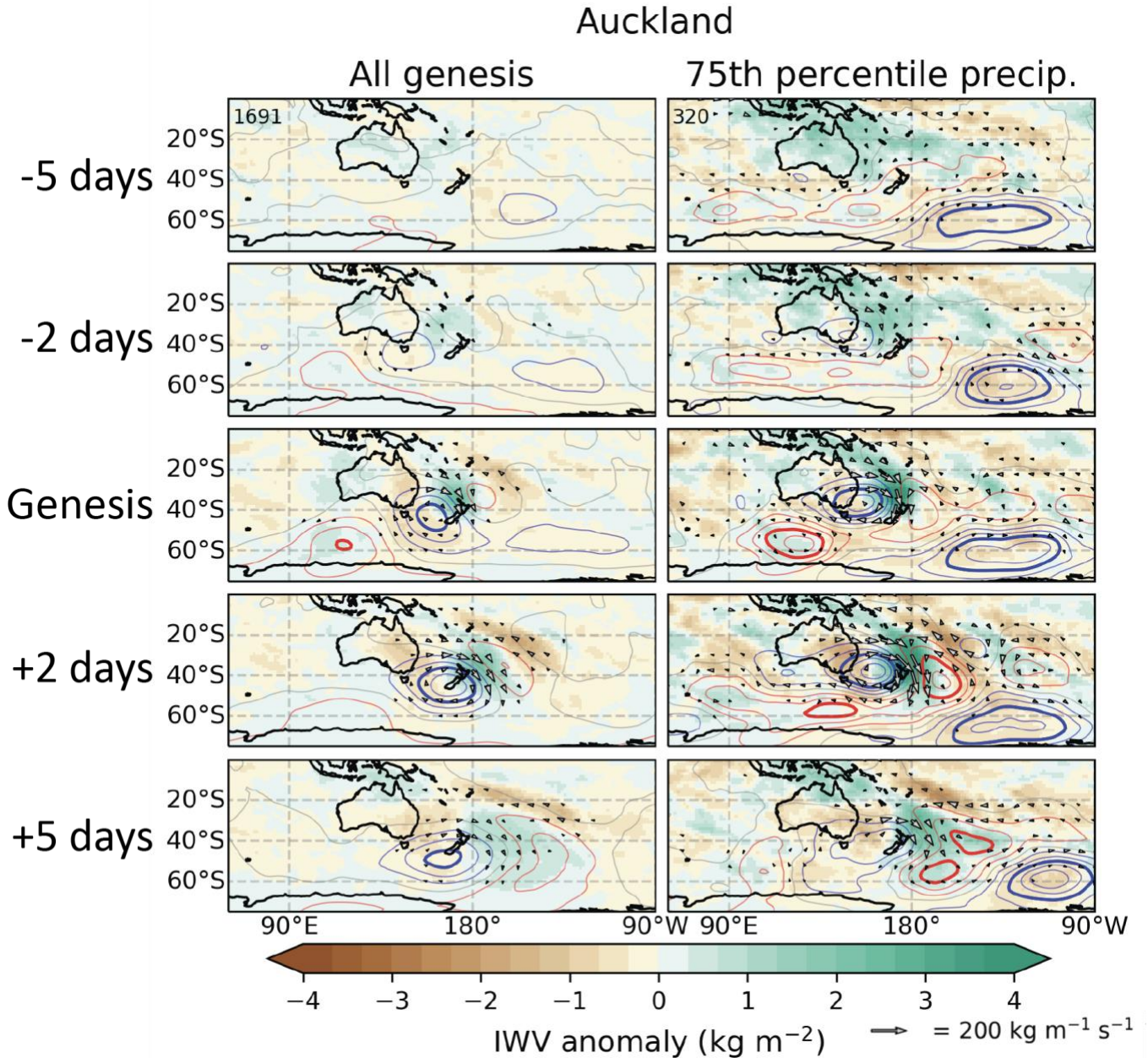
5 days. Impactful Hokitika ARs have a large moisture anomaly 2 days prior to genesis associated with a low that is passing to the south of Australia. Following genesis, impactful ARs are associated with a strengthening of all anomalies of pressure, IWV, and IVT observed up to 5 days following genesis.

Similar to Hokitika, Auckland AR genesis for all ARs does not have a signal in pressure, IWV or IVT at 5 days prior (Figure 9). At 2 days prior to genesis, moistening can be seen to the northwest of New Zealand with a low pressure in the south Tasman Sea in the composite. Following genesis, the cyclonic anomaly shifts eastward to be positioned over New Zealand which shifts the core of the enhanced moisture flux offshore to the east of Auckland, with all anomalies easing by 5 days following genesis. The lifecycle of impactful ARs for Auckland has some notable differences, namely, a large, stationary low pressure anomaly to the southeast of New Zealand, off the coast of Antarctica at about 135°W and 60°S. This low pressure remains relatively unchanged at a constant pressure anomaly and position over the 10 days centered around impactful ARs genesis. Another notable feature is the broad moist anomaly over much of Australia up to 5 days prior to impactful AR genesis. In the following 5 days leading up to genesis, a small cyclonic anomaly passes over the south of Australia, organizing this broad region of moisture into a narrow corridor along the leading edge of the cyclone, associated with the poleward flowing air of the circulation. By the time genesis occurs, the previously noted full planetary scale trough is apparent which persists for up to 5 days following genesis. As noted for Hokitika, the pressure anomalies tend to strengthen 2 days following genesis for impactful ARs, driving further development of the moisture flux in the events that produce substantial precipitation.

3.5 MJO impact on AR lifecycle characteristics

The role of the MJO on AR lifecycle characteristics is examined as an initial quantification of its impact on the weather systems that produce precipitation in New Zealand. The mean atmospheric conditions during the 8 MJO phases around New Zealand are shown in Supporting Information S4 and S5 accompanied by composites of New Zealand landfalling ARs that have genesis during each phase. Four individual AR lifecycle properties are examined at the four locations identified in Figure 6 during the 8 phases of the MJO: AR frequency, maximum IVT, AR travel speed, and median precipitation (Figure 10). AR travel speed is the mean speed that the AR object travels which will be broadly associated with the eastward translation of midlatitude

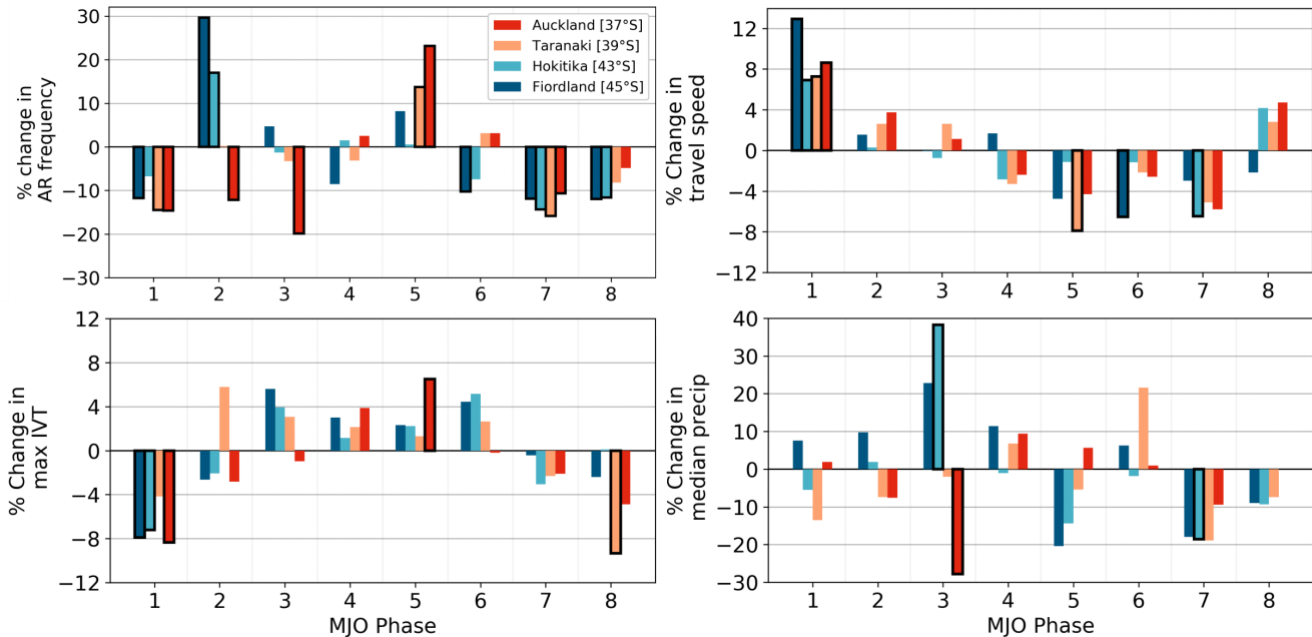
421 cyclones. A slower AR travel speed will be associated with a more stationary synoptic system
 422 possibly associated with blocking.



423 **Figure 9.** Synoptic-scale composites (of the same properties as Figure 7) on the day of genesis and
 424 2 and 5 days preceding and following the genesis of ARs that make landfall in Auckland for all
 425 ARs (left) and those that produce precipitation exceeding the 75th percentile (right).

426 Maximum IVT and AR travel speed both demonstrate a distinct modulation with the
 427 progression of the MJO. In phase 1 landfalling IVT is statistically significantly lower (an 8%
 428 decrease) in Auckland, Hokitika, and Fiordland. Moving through phases 2 to 4, the sign of the

429 difference changes to positive, however, these differences are not significant. At phase 5, Auckland
 430 experiences significantly greater maximum IVT (a 5% increase in magnitude). Then moving
 431 through to phase 8, the sign of the difference flips again with Taranaki experiencing significantly
 432 lower maximum IVT. Generally, it appears the IVT tends to be decreased during phases 1, 2, 7
 433 and 8, while IVT tends to be greater during phases 3 through to 6. AR travel speed (the speed that
 434 an AR object is translated geographically) also has a distinct cycle. ARs travel faster (statistically
 435 significant) for all landfall locations (up to 12% faster) in phase 1. Through phases 2 to 4 there is
 436 no substantial difference, while in phases 5, 6 and 7 ARs appear to travel slower with statistical
 437 significance in Fiordland, Hokitika, and Taranaki. Summarizing these two cycles, ARs tend to
 438 have lower landfalling IVT and travel faster in phases 1, 2 and 8, while having greater IVT and
 439 slower travel speeds in the middle phases, 4, 5, and 6.



440 **Figure 10.** Percent change in AR frequency, maximum IVT, AR travel speed and median
 441 precipitation for ARs that make landfall at the various locations in New Zealand during MJO
 442 phases. Statistically significant differences at the 95% level shown with bold outlines.

443 AR frequency has a complex relationship with MJO phase, however, cyclicity appears
 444 when examining individual landfall locations. In Auckland and Taranaki, AR frequency peaks in
 445 phase 5 with substantially lower frequencies during phase 1, 2, 3, 7, and 8. In Hokitika and
 446 Fiordland, AR frequency peaks in phase 2 with mostly reduced frequencies in all other phases.
 447 Median precipitation also exhibits an intriguing relationship with MJO phase, with the largest

anomalies occurring in phase 3 where Hokitika (and Fiordland to an extent) has increased median precipitation, while Auckland experiences significantly reduced median precipitation. All other phases do not have a significant impact on median precipitation, with the exception of phase 7, where there is an apparent reduction in all locations (significant in Hokitika). Interestingly, maximum IVT modulations and median precipitation statistics do not appear to covary with MJO phase.

To aid in the discussion of the role of MJO on New Zealand ARs, the spatial differences of AR lifecycle frequency is presented in Figure 11 (along with moisture, IVT, and pressure anomalies) for notable MJO phases 1, 2, 5, and 7. A positive anomaly in lifecycle frequency demonstrates that ARs (that makes landfall in New Zealand) tend to spend a longer duration at a given location than when considering all landfalling ARs. Phase 1 is characterized by reduced moisture to the north of New Zealand with a broad high pressure over the Tasman Sea and a low to the south of New Zealand. AR lifecycle frequencies are reduced over a large region of Australia and the South Pacific Ocean including much of New Zealand. Notably, the meridional pressure dipole produces a zonal moisture flux anomaly to the south of Australia, originating from the Indian Ocean that experiences increased AR occurrence and increased advection of moisture during phase 1. Phase 2 has a similar pattern that is translated eastward as the central region of tropical convection also shifts eastward. Increased atmospheric moisture in the eastern Indian Ocean allows for increased AR occurrence in the south of Australia, which stretches to the South Island of New Zealand. By phase 7 the region of increased moisture has shifted to be directly north of New Zealand, with increased AR occurrence over much of Australia and to the north of New Zealand. Phase 5 is associated with a poleward pointing geostrophic wind with a low pressure to the west of New Zealand and a high pressure to the east. Phase 5 is also associated with a large low pressure in the Amundsen-Bellingshausen Sea. Phase 7 has much drier conditions in the Indian Ocean with reduced AR occurrence over Australia and New Zealand. The region of convection is shifted into the Pacific Ocean with increased AR occurrence stretching across the Pacific Ocean.

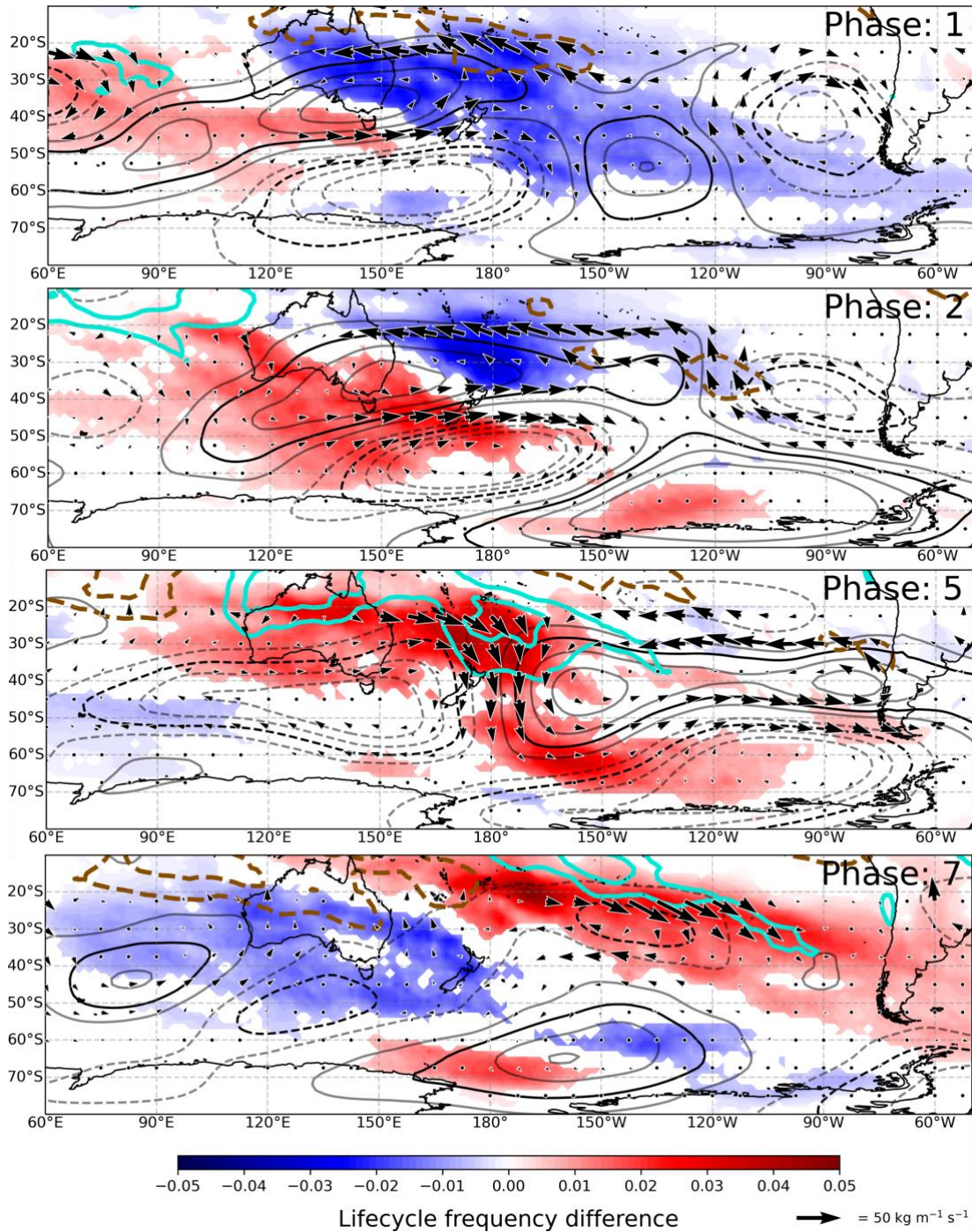


Figure 11. AR lifecycle frequency anomalies (red/blue shading) during selected MJO phases for ARs that make landfall in New Zealand (only significant anomalies at the 5% level are shown). 500z height anomalies shown with black contours (5 m interval; solid for positive, dashed for negative). IVT anomaly shown with black vectors (southward of 20°S). IWV anomalies in aqua/brown contours (+/- 1 and 2 mm of precipitable water). All atmospheric fields averaged from 10 day means following AR genesis within each MJO phase.

4 Discussion

4.1 New Zealand AR lifecycles

The composite and lagged-composite analysis (Figures 7, 8, and 9) allow for interpretation of the initial dynamical conditions that generate AR conditions for New Zealand, with a particular focus on impactful events. A schematic of the major geopotential and precipitable moisture anomalies during AR genesis is presented in Figure 12 for both the North and South Islands. Impactful South Island AR genesis tends to be associated with increased water vapor over much of Australia associated with a cyclone positioned to the south of Tasmania (50°S). The preconditioning of South Island ARs through moist anomalies over Australia has not been explicitly noted in previous studies. Prince et al. (2021a) and Kingston et al. (2021) identify the conditions during landfall with increased moisture advection immediately westward of New Zealand. We show here that this anomalous vapor flux landfalling on the South Island of New Zealand tends to be associated with greater than average precipitable water not just over the Tasman Sea but extending back over the Australian continent.

Impactful North Island AR genesis is characterized by a wavetrain within a broad trough with elevated moisture over the Coral Sea (northeast of Australia) and broad dry anomalies over Australia (Figure 12). The persistent low-pressure anomaly in the Amundsen Sea, lasting for over 10 days, speaks further to the stationary nature of this large scale trough (Figure 9). The location, magnitude, and size of this low-pressure anomaly resembles the characteristics of the Amundsen Sea Low (Raphael et al., 2016) suggesting, a linkage between Antarctic atmospheric dynamics and extreme weather in New Zealand. The same large-scale dynamics that initiate the Amundsen Sea Low may setup conditions favorable for impactful precipitation in the North Island of New Zealand.

The large-scale Rossby wave train for North Island ARs also bears resemblance to the synoptic conditions that produce Australian northwest cloudbands, a large-scale cloud feature related to widespread precipitation and warm advection over Australia (Reid et al., 2019; Black et al., 2021). Black et al. (2021) discuss the role of this large-scale trough in fluxing momentum equatorward, into the subtropical jet stream over New Zealand. This synoptic pattern is also associated with AR activity over Australia and the climatology of Australian northwest cloudbands also matches the climatology of ARs in New Zealand and Australia with maximum occurrence in

the summer (Prince et al., 2021a; Reid et al., 2019, 2022) The source of this planetary-scale wave that produces these numerous weather events for New Zealand and Australia requires further examination and remains an interesting research question. The presented composites also only resembles the mean conditions during AR genesis; an exploration of the various types of AR genesis for New Zealand would reveal further details to better constrain the synoptic drivers since they could vary somewhat between events, as have been studied for the Western U.S (e.g. Zhou and Kim, 2019; Prince et al., 2021b).

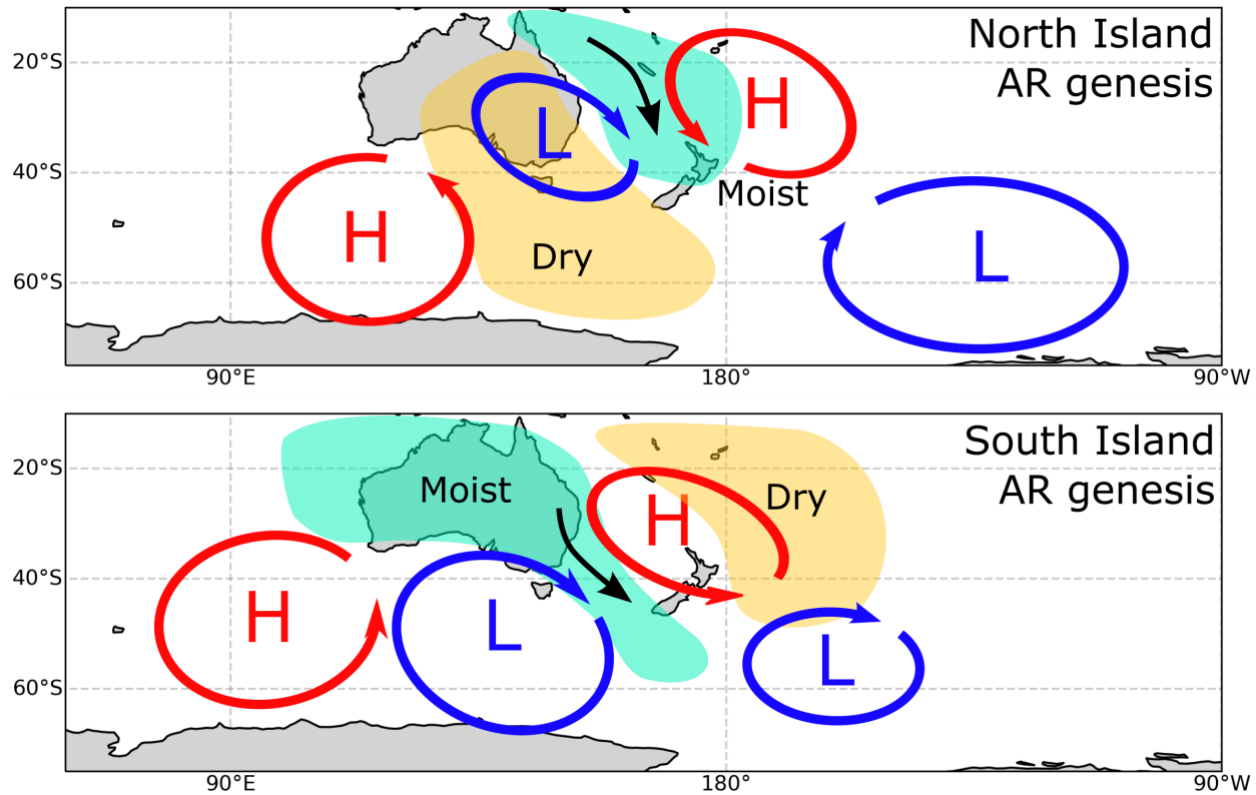


Figure 12. Schematic of the synoptic-scale setup for the genesis of impactful ARs that make landfall in the North (upper) and South (lower) Islands of New Zealand. Moisture anomalies shown with green and brown and pressure anomalies identified with blue and red regions.

The spatial extent of New Zealand AR genesis reveals insight in the passage of cyclones and accumulation of moisture that passes over New Zealand, highlighting the broad region of genesis extending back into the Indian Ocean through to termination in the South Pacific and extending through the Drake Passage. The maximum westward extent of New Zealand AR genesis extends approximately 90° west (with frequencies greater than 5%), almost half the longitudinal extent of AR genesis for corresponding west coast landfall locations in North America (Oregon

and Washington, between 35-40°N; Prince et al., 2021b). We speculate that the presence of the Australian landmass may be considered as the first order difference, inhibiting evaporation and initiating precipitation of transiting cyclones, limiting the supply of moisture available for progressing midlatitude storms. However, an adjacent moisture source is not necessarily a requirement of an AR, with examples from North Africa and the Middle East demonstrating the rapid advection of moisture over broad landmass and deserts (namely over the Arabian Peninsula; Esfandiari and Lashkari 2020; Dezfuli 2020) before initiating precipitation in mountainous regions. It is important to note however, that AR precipitable water does not necessarily come from the genesis region (Sodemann and Stohl, 2013), but rather ARs gain and lose moisture throughout their entire lifecycle. Therefore, the conditions immediately upstream of AR precipitation may be equally as important as the genesis region, suggesting that conditions in the Tasman Sea, such as sea surface temperature may be fundamentally important in controlling the amount of moisture that is advected over New Zealand. Further assessment of the source of moisture in New Zealand ARs could reveal fascinating insight into the particular regions of interest for the generation of moisture for New Zealand precipitation.

The dynamic difference between the North Pacific and westward of New Zealand (Tasman Sea and Southern Indian Ocean) cannot be ignored here and may be equally, if not more, important than the prior moisture source argument. The Northern Hemisphere jet stream maximum situated to the east of Japan (downwind of the Tibetan Plateau) is associated with substantial baroclinic growth in the north Pacific and consequently results in a broad region of enhanced transient eddy activity across the entire north Pacific basin (James, 1994), which is associated with broad AR genesis and elevated AR tracks (Zhang and Villarini, 2018; Guan and Waliser, 2019; Zhou and Kim, 2019; Prince et al., 2021b). The region of maximum cyclogenesis immediately westward of New Zealand is much closer to New Zealand than cyclogenesis for North America, with maximum cyclogenesis occurring over eastern Australia (Trenberth, 1991; Sinclair, 1994, 1995; Hoskins and Hodges, 2005). The cyclones that come further from the east, over the southern Indian Ocean (the hemispheric maximum in cyclone activity and eddy kinetic energy) tend to migrate poleward before reaching New Zealand, terminating well south of Australia (Sinclair, 1995; Hoskins and Hodges, 2005). While this westward region in the Indian Ocean does have enhanced AR genesis activity (Guan and Waliser, 2019), these ARs tend to have a substantial meridional component following the poleward migration of the cyclones, terminating to the south of Australia and

avoiding landfall with New Zealand. This understanding is in congruence with the results presented here; New Zealand ARs tend to come from a smaller upstream region stretching across Australia back to 90°E. The eastward propagation of New Zealand ARs following landfall, which extends well beyond 90° in longitude, further demonstrates that New Zealand is positioned closer to a region of AR genesis (and presumably cyclone genesis as demonstrated by Hoskins and Hodges, 2005), where ARs make landfall relatively early in their lifecycle. The unique characteristics of New Zealand AR lifecycles are crucial for understanding the occurrence of extreme precipitation in New Zealand and must be considered when interpreting future climate impacts for New Zealand.

4.2 Role of the MJO on New Zealand ARs

The presented connection between MJO and ARs in New Zealand generally agree with the role the MJO has on New Zealand weather types (Fauchereau et al., 2016). Phase 5 produces notable increases in North Island AR frequency, moisture flux and AR travel speed while aligns with the northerly flow and north Tasman Sea cyclone typically associated with this phase (Fauchereau et al., 2016). Interestingly, while phase 5 produces anomalous moisture flux and AR frequencies, it is not associated with increased precipitation, shown here and by Fauchereau et al. 2016. The anomalously low precipitation (and AR frequency) on the western coast during phase 7 (Figure 10) also agrees with the reduced west coast precipitation presented by Fauchereau et al. (2016), associated with anomalous easterly flow over the country. The increased AR frequency in phase 2 in the South Island is shown by Fauchereau et al. (2016) as increased precipitation on the South Island West Coast. The synoptic conditions are calculated as 10-day averages following the MJO phase following the methodology presented by Zhou et al. (2021) to capture the potential teleconnections initiated by the deep tropical convection associated with the MJO. Fauchereau et al. (2016) demonstrate that the geopotential height anomaly near New Zealand is stable within 10-days of a given MJO phase, consistent with the relevant timescales of stationary Rossby waves, providing confidence in the presented results.

The motivation to examine the potential role of the MJO on New Zealand AR genesis was to examine whether the geopotential anomalies associated with each phase resembled the conditions during AR genesis (as presented in Figures 7, 8, 9, and 12). The MJO does modulate the AR frequency for New Zealand landfalling ARs ($\pm 30\%$ in their occurrence). The associated

geopotential anomalies, especially associated with phase 5 sets up a low pressure in the Tasman Sea that has some resemblance to North Island AR composites. While the AR geopotential height composites will certainly involve interactions from a variety of wave sources, the position of the pressure dipole over New Zealand during phase 5 is certainly a feature expected to produce increased North Island AR activity. The exploratory analysis presented here acts as a benchmark to continue exploring the dynamical explanation for precipitation variability in New Zealand. Modern studies of MJO teleconnections have focused on North America, which has provided significant understanding of the role of tropical convection plays on seasonal-to-subseasonal forecasting (Wang et al. 2023). The results presented herein and by Fauchereau et al. (2016) highlight the potential of building understanding of tropical teleconnections for New Zealand.

5 Conclusions

In this study, we present the first assessment of New Zealand AR lifecycles, identifying the regions where New Zealand landfalling ARs are first detected and the synoptic conditions associated with initiating ARs conditions. The genesis conditions of the most impactful ARs are examined for various locations across New Zealand, with an assessment of the synoptic conditions prior to and following genesis. Impactful AR genesis for the North Island of New Zealand is associated with an embedded shortwave within a distinct planetary-scale trough extending over New Zealand. This identified synoptic pattern is not dissimilar to synoptic conditions that produce northwest cloudbands over Australia and the possible connection between Australian moisture anomalies and precipitation with New Zealand ARs is demonstrated. South Island AR genesis resembles a more typical synoptic scale wavetrain extending across New Zealand associated with moist conditions over Australia. North Island and South Island ARs appear to come from distinctly different geographic regions with the typical regions of genesis modulating for the most impactful events.

The role of MJO on modulating New Zealand AR lifecycles is also examined through 10-day composite analysis and changing AR characteristics. There is a distinct modulation in AR moisture flux and travel speed with phase 8 and 1 being associated with reduced AR frequency, low moisture flux, and faster travel speeds. The middle phases (4, 5, and 6) appear to be associated with increased moisture flux, increased AR frequency and slower travel speeds. These results appear consistent with the current understanding of MJO teleconnections in New Zealand. These

results highlight the potential for developing seasonal-to-subseasonal forecasts for the New Zealand region by identifying the role tropical dynamics play in generating midlatitude conditions that enhance precipitation.

Acknowledgments

This research undertaken by H. D. Prince is funded by Fulbright New Zealand.

Data Availability Statement

The AR data are available at <https://ucla.box.com/ARcatalog>. Development of the AR detection algorithm and databases was supported by NASA. AR detection is based on the algorithm originally introduced in Guan and Waliser (2015), refined in Guan et al. (2018), and further enhanced in Guan and Waliser (2019) with tracking capability. Precipitation data is retrieved from the NIWA CliFlo weather station network (<https://cliflo.niwa.co.nz/>). Atmospheric data is retrieved from the ECMWF ERA-Interim repository (<https://apps.ecmwf.int/datasets/data/interim-full-daily/levtype=sfc/>) and MJO timeseries is calculated by Wheeler and Hendon (2003) and retrieved from the Australian Bureau of Meteorology (<http://www.bom.gov.au/climate/mjo/>). Analysis was conducted in Python with figures produced primarily using the xarray and Cartopy packages.

References

- Black, A. S., Risbey, J. S., Chapman, C. C., Monselesan, D. P., Moore, T. S., Pook, M. J., Richardson, D., Sloyan, B. M., Squire, D. T. and Tozer, C. R. (2021). Australian Northwest cloudbands and their relationship to atmospheric rivers and precipitation. *Monthly Weather Review*, **149**(4), 1125–1139. <https://doi.org/10.1175/MWR-D-20-0308.1>
- Cullen, N. J., P. B. Gibson, T. Mölg, J. P. Conway, P. Sirguey, and D. G. Kingston (2019). The influence of weather systems in controlling mass balance in the Southern Alps of New Zealand. *J. Geophys. Res. Atmos.*, **124**, 4514–4529, <https://doi.org/10.1029/2018JD030052>.
- Dee, D. P., and Coauthors, 2011: The ERA-Interim reanalysis: Configuration and performance of the data assimilation system. *Quart. J. Roy. Meteor. Soc.*, **137**, 553–597, <https://doi.org/10.1002/qj.828>.
- Dezfuli, A. (2020). Rare atmospheric river caused record floods across the Middle East. *Bulletin of the American Meteorological Society*, **101**(4), E394–E400. <https://doi.org/10.1175/BAMS-D-19-0247.1>
- Esfandiari, N., and H. Lashkari, 2020: Identifying atmospheric river events and their paths into Iran. *Theor. Appl. Climatol.*, **140**, 1125–1137, <https://doi.org/10.1007/s00704-020-03148-w>

- Fauchereau, N., Pohl, B. and Lorrey, A. (2016). Extratropical impacts of the Madden-Julian Oscillation over New Zealand from a weather regime perspective. *Journal of Climate*, **29**(6), 2161–2175. <https://doi.org/10.1175/JCLI-D-15-0152.1>
- Fogt, R. L. and Marshall, G. J. (2020). The Southern Annular Mode: Variability, trends, and climate impacts across the Southern Hemisphere. *WIREs Climate Change*, **11**(4), e652. <https://doi.org/10.1002/wcc.652>
- Guan, B. and Waliser, D. E. (2019). Tracking atmospheric rivers globally: Spatial distributions and temporal evolution of life cycle characteristics. *J. Geophys. Res. Atmos.*, **124**, 12 523–12 552, <https://doi.org/10.1029/2019JD031205>.
- Guan, B., & Waliser, D. E. (2017). Atmospheric rivers in 20 year weather and climate simulations: A multimodel, global evaluation. *Journal of Geophysical Research: Atmospheres*, **122**, 5556–5581. <https://doi.org/10.1002/2016JD026174>
- Guan, B., and D. E. Waliser, (2015). Detection of atmospheric rivers: Evaluation and application of an algorithm for global studies. *J. Geophys. Res. Atmos.*, **120**, 12 514–12 535, <https://doi.org/10.1002/2015JD024257>
- Guan, B., Waliser, D. E., & Ralph, F. M. (2018). An intercomparison between reanalysis and dropsonde observations of the total water vapor transport in individual atmospheric rivers. *Journal of Hydrometeorology*, **19**(2), 321–337. <https://doi.org/10.1175/JHM-D-17-0114.1>
- Henderson, S. A., Maloney, E. D., Son, S.-W. (2017). Madden-Julian Oscillation Pacific Teleconnections: The impact of the basic state and MJO representation in General Circulation Models. *Journal of Climate*, **30**(12), 4567–4587. <https://doi.org/10.1175/JCLI-D-16-0789.1>
- Hoskins, B. J. and Hodges, K. I. (2005). A new perspective on Southern Hemisphere storm tracks. *Journal of Climate*, **18**(20), 4108–4129. <https://doi.org/10.1175/JCLI3570.1>
- Hoskins, B. J. and Karoly, D. J. (1981). The steady linear response of a spherical atmosphere to thermal and orographic forcing. *Journal of the Atmospheric Sciences*, **38**(6), 1179–1196. [https://doi.org/10.1175/1520-0469\(1981\)038<1179:TSLROA>2.0.CO;2](https://doi.org/10.1175/1520-0469(1981)038<1179:TSLROA>2.0.CO;2)
- ICNZ, 2023: Costs of natural disasters. Insurance Council of New Zealand, accessed 10 May 2023, <https://www.icnz.org.nz/natural-disasters/cost-of-natural-disasters/>
- James, I. N. (1994). Introduction to Circulating Atmospheres. *Cambridge University Press*, New York, USA
- Kidston, J., Renwick, J. A. and McGregor, J. (2009). Hemispheric-scale seasonality of the Southern Annular Mode and impacts on the climate of New Zealand. *Journal of Climate*, **22**(18), 4759–4770. <https://doi.org/10.1175/2009JCLI2640.1>
- Kim, S. and Chiang, J. C. H. (2021). Atmospheric river lifecycle characteristics shaped by synoptic conditions at genesis. *International Journal of Climatology*, **42**(1), 521–538. <https://doi.org/10.1002/joc.7258>
- Kingston, D. G., D. A. Lavers, and D. M. Hannah (2016). Floods in the Southern Alps of New Zealand: The importance of atmospheric rivers. *Hydrol. Processes*, **30**, 5063–5070, <https://doi.org/10.1002/hyp.10982>.
- Kingston, D. G., Lavers, D. A. and Hannah, D. M. (2021). Characteristics and large-scale drivers of atmospheric rivers associated with extreme floods in New Zealand. *International Journal of Climatology*, **42**(5), 3208–3224. <https://doi.org/10.1002/joc.7415>
- Kropač, E., Mölg, T., Cullen, N. J., Collier, E., Pickler, C. and Turton, J. V. (2021). A detailed, multi-scale assessment of an atmospheric river event and its impact on extreme glacier melt

- in the Southern Alps of New Zealand. *Journal of Geophysical Research: Atmospheres*, **126**, e2020JD034217. <https://doi.org/10.1029/2020JD034217>
- Lackman, G. M. (2002). Cold-frontal potential vorticity maxima, the low-level jet, and moisture transport in extratropical cyclones. *Monthly Weather Review*, **130**(1), 59-74. [https://doi.org/10.1175/1520-0493\(2002\)130<0059:CFPVMT>2.0.CO;2](https://doi.org/10.1175/1520-0493(2002)130<0059:CFPVMT>2.0.CO;2)
- Little, K., D. G. Kingston, N. J. Cullen, and P. B. Gibson (2019). The role of atmospheric rivers for extreme ablation and snowfall events in the Southern Alps of New Zealand. *Geophys. Res. Lett.*, **46**, 2761–2771, <https://doi.org/10.1029/2018GL081669>
- Mariotti, A., C. Baggett, E. A. Barnes, E. Becker, A. Butler, D. C. Collins, P.A. Dirmeyer, L. Ferranti, N. C. Johnson, J. Jones, B. P. Kirtman, A. L. Lang, A. Molod, M. Newman, A. W. Robertson, S. Schubert, D. E. Waliser, and J. Albers (2020). Windows of opportunity for skillful forecasts subseasonal to seasonal and beyond. *Bulletin of the American Meteorological Society*, **101**(5), E608-E625. <https://doi.org/10.1175/BAMS-D-18-0326.1>
- Orskaug, E., Scheel, I., Frigessi, A., Guttorp, P., Haugen J. E., Tveito, O. E. and Haug, O. (2011). Evaluation of a dynamic downscaling of precipitation over the Norwegian mainland. *Tellus*, **63A**, 746-756. <https://doi.org/10.1111/j.1600-0870.2011.00525.x>
- Pohl, B., Prince, H. D., Wille, J., Kingston, D. G., Cullen, N. J. and Fauchereau, N. (2023). Atmospheric rivers and weather types in Aotearoa New Zealand: a two-way story. *Journal of Geophysical Research: Atmospheres*, **Accepted**.
- Pohl, B., Sturman, A., Renwick, J., Quénol, H., Fauchereau, N., Lorrey and Pergaud, J. (2021). Precipitation and temperature anomalies over Aotearoa New Zealand analysed by weather types and descriptors of atmospheric centres of action. *International Journal of Climatology*, **43**(1), 331-353. <https://doi.org/10.1002/joc.7762>
- Porhemmat, R., Purdie, H., Zawar-Reza, P., Zammit, C. and Kerr, T. (2021). Moisture transport during large snowfall events in the New Zealand Southern Alps: The role of atmospheric rivers. *Journal of Hydrometeorology*, **22**(2), 425-444. <https://doi.org/10.1175/JHM-D-20-0044.1>
- Prince, H. D., Cullen, N. J., Gibson, P. B., Conway, J. and Kingston, D. G. (2021a). A climatology of atmospheric rivers in New Zealand. *Journal of Climate*, **34**(11), 4383-4402. <https://doi.org/10.1175/JCLI-D-20-0664.1>
- Prince, H. D., Gibson, P. B., DeFlorio, M. J., Corringham, T. W., Cobb, A., Guan, B., et al. (2021b). Genesis locations of the costliest atmospheric rivers impacting the western United States. *Geophysical Research Letters*, **48**, e2021GL093947. <https://doi.org/10.1029/2021GL093947>
- Ralph, F. M., J. J. Rutz, J. M. Cordeira, M. Dettinger, M. Anderson, D. Reynolds, L. J. Schick, and C. Smallcomb (2019). A scale to characterize the strength and impacts of atmospheric rivers. *Bull. Amer. Meteor. Soc.*, **100**, 269–289, <https://doi.org/10.1175/BAMS-D-18-0023.1>.
- Ralph, F. M., M. D. Dettinger, M. M. Cairns, T. J. Galarneau, and J. Eylander, 2018: Defining “atmospheric river”: How the Glossary of Meteorology helped resolve a debate. *Bull. Amer. Meteor. Soc.*, **99**, 837–839, <https://doi.org/10.1175/BAMS-D-17-0157.1>
- Raphael, M. N., Marshall, G. J., Turner, J., Fogt, R. L., Schneider, D., Dixon, D. A., Hoskings, J. S., Jones, J. M. and Hobbs, W. R. (2016). The Amundsen Sea Low: Variability, change, and impact on Antarctic Climate. *Bulletin of the American Meteorological Society*, **97**(1), 111-121. <https://doi.org/10.1175/BAMS-D-14-00018.1>

- Reid, K. J., King, A. D., Lane, T. P. and Hudson, D. (2022). Tropical, subtropical, and extratropical atmospheric rivers in the Australian region. *Journal of Climate*, **35**(9), 2697-2708. <https://doi.org/10.1175/JCLI-D-21-0606.1>
- Reid, K. J., Rosier, S. M., Harrington, L. J., King, A. D. and Lane, T. P. (2021). Extreme rainfall in New Zealand and its association with atmospheric rivers. *Environmental Research Letters*, **16**(4), 044012, <https://doi.org/10.1088/1748-9326/abeae0>
- Reid, K. J., Simmonds, I., Vincent, C. L. and King, A. D. (2019). The Australian Northwest Cloudband: Climatology, Mechanisms, and association with precipitation. *Journal of Climate*, **32**(20), 6665-6684. <https://doi.org/10.1175/JCLI-D-19-0031.1>
- Revell, M., Carey-Smith, T. and Moore, S. (2019). A severe frontal rain event over the lower North Island of New Zealand with intense embedded convective banding. *Weather and Climate*, **39**(1), 14-27. <https://doi.org/10.2307/26892909>
- Rhoades, A. M., Risser, M. D., Stone, D. A., Wehner, M. D. and Jones, A. D. (2021). Implications of warming on western United States landfalling atmospheric rivers and their flood damages. *Weather and Climate Extremes*, **32**, 100326. <https://doi.org/10.1016/j.wace.2021.100326>
- Salinger, M. J., Renwick, J. A. and Mullan, A. B. (2001). Interdecadal Pacific Oscillation and South Pacific Climate. *International Journal of Climatology*, **21**, 1705-1721. <https://doi.org/10.1002/joc.691>
- Sellars, S. L., Kawzenuk, B., Nguyen, P., Ralph, F. M., and Sorooshian, S. (2017). Genesis, pathways, and terminations of intense global water vapor transport in association with large-scale climate patterns. *Geophysical Research Letters*, **44**, 12465–12475. <https://doi.org/10.1002/2017gl075495>
- Shearer, E. J., Nguyen, P., Sellars, S. L., Analui, B., Kawzenuk, B., Hsu, K. and Sorooshian, S. (2020). Examination of global midlatitude atmospheric river lifecycles using an object-oriented methodology. *Journal of Geophysical Research: Atmospheres*, **125**, e2020JD033425. <https://doi.org/10.1029/2020jd033425>
- Shu, J., Shamseldin, A. Y. and Weller, E. (2021). The impact of atmospheric rivers on rainfall in New Zealand. *Scientific Reports*, **11**, 5869. <https://doi.org/10.1038/s41598-021-85297-0>
- Sinclair, M. R. (1994). An objective cyclone climatology for the Southern Hemisphere. *Mon. Wea. Rev.*, **122**, 2239–2256, [https://doi.org/10.1175/1520-0493\(1994\)122<2239:AOCFT.2.0.CO;2](https://doi.org/10.1175/1520-0493(1994)122<2239:AOCFT.2.0.CO;2)
- Sinclair, M. R. (1995). A climatology of cyclogenesis for the Southern Hemisphere. *Monthly Weather Review*, **123**(6), 1601-1619. [https://doi.org/10.1175/1520-0493\(1995\)123<1601:ACOCFT>2.0.CO;2](https://doi.org/10.1175/1520-0493(1995)123<1601:ACOCFT>2.0.CO;2)
- Sodemann, H., and A. Stohl, (2013). Moisture origin and meridional transport in atmospheric rivers and their association with multiple cyclones. *Mon. Wea. Rev.*, **141**, 2850–2868, <https://doi.org/10.1175/MWR-D-12-00256.1>
- Stone, D., Rosier, S. M., Bird, L., Harrington, L. J., Rana, S., Stuart, S. and Dean, S. M. (2022). The effect of experiment conditioning on estimates of human influence on extreme weather. *Weather and Climate Extremes*, **36**, 100427. <https://doi.org/10.1016/j.wace.2022.100427>
- Thompson, D. W. J. and Renwick, J. (2006). The Southern Annular Mode and New Zealand climate. *Water and Atmosphere*, **14**(2), 23-25
- Toride, K. and Hakim, G. J. (2022). What distinguished MJO events associated with atmospheric rivers? *Journal of Climate*, **35**(18), 6135-6149. <https://doi.org/10.1175/JCLI-D-21-0493.1>

- 788 Trenberth, K. E. (1991). Storm tracks in the Southern Hemisphere. *J. Atmos. Sci.*, **48**, 2159–2178,
789 [https://doi.org/10.1175/1520-0469\(1991\)048<2159:STITSH.2.0.CO;2](https://doi.org/10.1175/1520-0469(1991)048<2159:STITSH.2.0.CO;2).
- 790 Wang, J., DeFlorio, M. J., Guan, B. and Castellano, C. M. (2023). Seasonality of MJO impacts on
791 precipitation extremes over the Western United States. *Journal of Hydrometeorology*,
792 **24**(1), 151-166. <https://doi.org/10.1175/JHM-D-22-0089.1>
- 793 Wheeler, M. C., and H. H. Hendon, 2004: An all-season realtime multivariate MJO index:
794 Development of an index for monitoring and prediction. *Mon. Wea. Rev.*, **132**, 1917–1932,
795 [doi:10.1175/1520-0493\(2004\)132,1917:AARMMI.2.0.CO;2](https://doi.org/10.1175/1520-0493(2004)132<1917:AARMMI.2.0.CO;2).
- 796 Zhang, C., Adames, Á. F., Khouider, B., Wang, B. and Yang, D. (2020). Four theories of the
797 Madden-Julian Oscillation. *Reviews of Geophysics*, **58**, e2019RG000685.
798 <https://doi.org/10.1029/2019RG000685>
- 799 Zhang, W., and Villarini, G. (2018). Uncovering the role of the East Asian jet stream and
800 heterogeneities in atmospheric rivers affecting the western United States. *Proceedings of*
801 *the National Academy of Sciences of the United States of America*, **115**(50), 891–896.
802 <https://doi.org/10.1073/pnas.1717883115>
- 803 Zhang, Z., Ralph, F. M. and Zheng, M. (2019). The relationship between extratropical cyclones
804 strength and atmospheric river intensity and position. *Geophysical Research Letters*, **46**,
805 1814–1823. <https://doi.org/10.1029/2018GL079071>
- 806 Zhou, Y., and Kim, H. (2019). Impact of distinct origin locations on the life cycles of landfalling
807 atmospheric rivers over the U.S. West Coast. *Journal of Geophysical Research:*
808 *Atmospheres*, **124**, 11897–11909. <https://doi.org/10.1029/2019JD031218>
- 809 Zhou, Y., Kim, H. and Guan, B. (2018) Life cycle of atmospheric rivers: identification and
810 climatological characteristics. *Journal of Geophysical Research: Atmospheres*, **123**, 12–
811 715
- 812 Zhou, Y., Kim, H. and Waliser, D. E. (2021). Atmospheric river lifecycles responses to the
813 Madden-Julian Oscillation. *Geophysical Research Letters*, **48**, e2020GL090983.
814 <https://doi.org/10.1029/2020GL090983>

Supporting Information for

**The Lifecycle of New Zealand Atmospheric Rivers and Relationship with the
Madden-Julian Oscillation**

Hamish D. Prince¹, Peter B. Gibson², and Nicolas J. Cullen³

¹University of Wisconsin Madison, Department of Atmospheric and Oceanic
Sciences, USA

²National Institute of Water and Atmospheric Research, NZ

³University of Otago, School of Geography, NZ

Contents of this file

Figures S1 to S5

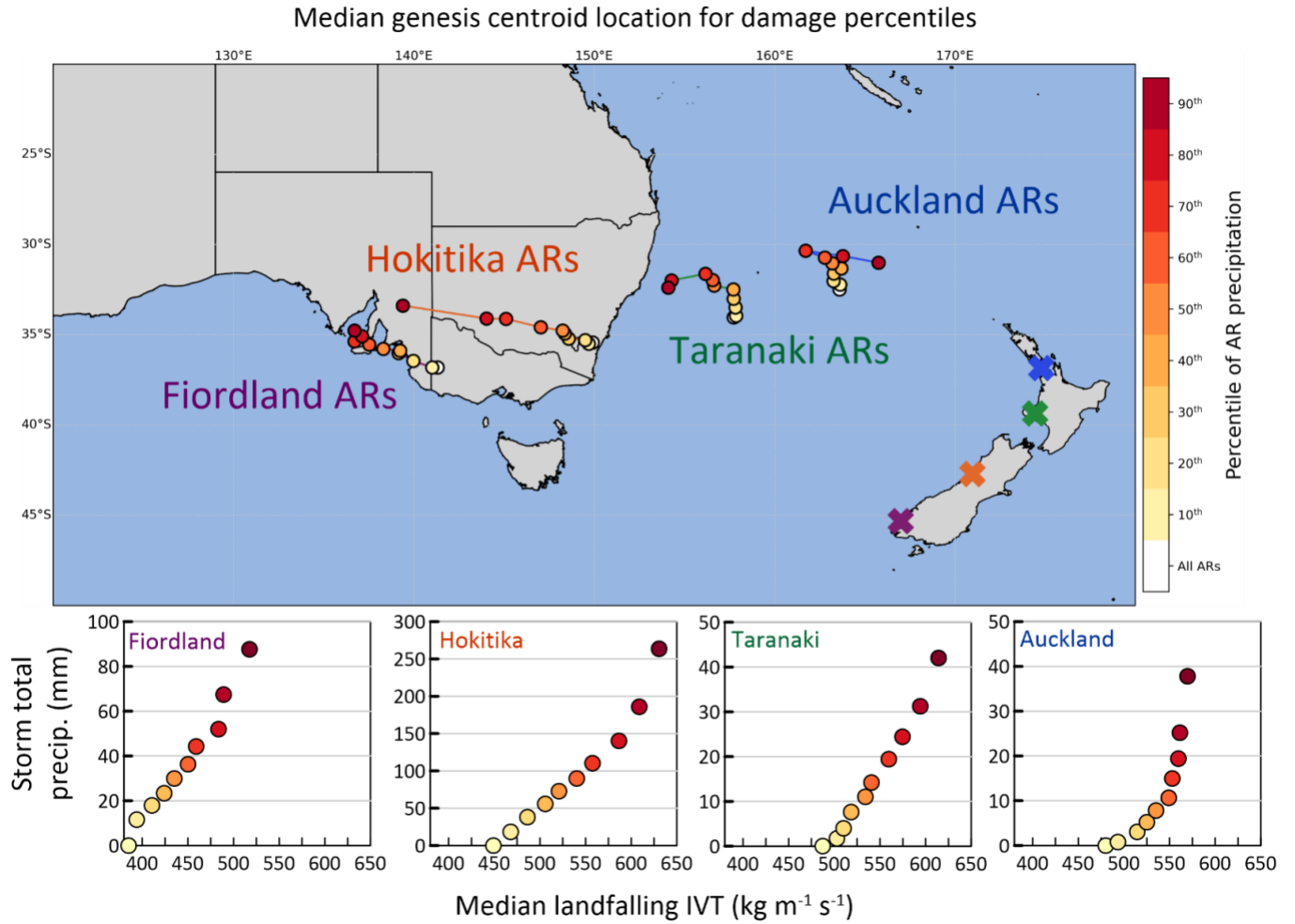


Figure S1. (upper) Median genesis location for ARs that make landfall at each weather station separated by precipitation percentile. (lower) The relationship between median landfalling IVT and storm total precipitation at the four weather stations.

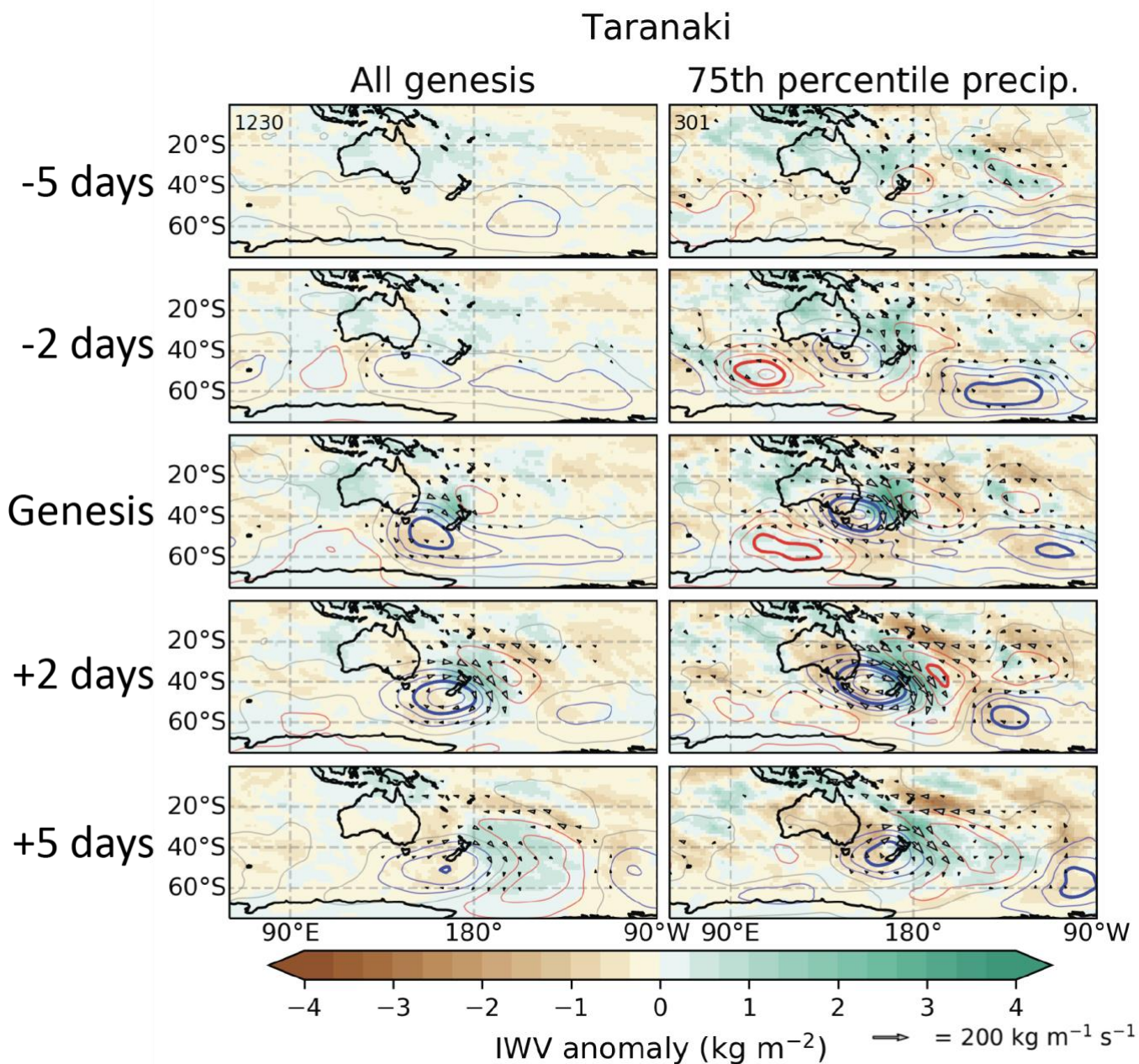


Figure S2. Synoptic-scale composites (of the same properties as Figure 7) on the day of genesis and 2 and 5 days preceding and following the genesis of ARs that make landfall in Taranaki for all ARs (left) and those that produce precipitation exceeding the 75th percentile (right).

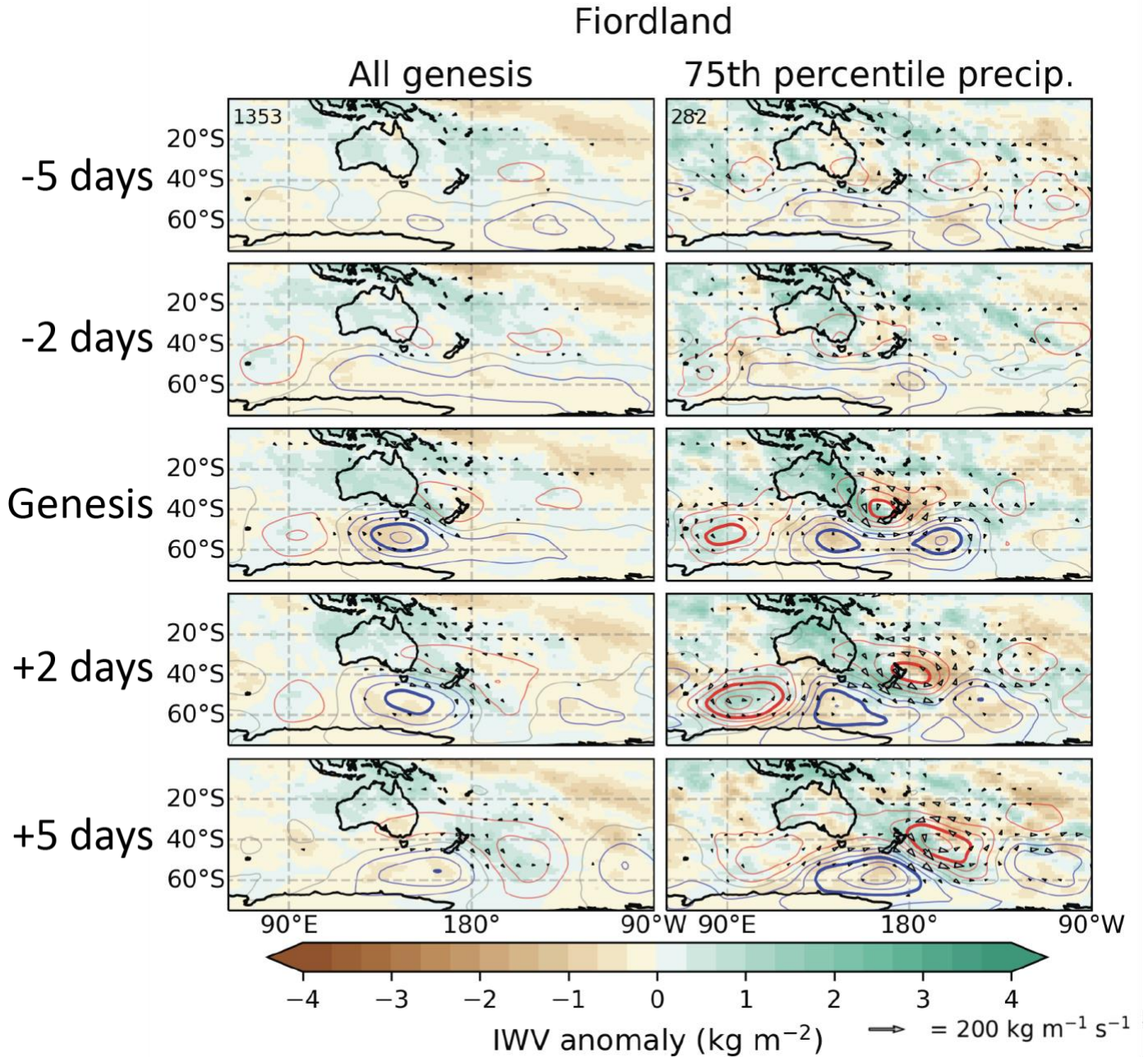


Figure S3. Synoptic- scale composites (of the same properties as Figure 7) on the day of genesis and 2 and 5 days preceding and following the genesis of ARs that make landfall in Fiordland for all ARs (left) and those that produce precipitation exceeding the 75th percentile (right).

All MJO

NZ AR MJO

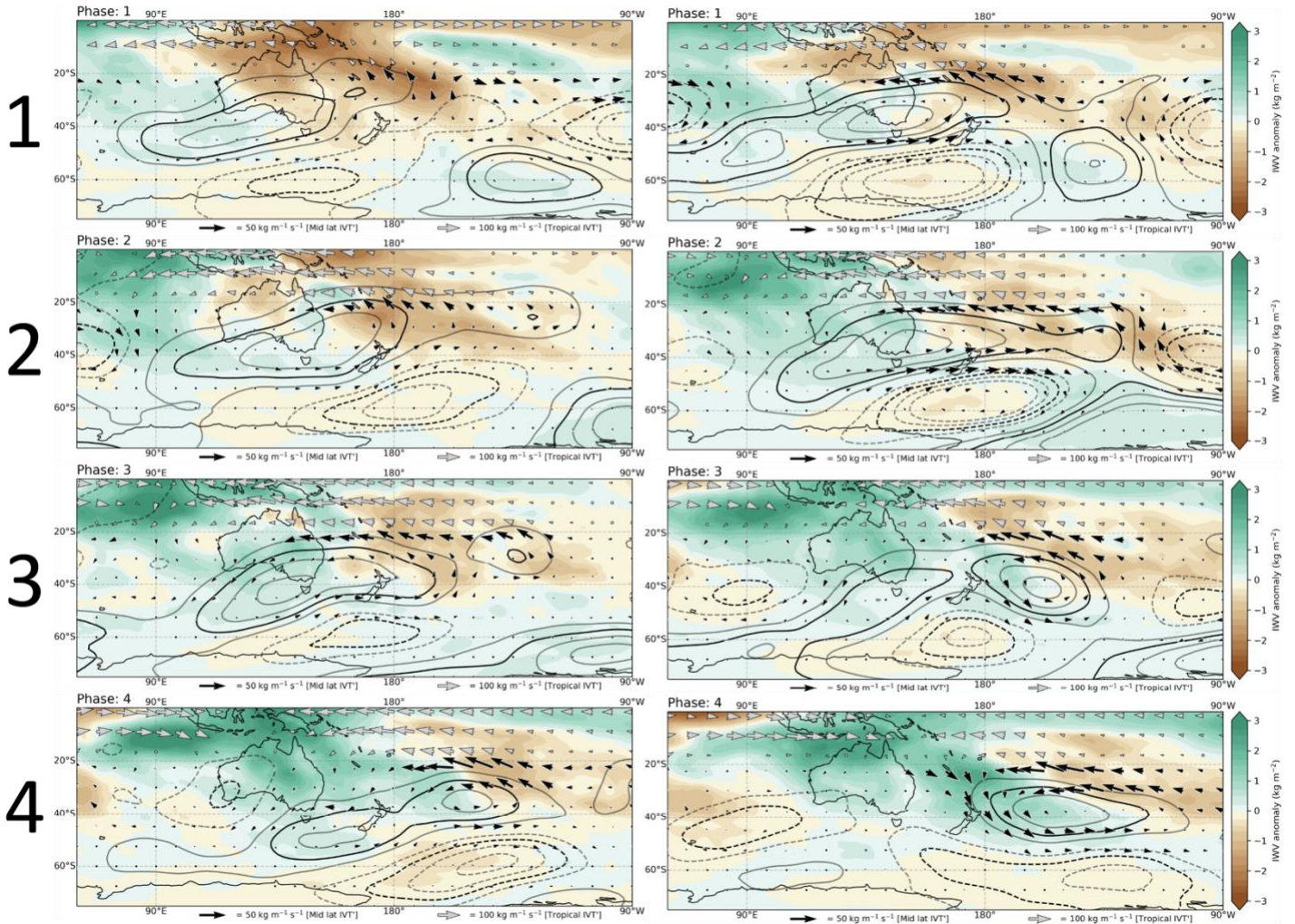


Figure S4. Atmospheric composites during MJO phases (left) and landfalling New Zealand ARs during MJO phase (right) of vertically integrated water vapor (IWV; green and brown), 500 hPa height anomalous (black 5 m contours, 10 m in bold) and vapor flux vector anomaly (arrows). Composites and anomalies are calculated from 10-day averaged starting from day of MJO phase or AR genesis during an MJO phase. The vapor flux anomalies are separated into tropical (gray arrows) and midlatitude vapor flux anomalies due to the difference in scale with the midlatitude vapor flux anomalies bring half the magnitude for the same scale.

All MJO

NZ AR MJO

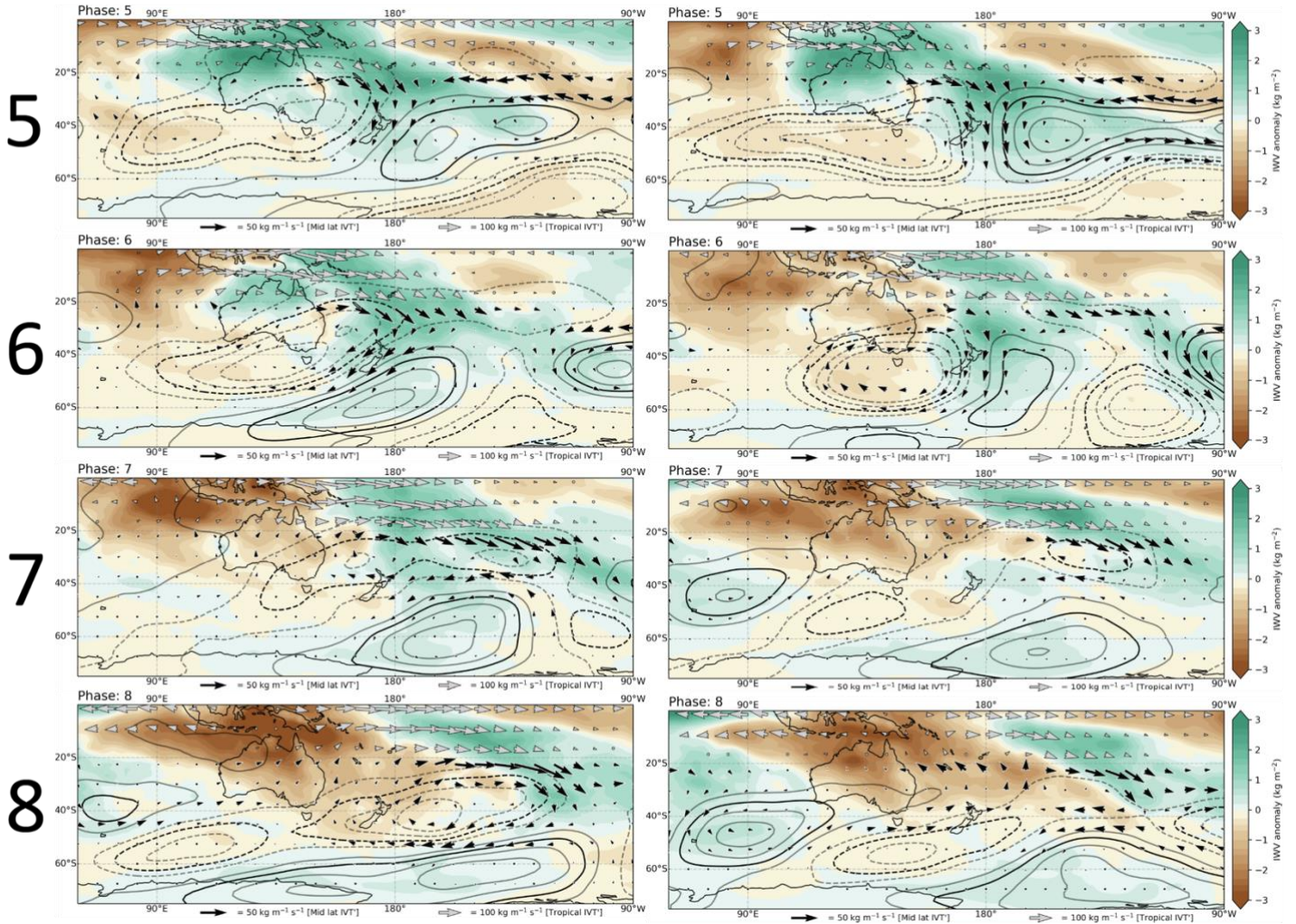


Figure S5. Atmospheric composites during MJO phases (left) and landfalling New Zealand ARs during MJO phase (right) of vertically integrated water vapor (IWV; green and brown), 500 hpa height anomalous (black 5 m contours, 10 m in bold) and vapor flux vector anomaly (arrows). Composites and anomalies are calculated from 10-day averaged starting from day of MJO phase or AR genesis during an MJO phase. The vapor flux anomalies are separated into tropical (gray arrows) and midlatitude vapor flux anomalies due to the difference in scale with the midlatitude vapor flux anomalies bring half the magnitude for the same scale.